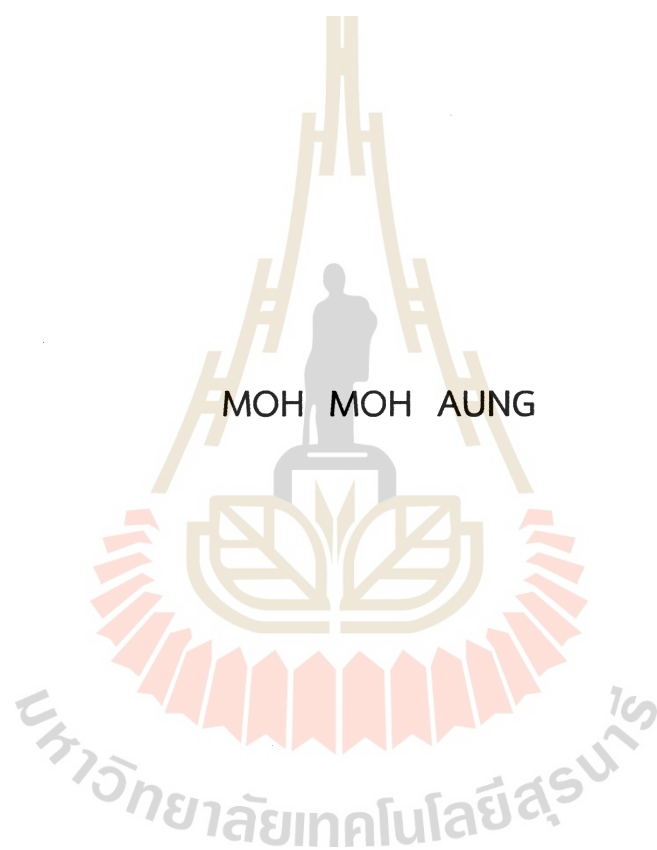


ELECTROMAGNETIC FORM FACTORS OF Delta-N TRANSITION



A Thesis Submitted in Partial Fulfillment of the Requirements for the
Degree of Doctor of Philosophy in Physics
Suranaree University of Technology
Academic Year 2023

ฟอร์มแฟกเตอร์เชิงแม่เหล็กไฟฟ้าของการเปลี่ยนสถานะของ
อนุภาคเดลตา-นิวคลีออน



นางสาวโม โม ออง

วิทยานิพนธ์นี้เป็นส่วนหนึ่งของการศึกษาตามหลักสูตรปริญญาวิทยาศาสตรดุษฎีบัณฑิต
สาขาวิชาฟิสิกส์
มหาวิทยาลัยเทคโนโลยีสุรนารี
ปีการศึกษา 2566

ELECTROMAGNETIC FORM FACTORS OF Delta-N TRANSITION

Suranaree University of Technology has approved this thesis submitted in partial fulfillment of the requirements for the Degree of Doctor of Philosophy.

Thesis Examining Committee

Daris Samart

(Assoc. Prof. Dr. Daris Samart)

Chairperson

Yupeng Yan

(Prof. Dr. Yupeng Yan)

Member (Thesis Advisor)

Stefan Leupold

(Prof. Dr. Stefan Leupold)

Member (Thesis Co-advisor)

Ayut Limphirat

(Assoc. Prof. Dr. Ayut Limphirat)

Member

Khanchai Khosonthongkee

(Asst. Prof. Dr. Khanchai Khosonthongkee)

Member

Yupaporn Ruksakulpiwat

(Assoc. Prof. Dr. Yupaporn Ruksakulpiwat)

Vice Rector for Academic Affairs
and Quality Assurance

Santi Maensiri

(Prof. Dr. Santi Maensiri)

Dean of Institute of Science


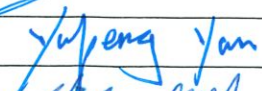

โม โม ออง : ฟอรั่ม แฟกเตอร์ เชิงแม่เหล็กไฟฟ้า ของ การเปลี่ยนสถานะ ของ
อนุภาคเดลตา-นิวคลีออน (ELECTROMAGNETIC FORM FACTORS OF Delta-N
TRANSITION) อาจารย์ที่ปรึกษา : ศาสตราจารย์ ดร.ยูเป้ง แยน, 136 หน้า

คำสำคัญ: ฟอรั่มแฟกเตอร์การเปลี่ยนสถานะเชิงแม่เหล็กไฟฟ้า, ฟิสิกส์ของฮาดรอน

การศึกษาฟอรั่มแฟกเตอร์การเปลี่ยนสถานะทางแม่เหล็กไฟฟ้าทำให้ทราบคุณสมบัติของ
โครงสร้างภายในของฮาดรอน เช่น Δ และ N เป็นต้น ในงานวิจัยนี้ได้ศึกษาฟอรั่มแฟกเตอร์การ
เปลี่ยนสถานะในปฏิกิริยา $\Delta(1232) \rightarrow N\gamma$ โดยใช้ทฤษฎีการรบกวนเชิงไครล์ของแบรีออนและความ
สัมพันธ์การกระจายตัวในการศึกษาที่บริเวณ q^2 ต่ำ เราศึกษาฟอรั่มแฟกเตอร์แบบหลายชั่วของ
Jone-Scadron ในความสัมพันธ์การกระจายแบบลบบอกและแบบไม่ลบบอก ทั้งสามรูปแบบ ดังนี้
 G_M^* , G_E^* และ G_C^* อีกทั้งยังนำผลลัพธ์ทางทฤษฎีของฟอรั่มแฟกเตอร์เชิงแม่เหล็กแบบชั่วคู่ซึ่งเป็น
ฟังก์ชันของ q^2 มาเปรียบเทียบกับข้อมูลการทดลองของเรโซแนนซ์ของแม่เหล็กหลายชั่ว $\text{Im}M^{3/2,+}$
ของการกระเจิง $e^-N \rightarrow e^-\Delta(1232)$ ในบริเวณ $q^2 < 0$

ความสัมพันธ์การกระจายแบบลบบอกถูกใช้มาคำนวณอัตราส่วน $R_{EM} = G_E^*/G_M^*$ และ
 $R_{SM} = G_C^*/G_M^*$ และเปรียบเทียบกับข้อมูลจากการทดลอง เราได้คำนวณความกว้างของการสลาย
ตัวเชิงอนุพันธ์ของกระบวนการสลายตัวแบบสองอนุภาค $\Delta(1232) \rightarrow N\gamma$ และการสลายตัวของ
Dalitz $\Delta(1232) \rightarrow Ne^+e^-$ ด้วยทฤษฎีควอนตัมสนามแบบมาตรฐานและในรูปของฟอรั่มแฟกเตอร์
สำหรับสามอนุภาคของ Jone-Scadron อีกทั้งยังคำนวณภาคตัดขวางเชิงอนุพันธ์ของการกระเจิงของ
 $e^+e^- \rightarrow \bar{\Delta}(1232)N$ ในบริเวณ $q^2 > 0$

สาขาวิชาฟิสิกส์
ปีการศึกษา 2566

ลายมือชื่อนักศึกษา 
ลายมือชื่ออาจารย์ที่ปรึกษา 
ลายมือชื่ออาจารย์ที่ปรึกษาร่วม 


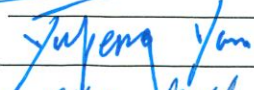

MOH MOH AUNG : ELECTROMAGNETIC FORM FACTORS OF Delta-N
TRANSITION. THESIS ADVISOR : PROF. YUPENG YAN, Ph.D. 136 PP.

Keyword: Electromagnetic transition form factors, Hadron physics

The investigation of electromagnetic transition form factors provides the intrinsic structural properties of hadrons such as Δ and N . In our work, the transition form factors in the $\Delta(1232) \rightarrow N\gamma$ reaction are studied in the combination of baryon chiral perturbation theory and dispersion relations at low q^2 regions. We explore the three Jone-Scadron multipole form factors G_M^* , G_E^* and G_C^* in the unsubtracted and subtracted dispersion relations. The q^2 -dependence of our theoretical results of magnetic dipole form factors is compared with the experimental data on the resonant multipole $\text{Im}M_{1+}^{3/2}$ of the $e^-N \rightarrow e^-\Delta(1232)$ scattering in the space-like $q^2 < 0$ region.

The two ratios $R_{EM} = G_E^*/G_M^*$ and $R_{SM} = G_C^*/G_M^*$ are fitted to the data in the subtracted dispersion relations. After fitting the transition form factors of subtracted method, we have calculated the differential decay width of the two-body decay process $\Delta(1232) \rightarrow N\gamma$ and Dalitz decay $\Delta(1232) \rightarrow Ne^+e^-$ in the standard quantum field theory as well as in terms of three Jone-Scadron form factors. The differential cross-section of the $e^+e^- \rightarrow \bar{\Delta}(1232)N$ scattering is calculated in the time-like $q^2 > 0$ regions.

School of Physics
Academic Year 2023

Student's Signature 
Advisor's Signature 
Co-Advisor's Signature 

ACKNOWLEDGEMENTS

I would like to express my deepest gratitude to my role model teachers: Prof. Dr. Yupeng Yan, the thesis advisor, and Prof. Dr. Stefan Leupold, the thesis co-advisor, for their super-patient guidance during my entire Ph.D. studying life. They have not only shared physics knowledge but also their life experiences, providing me with a great chance to study at Suranaree University of Technology and Uppsala University. They trusted me in all conditions, protected me kindly, and offered unwavering support. There are no words to adequately express my gratitude to my teachers. Without their excellent supervision and guidance, I could not have advanced so far in my Ph.D. studies.

When I started this Ph.D. journey at the School of Physics, SUT, everything was new, including fundamental knowledge of theoretical physics. Prof. Dr. Yupeng Yan diligently taught and trained me before my departure to Uppsala University, Sweden. His comments and suggestions during my thesis work were invaluable. Additionally, I appreciate their continuous support, assistance in participating in conferences, and helping me whenever needed. Special thanks to Pee Yanling Hua for very delicious meals. Prof. Dr. Yupeng Yan is truly deserving of immense thanks.

I am immensely grateful to my co-supervisor, Prof. Dr. Stefan Leupold, for visiting SUT before my departure to Uppsala. I extend my great thanks to Stefan for his lectures on QCD and EFT before I began my thesis, sharing his knowledge about hadron physics, and offering assistance whenever needed. I appreciate his efforts to motivate and guide me, always simplifying complex points. I also want to acknowledge the warmth and generosity of Stefan and Sabrina, making their home feel like my second home. I will always cherish the memories of delicious meals and the insightful advice from Sabrina. Stefan, you truly deserve a huge thanks as my role model teacher.

I extend a huge thanks to the scholarship organizations under the Thai-Swedish Trilateral Development Cooperation Programme. My heartfelt gratitude goes to TICA, TSRI, NRCT from the RGJ Program, and CoE for their financial support during my studies at Suranaree University of Technology. Special thanks to Ms.

Chachsaran Lertkiattiwong from TICA for her warm welcome and assistance on my first day in Bangkok. I also appreciate the support from Sida and ISP during my studies at Uppsala University. Thanks to Carla Puglia, Ulrika Kolsmyr, and all people from ISP for their warm welcome and support. Thanks Ulrika a lot for picking me up on my first day in Sweden and the unforgettable Fika times.

I express my gratitude to the steering committee of my thesis, with Assoc. Prof. Dr. Daris Samart as the chairperson, and committee members Prof. Dr. Yupeng Yan, Prof. Dr. Stefan Leupold, Assoc. Prof. Dr. Ayut Limphirat, and Asst. Prof. Dr. Khanchai Khosonthongkee, for their patient support in both the thesis proposal and final defense.

I appreciate our theoretical physics group, including seniors, teachers, and staff at Suranaree University of Technology and Uppsala University. Special thanks to Dr. Elisabetta Perotti, Dr. Kai Xu, Dr. Attaphon Kaewsnod, Dr. Thanat Sangkhakrit, and Dr. Zhao Zheng for their suggestions, discussions, cross-checking calculations, knowledge sharing, and assistance in my proposal writing.

I extend my thanks to Prof. Dr. Khin Swe Myint, Assoc. Prof. Dr. Khin Mar Win from Mandalay University and Prof. Dr. Khin Maung Maung from the University of Southern Mississippi for their help and encouragement in applying for the scholarship. I am profoundly grateful to all my teachers who have guided me throughout my PhD study.

Many thanks to my international and local friends for their help whenever needed. Special thanks to my younger sister and brother, Miss KyalCynn Lin and Mr. Aung Hein Kyaw for always taking care of me when I was sick. I also appreciate the support from spiritual mentor Sister Arabelle Yee for her courses on self-awareness.

My deepest gratitude goes to my beloved family for their support throughout my entire life. To my lovely dad and mom, Mr. Myint Swe and Mrs. Tin Yee, I am proud to be your daughter. Thanks for your incredible care, nourishment, and support in education and health. I wish you both continued health and happiness. Thanks to my younger brother, Mr. Ye Yint Thu, for his support, and my little brother, Mr. Htet Wai Yan, for his kindness.

In conclusion, I express my appreciation and gratitude to every person who deserves thanks during my long educational journey in Myanmar, Thailand, and Sweden. It will serve as a reminder to help me maintain a balanced life in

the future. I wish to close by sharing one of the Arab proverbs “Everything that happens once can never happen again. But everything that happens twice will surely happen a third time” for every believer in their life journey.

Moh Moh Aung



CONTENTS

	Page
ABSTRACT IN THAI	I
ABSTRACT IN ENGLISH	II
ACKNOWLEDGEMENTS	III
CONTENTS	V
LIST OF TABLES	VII
LIST OF FIGURES	VIII
LIST OF ABBREVIATIONS	XI
 CHAPTER	
I INTRODUCTION	1
II CUTTING RULES OF DISPERSIVE FRAMEWORK	7
2.1 Cutkosky theorem to dispersive integrals	7
2.2 Cutkosky's cutting rules to optical theorem	10
2.3 Scalar direct loop calculation	13
2.4 Analytic properties of the unitarity discontinuity	16
2.5 Dispersive expansions to anomalous discontinuity	20
III DISPERSIVE REPRESENTATION TO TRANSITION FORM FACTORS	25
3.1 Dispersion relations for the transition form factors	25
3.1.1 Unsubtracted dispersion relations	26
3.1.2 Subtracted dispersion relations	28
3.2 Jone-Scadron form factors	28
3.3 Pion-baryon scattering amplitude $T_m(s)$	33
3.4 Omnès function and pion p-wave phase shift	39
IV HELICITY AMPLITUDES OF PROJECTION FORMALISM	43
4.1 Baryon chiral perturbation theory	43
4.2 Feynman amplitude of the scattering process $\Delta^0 \bar{N} \rightarrow \pi^+ \pi^-$	48
4.3 Projection formalism	50
4.4 Helicity amplitudes	53
V DIFFERENTIAL DALITZ DECAY OF BARYONS	56
5.1 Decay width of Dalitz decay $\Delta^0 \rightarrow N e^+ e^-$	56

CONTENTS (Continued)

	Page
5.2 Decay width of two-body decay $\Delta^0 \rightarrow N\gamma$	68
5.3 Differential cross section of $e^+e^- \rightarrow \bar{\Delta}^0 N$ scattering	70
VI RESULTS AND DISCUSSIONS	76
6.1 Results of unsubtracted dispersion relation	76
6.2 Results of subtracted dispersion relation	78
6.3 Results of Dalitz decay	82
VII CONCLUSIONS	84
REFERENCES	85
APPENDICES	
APPENDIX A DERIVATION OF SCALAR ONE-LOOP FUNCTION	96
APPENDIX B STEPS OF DELTA FUNCTION	104
APPENDIX C DERIVATION OF JONE-SCADRON FORM FACTORS	105
APPENDIX D COEFFICIENT FUNCTIONS	115
APPENDIX E VECTOR SPINORS	119
APPENDIX F SOLUTION OF OMNÈS FUNCTION	121
APPENDIX G DERIVATION OF TWO BODY PHASE-SPACE	123
APPENDIX H DERIVATION OF THREE BODY PHASE-SPACE	126
CURRICULUM VITAE	136

LIST OF TABLES

Table		Page
6.1	c_F , $G_m(0)$ and $G_M^*(0)$ determined in the unsubtracted dispersion relation with cutoff $\Lambda=2$ GeV.	77
6.2	Polynomial constants P_M^* determined in the unsubtracted dispersion relation for different c_F	77
6.3	The values of the magnetic, electric and charge form factors at the real photon point in subtracted dispersion relation. . . .	78
6.4	Jones-Scadron form factors G_M^* , G_E^* , G_C^* at the photon point with the cutoff $\Lambda=1$ GeV and $\Lambda=2$ GeV. Here $h_A=2.67$ and $H_A=2.27$	78
6.5	Jones-Scadron form factors G_M^* , G_E^* , G_C^* and corresponding radii with different h_A , H_A at the cutoff $\Lambda=2$ GeV.	80
6.6	Comparison of the two parameters A and B in the QED approximation and our calculation in $\Delta^0 \rightarrow Ne^+e^-$ Dalitz decay. . .	82

LIST OF FIGURES

Figure		Page
1.1	Schematic diagrams of the space-like ($q^2 < 0$) and time-like ($q^2 > 0$) form factors in different regions.	1
1.2	The Q^2 -dependance of $N\Delta(1232)$ transition FFs for the magnetic dipole $\text{Im}M_{1+}^{3/2}$, the electric quadrupole ratio R_{EM} and the Coulomb quadrupole ratio R_{SM} . The data are taken from: BATES (blue squares) (Sparveris et al., 2005), MAMI (red circles) (Beck et al., 2000; Stave et al., 2006; Sparveris et al., 2007), JLab/Hall C (open circles) (Frolov et al., 1999), JLab/CLAS (black squares) (Joo et al., 2002) and inverted triangles (Ungaro et al., 2006), and JLab/Hall A (blue stars) (Kelly et al., 2005).	3
2.1	Schematic diagram of the contour integral on the branch curve Γ we defined in the relation Eq. (2.1).	8
2.2	Sketch of the optical theorem.	12
2.3	Graphic representation of one-loop triangle diagram with the p and Δ exchanged in the two-pion intermediate approximation.	12
2.4	Schematic one-loop Feynman diagram. The internal masses are m_1 for the momentum q , m_2 for the momentum $q + p_1$, etc..	14
2.5	Schematic diagram of the scalar three point triangle function with p_1 and p_2 for incoming momenta, m_π for two internal pions, and m_{ex} for an exchanged baryon.	15
2.6	Sketch of the unitarity cut along the two internal pions lines.	17
2.7	One-loop triangle contribution diagram of the anomalous threshold cut and the unitarity cut of the $\Delta - N$ TFFs.	20
2.8	Graphic representation of a new integration contour in the complex plane. The trajectory of unitarity cut along the real axis is shown in blue line and the path of branch point through the anomalous threshold cut onto the physical sheet is shown in red.	21

LIST OF FIGURES (Continued)

Figure		Page
3.1	Sketch of the Feynman diagram of $\Delta^0 \bar{n}$ interaction in the Lowest order approximation (red blob), including the $\pi\pi$ rescattering consideration (gray blob).	34
3.2	Parametrization results of the pion p-wave phase shift in line with (3.58) at the specific range, $0 < s(\text{GeV}^2) < 1.4$. In the plot, we start the energy range from 0 GeV^2 instead of starting at $4m_\pi^2 \text{ GeV}^2$	41
3.3	Real and imaginary part of the Omnès function as parameterized in the pion p-wave phase shift at a given physical range, $0 < s(\text{GeV}^2) < 1.4$	42
3.4	The absolute parameterization result of Omnès function in the range, $0 < s(\text{GeV}^2) < 1.4$. All the parameterization results are similar to the works of (Garcia-Martin et al., 2011; Hanhart, 2012).	42
4.1	Feynman diagrams for the scattering process $\Delta^0 \bar{n} \rightarrow \pi^+ \pi^-$	48
5.1	Sketch of Feynman of Dalitz decay $\Delta^0 \rightarrow N e^+ e^-$ with respect to the one-photon approximation. Here, the baryon vertex is represented by a gray blob and the QED vertex is denoted with $e^- e^+ \gamma$	61
5.2	Graphic representation of the Dalitz decay $\Delta^0 \rightarrow N e^- e^+$ in the C-M frame.	61
5.3	Sketch of Feynman diagram for the two-body decay $\Delta^0 \rightarrow N \gamma$	68
5.4	Sketch of Feynman diagram for the 2 to 2 scattering $e^- e^+ \rightarrow \bar{\Delta}^0 N$	70
6.1	Magnetic dipole form factor G_M^* , electric quadrupole form factor G_E^* and Coulomb quadrupole form factor G_C^* in the region, $-0.7 \ll q^2(\text{GeV}^2) \ll (m_\Delta - m_n)^2$. The polynomial constants are fixed to be $P_M^* = 406.12 \text{ GeV}^{-2}$, $P_E^* = 10.24 \text{ GeV}^{-2}$ and $P_C^* = 122.89 \text{ GeV}^{-2}$. The cutoff $\Lambda = 2 \text{ GeV}$	79

LIST OF FIGURES (Continued)

Figure		Page
6.2	Q^2 -dependence of $\text{Im}M_{1+}^{3/2}$, R_{EM} and R_{SM} . Red dot-dashed curve shows the results for the central parameters h_A and H_A , the magenta and green color lines show the results with h_A varied by $\pm 10\%$, and the orange and brown lines for the results with H_A varied by $\pm 10\%$. Data are taken from BATES (blue color) (Sparveris et al., 2005), MAMI (red color) (Sparveris et al., 2007; Stave et al., 2006), and CLAS (black color) (Aznauryan et al., 2009).	81
6.3	Single-differential decay width of the $\Delta^0 \rightarrow Ne^+e^-$ Dalitz decay in comparison with the QED-type approximation in the range, $4m_e^2 \leq q^2 (\text{GeV}^2) \leq (m_\Delta - m_n)^2$. The green line represents the results we calculated using the model parameters fixed in subtracted dispersion relation and red line represents the QED analogue results.	83
A.1	Two integral triangle boundaries in the step Eq. (A.22).	101

LIST OF ABBREVIATIONS

eTFFs	electromagnetic Transition Form Factors
LEGS	Laser Electron Gamma Source
BATES	Bates Linear Accelerator Center
ELSA	ELectron Stretcher Accelerator
MAMI	Mainz Microtron
CLAS	CEBAF Large Acceptance Spectrometer
Jlab	Jefferson Laboratory
HADES	High heAt load tESt
QCD	Quantum Chromodynamics
QED	Quantum Electrodynamics
EFT	Effective Field Theory
Im	Imaginary
Re	Real
disc	Discontinuous
CM	Center of Mass
MO	Muskhelishvili Omnès
LO	Leading Order
NLO	Next to Leading Order

มหาวิทยาลัยเทคโนโลยีสุรนารี

CHAPTER I

INTRODUCTION

Electromagnetic transition form factors have been studied for decades and have played an important role in revealing the intrinsic structure of hadronic matters, see e.g. (Jones and Scadron, 1973; Cardarelli et al., 1996; Alexandrou et al., 2005; Burkert and Lee, 2004; Pascalutsa et al., 2007; Leupold, 2018; Aznauryan and Burkert, 2012a; Elsner et al., 2006; Stave et al., 2008; Aznauryan et al., 2009; Blomberg et al., 2016; Kaewsnod et al., 2022) and references therein. Form factors, as functions of the four momentum transfer Q^2 , describe the charge and current distributions in momentum space. Among all form factors, the magnetic and electric form factors received most attentions since they supply necessary information on the electroweak hadron structure, and also help us understand electromagnetic and weak interactions of hadrons. The form factors are also experimentally defined in different kinematical regimes with distinct processes (see in Figure 1.1). In the space-like region, the magnetic and electric form factors are accessed by scattering electrons on a fixed target experiment, like $e^- B_1 \rightarrow e^- B_2$. In the time-like region, the form factors are explored via Dalitz decays into a lighter baryon and an electron-positron pair, $B_1 \rightarrow B_2 e^+ e^-$ at low energies and via the electron-positron scattering $e^+ e^- \rightarrow B_1 \bar{B}_2$ at high energies.

The $\Delta(1232)$ resonance, as the lowest spin 3/2 particle, plays a crucial role

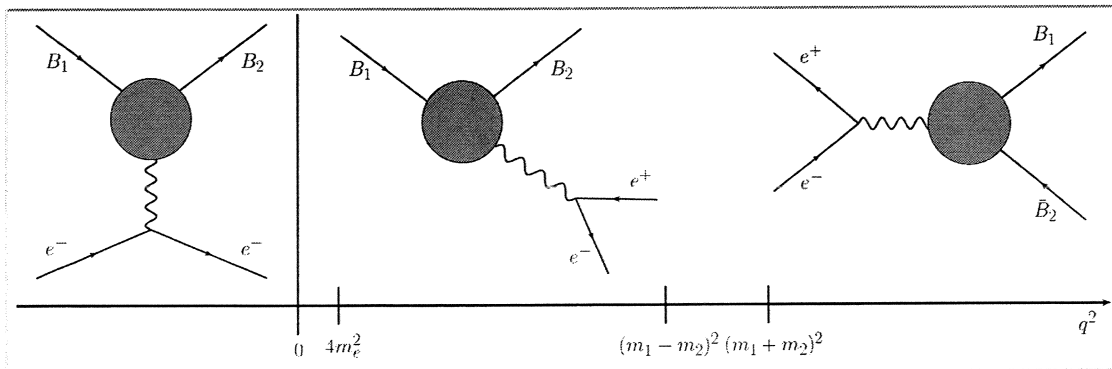


Figure 1.1 Schematic diagrams of the space-like ($q^2 < 0$) and time-like ($q^2 > 0$) form factors in different regions.

in many nuclear processes, i.e, the pion-production threshold (Brown and Weise, 1975), the pion photo- and electro-production and so on. $\Delta(1232)$ electromagnetic properties which mainly are three transition-multipoles: the magnetic dipole $M1(G_M^*)$, the electric quadrupole $E2(G_E^*)$, the coulomb quadrupole $C2(G_C^*)$ and also their ratios $R_{EM} = E2/M1$ and $R_{SM} = C2/M1$ provide valuable information on the quark-quark interaction.

In the recent years, the nucleon $\Delta(1232)$ transition has been well measured in a large Q^2 range by means of electromagnetic probes with the advent of the new generation of electron beam facilities, such as LEGS, BATES, ELSA, MAMI, and Jefferson Lab (Pascalutsa and Vanderhaeghen, 2006). The current experimental data of the $N\Delta(1232)$ transition form factors in the space-like extracted from $e^-N \rightarrow e^-\Delta$ are presented in Figure 1.2 (Pascalutsa et al., 2007; Burkert, 2018). The data are compared to three different models: dashed-dotted curves are the results obtained from Dubna-Mainz-Tapei (DMT) model, the dashed curves are from the Sato-Lee (SL) model and the solid curves are from the dynamical Utrecht-Ohio (DUO) model, see more detailed in (Pascalutsa et al., 2007). The high precision experimental data of $N\Delta(1232)$ transition and the interests in the differential decay rate of the Dalitz decay $\Delta^0 \rightarrow Ne^+e^-$ have inspired us to carry out the present study of the electromagnetic form factors of $N-\Delta(1232)$ transition. The early study of form factors was carried out with QCD in the perturbative QCD regime at high Q^2 (Carlson, 1986). At low Q^2 regions, the pion-cloud was expected to make a sizable contribution to the electromagnetic form factors (Pascalutsa et al., 2007). One may tackle the electromagnetic form factors of $\Delta-N$ transition at low Q^2 region in the chiral perturbation theory (χ PT) which is more or less a model-independent approach for the low-energy QCD (Bissegger and Fuhrer, 2007; Gasser and Leutwyler, 1984; Scherer, 2003; Scherer and Schindler, 2012c) together with the dispersion theory which relates the pion vector form factor to the low-energy electromagnetic transition form factors (Frazer and Fulco, 1960; Hohler et al., 1976; Mergell et al., 1996; Hoferichter et al., 2016a).

There are several theoretical frameworks to describe the $N-\Delta$ transition. In the 1980's, perturbative QCD was used to study the electromagnetic $N-\Delta$ transition at high Q^2 where the helicity of the hadrons is conserved (Carlson, 1986). The electromagnetic $N-\Delta$ transition form factors was investigated in the chiral effective field theory (Davidson et al., 1991; Hanstein et al., 1996; Kalleicher

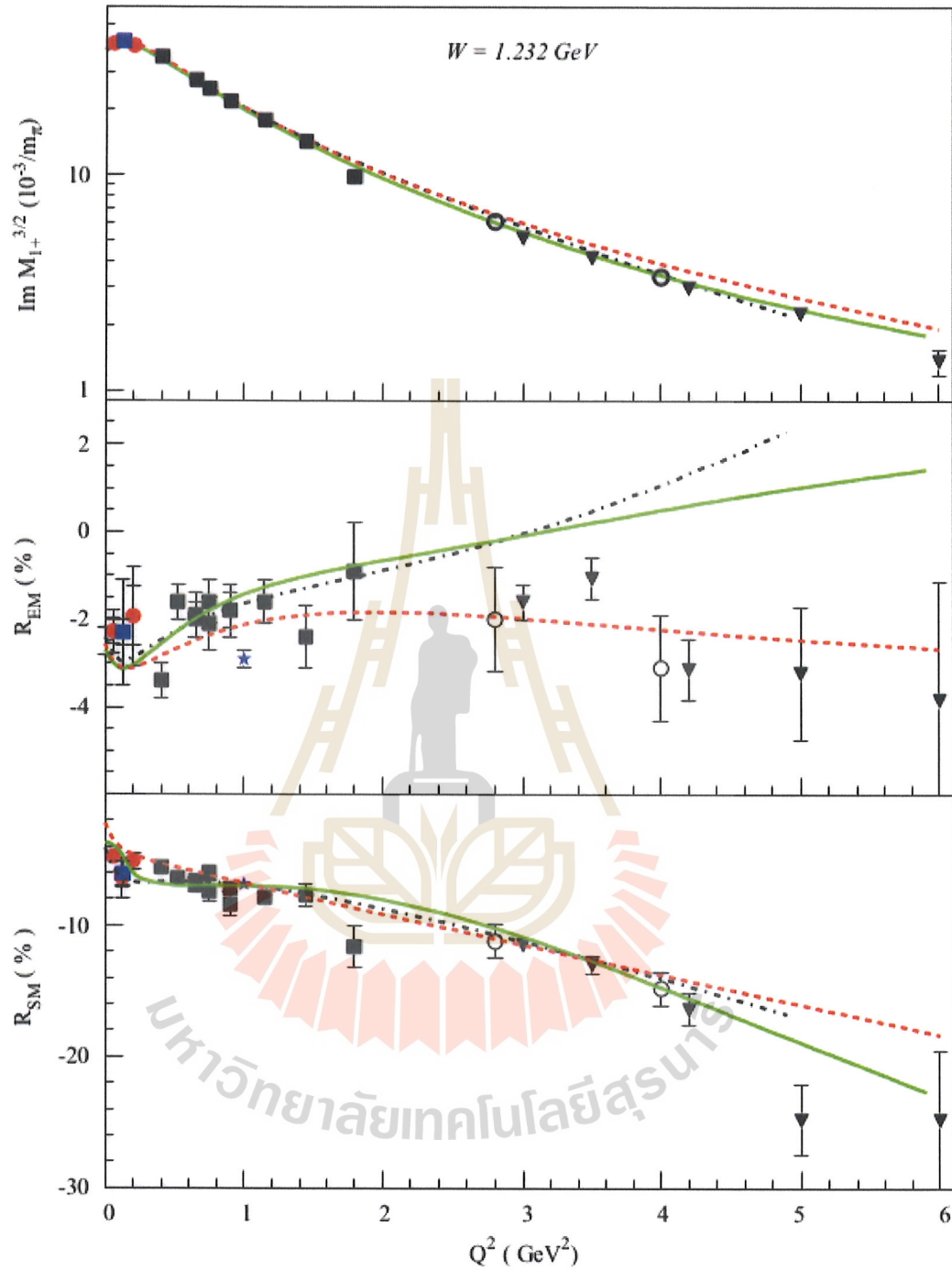


Figure 1.2 The Q^2 -dependance of $N\Delta(1232)$ transition FFs for the magnetic dipole $\text{Im}M_{1+}^{3/2}$, the electric quadrupole ratio R_{EM} and the Coulomb quadrupole ratio R_{SM} . The data are taken from: BATES (blue squares) (Sparveris et al., 2005), MAMI (red circles) (Beck et al., 2000; Stave et al., 2006; Sparveris et al., 2007), JLab/Hall C (open circles) (Frolov et al., 1999), JLab/CLAS (black squares) (Joo et al., 2002) and inverted triangles (Ungaro et al., 2006), and JLab/Hall A (blue stars) (Kelly et al., 2005).

et al., 1997; Gellas et al., 1999), which predicted the Q^2 dependence of the three transition-multipoles: the magnetic dipole $M1(G_M^*)$, the electric quadrupole $E2(G_E^*)$, and the coulomb quadrupole $C2(G_C^*)$, and also their ratios $R_{EM} = EMR = E2/M1$ and $R_{SM} = CMR = C2/M1$ as well. These three form factors are also named as Jones-Scadron form factors which are the main physical observables in this work.

The behavior of the quadrupole amplitudes at low photon virtualities Q^2 and the ratios of the $E2/M1$ and $C2/M1$ of the multipole amplitudes for electroproduction of the $\Delta(1232)$ were also calculated in the chiral chromodielectric model and linear σ model (Fiolhais et al., 1996). In addition, the helicity amplitudes $A_{1/2}$ and $A_{3/2}$ were reasonably well-reproduced except for the low Q^2 regions. The helicity amplitudes $A_{1/2}$ and $A_{3/2}$ of the $\gamma^*N \rightarrow \Delta$ transition were also evaluated in the perturbative chiral quark model (Pumsa-ard et al., 2003) which gave rather good fitting to the experimental data by including the meson cloud contribution. In particular, the meson cloud effects were found to be quite important in not only the $\gamma^*N \rightarrow \Delta$ transition (Dong et al., 2001; Ledwig et al., 2012) but also other cases, for example, the weak pion production reactions and the Roper resonance (Sato and Lee, 2001).

With the spectator quark model, the electromagnetic form factors for the $\Delta \rightarrow N\gamma^*$ were related to Dalitz decay $\Delta \rightarrow Ne^+e^-$ in the timelike region, and the Q^2 dependence of the form factors and partial width decays widths of these processes were estimated (Ramalho and Pena, 2009; Ramalho and Pena, 2012). The quark core contribution to electroexcitation amplitudes of the resonances $\Delta(1232)$ and $N(1440)$ was predicted in the light-front relativistic quark model (Aznauryan and Burkert, 2012b). The pion-cloud contribution might again play an important role in the magnetic and electric FFs at very small Q^2 , while at high Q^2 this contribution was negligible. The Q^2 dependence for the $\gamma^*N \rightarrow \Delta(1232)$ transitions up to virtuality $Q^2 = 12 \text{ GeV}^2$ was later evaluated within the approach of light-front relativistic quark model (Aznauryan and Burkert, 2015), only at the $Q^2 < 4 \text{ GeV}^2$ region the magnetic dipole FFs and the ratios R_{EM} , and R_{SM} fitted well to the experiment data.

The dispersion theory (Frazer and Fulco, 1960; Hohler et al., 1976; Mergell et al., 1996; Hoferichter et al., 2016a) was developed to relate the lightest hadronic state that couples to electromagnetism. Using the dispersion theory, the low-energy electromagnetic form factors of the nucleon are related to the pion vector form factor (Leupold, 2018). The pion-nucleon scattering amplitudes were determined by

relativistic NLO chiral perturbation theory including the nucleons and optionally the Δ resonances. The pion rescattering was considered by solving the Muskhelishvili-Omnès (MO) equation (Granados et al., 2017) and using N/D (Alarcón et al., 2017) approach. A fully dispersive calculation of the pion-nucleon amplitudes based on Roy-Steiner (RS) equation (Hoferichter et al., 2016b) has shown us that the inclusion of Δ resonances was necessary to obtain reasonable results. And the method has been applied to the electromagnetic form factors of the transition from the spin-3/2 Σ to the ground-state Λ in the Uppsala group very recently (Junker et al., 2020), to predict the form factors in the hyperon sector (Granados et al., 2017; Alarcón et al., 2017), as well as the Δ - n TFFs (purely isovector form factors) (Leupold, 2018). In the magnetic sector of the nucleon Δ transition, the combination of the dispersion relation theory and χ PT at NLO works very well (Leupold, 2018).

In this thesis, we derive the electromagnetic Δ to nucleon transition in the dispersion theory and chiral perturbation theory (χ PT) at the low Q^2 regions. The differential decay rate of two-body $\Delta^0 \rightarrow N\gamma$, the Dalitz decay $\Delta^0 \rightarrow Ne^+e^-$ are calculated in the one-photon approximation. The radii of the magnetic, electric and Coulomb form factors are determined in the time-like regions as well. Finally, we calculate the differential cross-section of $e^+e^- \rightarrow \bar{\Delta}^0 N$ scattering within the framework of the quantum field theory to complete the whole time-like $q^2 > 0$ at the kinematic diagram of 1.1. All theoretical outcoming values are well fitted to the experimental data up to the energy range $Q^2 = 0.7 \text{ GeV}^2$.

The thesis is organized as follows. In Chapter II, we present and discuss how the anomalous cut structure of the scalar triangle diagram is relative to the dispersive representation according to the fundamental Cutkosky's cutting rules and principles. The technical ways of special attention such as the optical theorem in the language of dispersion theory approach for eTFFs are described in Chapter II. The main part of the thesis works including the technical developments of how the Jone-Scadron form factors relate to our transition form factors are mentioned in Chapter III. The interest of all input sources of projection formalism through Feynman matrix elements for $\Delta^0 \bar{N} \rightarrow \pi^+ \pi^-$ interaction and the corresponding helicity amplitudes are presented in Chapter IV. Chapter V contains a main computation for the differential cross section of $e^+e^- \rightarrow \bar{\Delta}^0 N$ reaction in addition to the predictions of differential decay width of decay $\Delta^0 \rightarrow N\gamma \rightarrow Ne^+e^-$ in the similar direction of time-like Q^2 regions. Our theoretical results of the multipole form factors for the

interaction $\Delta \rightarrow N\gamma$ in comparison with the experimental data are also mentioned describing both options of the present work in Chapter VI. Numerical results of the radii of TFFs, the decay width of two-body $\Delta \rightarrow N\gamma$ and Dalitz decay $\Delta^0 \rightarrow Ne^+e^-$ are provided in the same Chapter VI. The conclusions and outlooks are finally summarized in Chapter VII.



CHAPTER II

CUTTING RULES OF DISPERSIVE FRAMEWORK

In the present chapter, we describe systematically a basic framework for the Cutkosky's cutting rules which are applied to the expansion of the dispersion technique. Then we address in general analytic functions relative to the dispersion relations and also the analytic cut structure of the scalar triangle diagram. And the proof of analytic properties of the discontinuity is described for the dispersive representation. In the end, we will see the simplest form of the dispersive framework that is very important for calculating $\Delta-N$ TFFs in the thesis.

2.1 Cutkosky theorem to dispersive integrals

We start from the Cauchy integral

$$f(z) = \frac{1}{2\pi i} \oint_{\Gamma} dz' \frac{f(z')}{z' - z}. \quad (2.1)$$

where $f(z)$ is analytical inside the contour Γ , and the contour of $\Gamma = \Gamma_1 + \Gamma_R + \Gamma_2 + \Gamma_\epsilon$ does not cross any singularity, as shown in Figure 2.1. Assuming that the integral holds at the boundaries $\Gamma_R \rightarrow 0$ and $\Gamma_\epsilon \rightarrow 0$ as $R \rightarrow \infty$ and $\epsilon \rightarrow 0$, we may rewrite the relation of Eq. (2.1) as the sum of two integrals separately,

$$f(z) = \frac{1}{2\pi i} \left(\int_0^\infty dz' \frac{f(z' + i\epsilon)}{z' - z} + \int_\infty^0 dz' \frac{f(z' - i\epsilon)}{z' - z} \right), \quad (2.2)$$

$$f(z) = \frac{1}{2\pi i} \int_0^\infty dz' \frac{\text{disc} f(z')}{z' - z}.$$

For very point on the real axis, the function f also satisfies the Schwarz's reflection principle (Zwicky, 2017), that is,

$$f(z + i\epsilon) = f(z - i\epsilon), \quad (2.3)$$

$$\text{Re} f(z + i\epsilon) = \text{Re} f(z - i\epsilon),$$

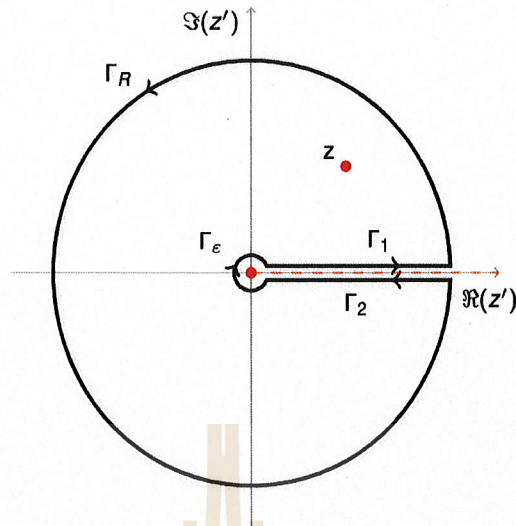


Figure 2.1 Schematic diagram of the contour integral on the branch curve Γ we defined in the relation Eq. (2.1).

$$\text{Im} f(z + i\epsilon) = -\text{Im} f(z - i\epsilon). \quad (2.4)$$

Then we have the discontinuities function related to the imaginary part along the branch cut by

$$\text{disc} f(z) = f(z + i\epsilon) - f(z - i\epsilon) = 2i \text{Im} f(z + i\epsilon). \quad (2.5)$$

and then

$$f(z) = \frac{1}{\pi} \int_0^\infty dz' \frac{\text{Im} f(z')}{z' - z}. \quad (2.6)$$

It is well known as the formal dispersion relation, where an integral expression constitutes both real and imaginary parts of the analytic continuation of the function $f(z)$. Note, however, that there are functions, where the boundary integral along Γ_R does not vanish when $R \rightarrow \infty$. One may make the well-known dispersion representation above converge when $z \rightarrow \infty$ by using the derivative of the function $f(z)$,

$$f'(z) = \frac{1}{2\pi i} \int_{z_0}^\infty dz' \frac{\text{disc} f'(z')}{z' - z}, \quad (2.7)$$

$$f'(z) = \frac{1}{2\pi i} \left[\frac{\text{disc} f(z)}{z' - z} \Big|_{z_0}^{\infty} + \int_{z_0}^{\infty} dz' \frac{\text{disc} f(z')}{(z' - z)^2} \right]. \quad (2.8)$$

The lowest threshold state z_0 is indeed $4m_\pi^2$ in our dispersion integral of transition form factors evaluation. Assuming the first integral term drops out at the boundaries, then integrating over both sides of the above equation leads to

$$\begin{aligned} \int_{z_1}^{z_2} dz f'(z) &= \frac{1}{2\pi i} \int_{z_1}^{z_2} dz \int_{z_0}^{\infty} dz' \frac{\text{disc} f(z')}{(z' - z)^2}, \\ f(z_2) - f(z_1) &= \frac{1}{2\pi i} \int_{z_0}^{\infty} dz' \left[\frac{\text{disc} f(z')}{(z' - z)} \right]_{z_1}^{z_2}, \\ f(z_2) &= f(z_1) + \frac{1}{2\pi i} \int_{z_0}^{\infty} dz' \left[\frac{\text{disc} f(z')}{(z' - z_2)} - \frac{\text{disc} f(z')}{(z' - z_1)} \right], \\ f(z) &= f(z_1) + \frac{(z - z_1)}{2\pi i} \int_{z_0}^{\infty} dz' \frac{\text{disc} f(z')}{(z' - z)(z' - z_1)}. \end{aligned} \quad (2.9)$$

This is the so-called once-subtracted dispersion relation. The first subtraction constant parameter, $f(z_1)$ shall be taken from the experiment directly since there is no capability for the dispersive method to deal with the high energy physics yet. The convergence of the second term is improved due to the contribution of the extra factor $\frac{1}{z' - z_1}$. The subtraction procedure can be carried out repeatedly, resulting more free parameters. For a general n -power case, we can formulate the subtracted dispersion relation based on the derivative of $f(z)$ in a cut plane with the branch point z_1 as:

$$\begin{aligned} f(z) &= f(z_1) + \sum_{i=1}^{n-1} B_i (z - z_1)^i + \frac{(z - z_1)^n}{2\pi i} \int_{Br} dz' \frac{\text{disc} f(z')}{(z' - z)(z' - z_1)^n}, \\ f(z) &= f(z_1) + \sum_{i=1}^{n-1} B_i (z - z_1)^i + \frac{(z - z_1)^n}{\pi} \int_{Br} dz' \frac{\text{Im} f(z')}{(z' - z)(z' - z_1)^n}, \end{aligned} \quad (2.10)$$

The model independent parameters B_i are to be determined experimentally.

2.2 Cutkosky's cutting rules to optical theorem

Introducing the Cutkosky cutting rules in this section aims to identify the imaginary part of the full amplitude when the internal propagators are compatible with the on-shell condition $s = q^2$.

The integration resulted from Feynman diagram of L -loop of momenta $k_i (i = 1, \dots, L)$, N propagators, external momenta p_i may have a form,

$$I = \int Dk \frac{1}{\prod_{i=1}^N (q_i^2 - m_i^2 + i\varepsilon)}, \quad \text{with} \quad Dk = \prod_{i=1}^L d^4 k_i. \quad (2.11)$$

where $q_i = q_i(p_j, k_l)$ are the momenta of the propagators. Here, we are not going to deal with problems far away from the on-shell contribution since there is no imaginary part in the amplitude if $i\varepsilon = 0$ in the propagators. In (Cutkosky, 1960), Cutkosky has proven rigorously that the imaginary part can be computed by carrying out all possible cuts to propagators, which lead to on-shell processes. We have (Zwicky, 2017),

$$\text{disc}(I) = \sum_{\text{all possible cuts}} \int (-2\pi i) Dk \frac{\prod_{i=1}^n \delta_+(q_i^2 - m_i^2)}{\prod_{j=1}^M (q_j^2 - m_j^2 + i\varepsilon)} = 2i \text{Im}(I). \quad (2.12)$$

where the sum is over all possible cuts to the propagators $i = 1, \dots, n < M$, leading to on-shell processes, and we have applied the rules,

$$\begin{aligned} \frac{1}{q_i^2 - m_i^2 + i\varepsilon} &\rightarrow -2\pi i \delta_+(q_i^2 - m_i^2), \quad \text{and} \\ \frac{1}{q_j^2 - m_j^2 + i\varepsilon} &\rightarrow \frac{1}{q_j^2 - m_j^2 + i\varepsilon} \quad \text{for } j = n+1, \dots, M, \end{aligned} \quad (2.13)$$

with the substitution of positive delta functions, $\delta^{(+)}(q_i^2 - m_i^2) = \delta(q_i^2 - m_i^2) \Theta(q_0)$ to assure the correct energy following through the external momentum in the diagram.

It is straightforward to derive the optical theorem by considering the unitarity of S-matrix,

$$\mathbb{1} = SS^\dagger = \mathbb{1} + i \underbrace{(T - T^\dagger)}_{-2\text{Im}[T]} + |T|^2, \quad (2.14)$$

then

$$2\text{Im}T = |T|^2, \quad (2.15)$$

$$\text{Im}T_{A \rightarrow B} = \frac{1}{2} \sum_X T_{A \rightarrow X} T_{X \rightarrow B}^\dagger,$$

where A and B are symbolized for the initial and final particles, and X refers to all intermediate states. Figure 2.2 shows how the propagators contribute to the unitarity cut of the optical theorem.

In our study of the process $\Delta\bar{n} \rightarrow \gamma$, we consider the lowest order approximation, that is, only two-pion intermediate states included since the lightest hadronic states dominantly contribute to the low energy TFFs. The pions are brought to the on-shell condition for the system $\Delta\bar{n}$ coupled to the real photon, as shown in the triangle diagram, Figure 2.3. For the unitarity cut, the two pions threshold is located at the starting branch point $4m_\pi^2$ along the real positive axis. And the imaginary part of the scattering amplitude can be identified by cutting the triangle diagram in all possible ways with the internal pions propagators according to the cutting rules.

In the particular case of lightest state exchanged, there will be a need to consider the additional anomalous threshold cut in the dispersive approach beside the unitarity cut in the triangle diagram. To be concrete, the dispersive formalism involves more integration whenever an extra threshold produces a new cut at low energies. However, the intermediate state of Δ has occupied a big enough mass, so we can directly imply the unitarity integral for our dispersive representation. The aspects of the vector meson dominance inclusion such as loop diagrams for which the photon couples to the baryons by two pions and how the anomalous cut comes out in the implementation of the dispersion relation are examined with respect to the scalar triangle diagram. The scalar direct loop representation in the next topic is done based on the step-by-step calculation of 't Hooft and Veltman (Phan, 2017).

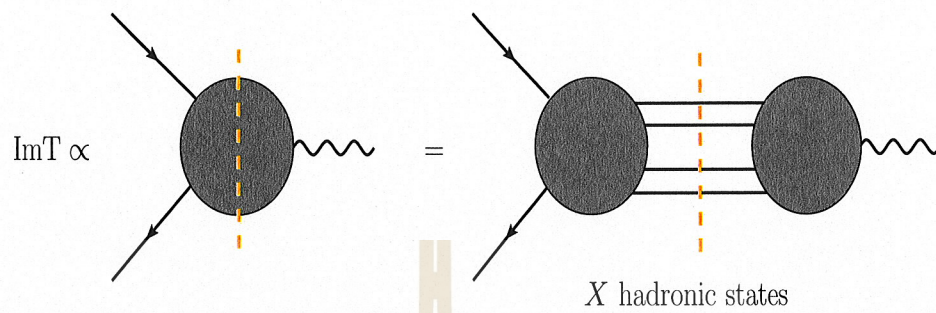


Figure 2.2 Sketch of the optical theorem.

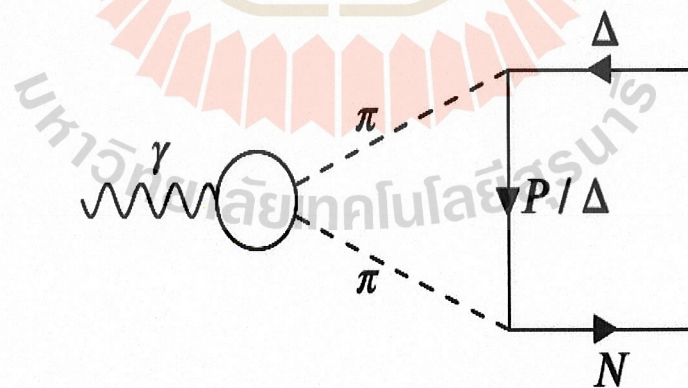


Figure 2.3 Graphic representation of one-loop triangle diagram with the p and Δ exchanged in the two-pion intermediate approximation.

2.3 Scalar direct loop calculation

In this section, we present the scalar three-point function calculation to reveal whether the anomalous threshold cut can be directly connected with the dispersion relations. Applying the Feynman rules to the diagram in Figure 2.4, one may write the scalar one loop n-point function may in the integral,

$$C_n = \int d^4q \frac{1}{(q^2 - m_1^2)((q + p_1)^2 - m_2^2)((q + p_1 + p_2)^2 - m_3^2) \dots}, \quad (2.16)$$

Note that we have omitted the $-i\epsilon$ for every propagators. In our case, we are interested in $\Delta^0 \bar{n} \rightarrow \pi^+ \pi^-$ couple to the photon with the exchanged particles either p or Δ , as shown in Figure 2.5, where the mass of the exchanged state is denoted by m_{ex} and internal two-pion lines are labeled m_π . There are also five variable functions, i.e the external momenta $p_1, p_2, (p_1 + p_2)^2 = s, p_1^2 = m_\Delta^2$ and $p_2^2 = m_n^2$ in the three-point integral representation. We have

$$C_3(s) = \frac{1}{i\pi^2} \int d^4q \frac{1}{(q^2 - m_{ex}^2)((q + p_1)^2 - m_\pi^2)((q - p_2^2 - m_\pi^2)}, \quad (2.17)$$

where $\frac{1}{i\pi^2}$ is a constant for later convenience. By applying Feynman parametrization,

$$\frac{1}{B_1 B_2 \dots B_n} = \int_0^1 dx_1 \dots dx_n (n-1)! \frac{\delta(1 - \sum_{i=1}^n x_i)}{[\sum_{i=1}^n x_i B_i]^n}, \quad (2.18)$$

with the particular identification of each parameters in our case

$$\begin{aligned} B_1 &= ((q - p_2)^2 - m_\pi^2), B_2 = ((q + p_1)^2 - m_\pi^2), \\ B_3 &= (q^2 - m_{ex}^2). \end{aligned} \quad (2.19)$$

we can rewrite the integral in Eq. (2.17) in the form,

$$C_3(s) = \frac{2}{i\pi^2} \int d^4q \int_0^1 dx dy dz \delta(1 - x - y - z) \frac{1}{A^3}, \quad (2.20)$$

with $A = z(q^2 - m_{ex}^2) + y((q + p_1)^2 - m_\pi^2) + x((q - p_2)^2 - m_\pi^2)$, where the mass parameters should be understood as $m_i^2 - i\epsilon$. The integration over x and z , as detailed in

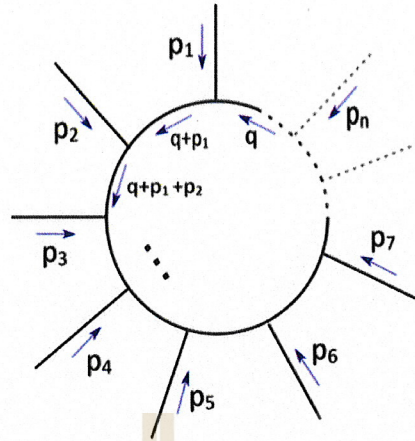


Figure 2.4 Schematic one-loop Feynman diagram. The internal masses are m_1 for the momentum q , m_2 for the momentum $q + p_1$, etc..

Appendix (A), leads to

$$\begin{aligned}
 -C_3(s) = & \int_{-\tau}^{(1-\tau)} dy \frac{1}{P} \log(P + by^2 + ey + f) \\
 & - \int_0^{(1-\tau)} dy \frac{1}{P} \log\left(y \frac{P}{1-\tau} + by^2 + ey + f\right) \\
 & + \int_0^{-\tau} dy \frac{1}{P} \log\left(-y \frac{P}{\tau} + by^2 + ey + f\right).
 \end{aligned} \tag{2.21}$$

One may add one extra term into each integral in the above equation to make the integration convergent when $P(y_0) = 0$. That is

$$\begin{aligned}
 -C_3(s) = & \int_{-\tau}^{(1-\tau)} dy \frac{1}{P} \left(\log(P + by^2 + ey + f) - \log(by_0^2 + ey_0 + f) \right) \\
 & - \int_0^{(1-\tau)} dy \frac{1}{P} \left(\log\left(y \frac{P}{1-\tau} + by^2 + ey + f\right) - \log(by_0^2 + ey_0 + f) \right) \\
 & + \int_0^{-\tau} dy \frac{1}{P} \left(\log\left(-y \frac{P}{\tau} + by^2 + ey + f\right) - \log(by_0^2 + ey_0 + f) \right),
 \end{aligned} \tag{2.22}$$

where the term $y_0 = -(e\tau + d)/(c + 2\tau d)$. If we take into account the component τ as a purely real value, the defining Feynman parameters for the three-point

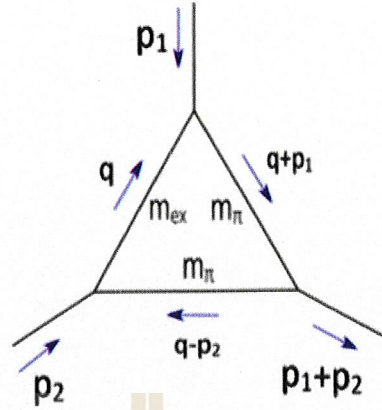


Figure 2.5 Schematic diagram of the scalar three point triangle function with p_1 and p_2 for incoming momenta, m_π for two internal pions, and m_{ex} for an exchanged baryon.

function described in Eq. (A.17) can be used directly in our case. However, it must be noted that the boundaries of the integration are unambiguously defined in the complex space for the argument τ ($\tau \in \mathbb{C}$). By doing the replacements, $y = y' - \tau$, $y = (1 - \tau)y''$ and $y = -\tau y'''$ in the three integrals in Eq. (2.22), respectively, one may simplify the integration boundaries,

$$\begin{aligned}
 -C_3(s) = & \int_0^1 dy \frac{1}{(c + 2\tau b)y + \tau e + d + 2a + c\tau} \\
 & \times (\log(by^2 + (e + c)y + a + d + f) - \log(by_0^2 + ey_0 + f)) \\
 & - \int_0^1 dy \frac{(1 - y)}{(c + 2\tau b)(1 - \tau)y + \tau e + d} \\
 & \times (\log((a + b + c)y^2 + (e + d)y + f) - \log(by_0^2 + ey_0 + f)) \\
 & + \int_0^1 dy \frac{-\tau}{-(c + 2\tau b)\tau y + \tau e + d} \\
 & \times (\log(ay^2 + dy + f) - \log(by_0^2 + ey_0 + f)).
 \end{aligned} \tag{2.23}$$

This function is a standard representation of the scalar loop integration.

2.4 Analytic properties of the unitarity discontinuity

In the following, we calculate the imaginary part of the triangle diagram shown in Figure 2.6 on the Cutkosky cutting rules. When the two pions are on the mass threshold $4m_\pi^2$ on the real axis, the scalar triangle function itself involves an imaginary part of the amplitude, i.e the discontinuous dependence on on-shell condition. If the triangle function is analytic, the integral takes the form,

$$\begin{aligned} \text{disc } C_3(s) = & \frac{1}{i\pi^2} \int d^4q \frac{1}{q^2 - m_{ex}^2} (-2\pi i) \delta((q + p_1)^2 - m_\pi^2) \Theta(q^0 + p_1^0) \\ & (-2\pi i) \delta((q - p_2)^2 - m_\pi^2) \Theta(q^0 - p_2^0). \end{aligned} \quad (2.24)$$

For convenience, we make a shift of integration variables $\hat{q} + \vec{p}_1 \rightarrow \vec{q}$ and work in the center of mass frame, that is, $\vec{p}_1 = -\vec{p}_2$. The above integration becomes,

$$\begin{aligned} \text{disc } C_3(s) = & 4i \int d^4q \frac{1}{q_0^2 - \vec{q}^2 - m_{ex}^2} \delta((q^0 + p_1^0)^2 - |\vec{q}|^2 - m_\pi^2) \Theta(q^0 + p_1^0) \\ & \delta((q^0 - p_2^0)^2 - |\vec{q}|^2 - m_\pi^2) \Theta(q^0 - p_2^0), \end{aligned} \quad (2.25)$$

and then

$$\begin{aligned} \text{disc } C_3(s) = & 4i \int d^4q \frac{1}{q_0^2 - (\vec{q} - \vec{p}_1)^2 - m_{ex}^2} \underbrace{\delta((q^0 + p_1^0)^2 - |\vec{q}|^2 - m_\pi^2)}_{=f(q^0, |\vec{q}|)} \\ & \underbrace{\delta((q^0 - p_2^0)^2 - |\vec{q}|^2 - m_\pi^2)}_{=g(q^0, |\vec{q}|)} \Theta(q^0 + p_1^0) \Theta(q^0 - p_2^0). \end{aligned} \quad (2.26)$$

The above integral includes two delta functions of the two integration variables, so it necessary to write the delta functions into one dimensional functions by applying

$$\delta(f(x)) = \sum_{x_i} \frac{\delta(x - x_i)}{|f'(x_i)|}. \quad (2.27)$$

Assuming that the smooth functions $f(x, y)$ and $g(x, y)$ are differentiable at least once in the interval of integration, we derive the zero points of the two delta

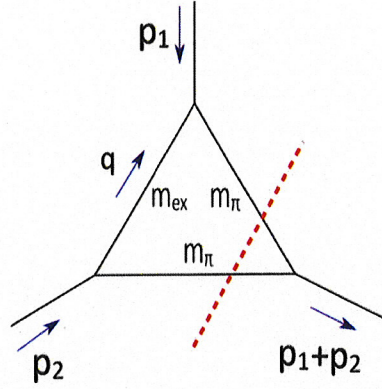


Figure 2.6 Sketch of the unitarity cut along the two internal pions lines.

functions, as shown in the detail in Appendix (B). Substituting all these results into the discontinuity relation of Eq. (2.26), we get

$$\begin{aligned}
 \text{disc } C_3(s) &= \frac{i}{\sqrt{s}|\vec{q}|^*} \int d^4q \frac{1}{q_0^2 - (\vec{q} - \vec{p}_1)^2 - m_{ex}^2} \delta(q^0 - q^{0*}) \delta(|\vec{q}| - |\vec{q}|^*), \\
 &= \frac{i}{\sqrt{s}|\vec{q}|^*} \int |\vec{q}|^2 d|\vec{q}| d\Omega \frac{1}{(q^{0*})^2 - (\vec{q} - \vec{p}_1)^2 - m_{ex}^2} \delta(|\vec{q}| - |\vec{q}|^*), \\
 &= \frac{2\pi i |\vec{q}|^{2*}}{\sqrt{s}|\vec{q}|^*} \int_{-1}^1 d\cos(\theta) \frac{1}{(q^{0*})^2 - |\vec{q}|^{2*} + 2|\vec{q}|^* |\vec{p}_1| \cos(\theta) - |\vec{p}_1|^2 - m_{ex}^2}.
 \end{aligned} \tag{2.28}$$

This allows us to redefine as

$$\begin{aligned}
 \text{disc } C_3(s) &= \frac{-4\pi i |\vec{q}|^*}{\sqrt{s}} \int_{-1}^1 dz \frac{1}{a(s) - b(s)z}, \\
 a(s) &= 2|\vec{q}|^{2*} + 2|\vec{p}_1|^2 + 2(q^{0*})^2 + 2m_{ex}^2, \\
 b(s) &= 4|\vec{q}|^* |\vec{p}_1|^*,
 \end{aligned} \tag{2.29}$$

which gives rise to

$$\text{disc } C_3(s) = \frac{-4\pi i |\vec{q}|^*}{\sqrt{s}} \frac{1}{b(s)} \log \frac{a(s) + b(s)}{a(s) - b(s)}. \tag{2.30}$$

Suppose that the chosen momentum value in the CM frame: $|\vec{p}_1| = |\vec{p}_\Delta| = \frac{\sqrt{\lambda(s, m_\Delta^2, m_n^2)}}{2\sqrt{s}}$,

we rewrite it in a convenient form as follow:

$$\text{disc} C_3(s) = \frac{-2\pi i}{\sqrt{\lambda(s, m_\Delta^2, m_n^2)}} \log \frac{a(s) + b(s)}{a(s) - b(s)} \Theta(s - 4m_\pi^2), \quad (2.31)$$

describing the step Θ -function occurs when the two pion propagators can simultaneously go on-shell. The explicit form of imaginary part which relative to the unitary cut of three point function can be written as:

$$\text{Im} C_3(s) = \frac{-\pi}{\sqrt{\lambda(s, m_\Delta^2, m_n^2)}} \log \frac{a(s) + b(s)}{a(s) - b(s)} \Theta(s - 4m_\pi^2), \quad (2.32)$$

with the components of the logarithm

$$\begin{aligned} a(s) &= s + 2m_{ex}^2 - m_\Delta^2 - m_n^2 - 2m_\pi^2 \equiv Y(s), \\ b(s) &= \sqrt{\lambda(s, m_\Delta^2, m_n^2)} \sqrt{1 - \frac{4m_\pi^2}{s}} \equiv k(s). \end{aligned} \quad (2.33)$$

It is convenient to say that the branch point of the logarithm in the discontinuity is actually laid on the Riemann sheet of the unitarity cut. The anomalous cut associated with the dispersive integral will include all contributions of the complex plane located at the branch point of the Riemann sheet. Notice here that there is no longer contribution for anomalous threshold if a branch point lies on a different Riemann sheet. Consequently, the tracking of the branch points location on the Riemann sheet for the discontinuity has been checked in the Uppsala group. So, we now turn to introduce the different interval points of the logarithm concerned with the discontinuous function on the real axis in order to evaluate the anomalous contribution in the dispersive integral conveniently. They are

$$\begin{aligned} s_{2\pi} &= 4m_\pi^2, \\ s_{dt} &= (m_\Delta - m_n)^2, \\ s_c &= 5m_\pi^2, \\ s_Y &= m_\Delta^2 + m_n^2 + 2m_\pi^2 - 2m_p^2, \end{aligned} \quad (2.34)$$

$$s_{st} = (m_{\Delta} + m_n)^2, \quad (2.35)$$

where $s_{2\pi}$ refers to the two pions threshold, the decay threshold is assigned by s_{dt} , s_c represents for the branch point and s_{th} represents for the scattering region. In line with all these intervals, the unitarity integral of the scalar triangle function is specifically defined as:

$$\text{disc } C_3(s) = 2i \begin{cases} -\pi \frac{\sigma(s)}{k(s)} \left(\log \frac{Y(s)+k(s)}{Y(s)-k(s)} \right) & \text{for } s_{2\pi} < s < s_{dt}, \\ -2\pi \frac{\sigma(s)}{k(s)} \left(\arctan \frac{|k(s)|}{Y(s)} \right) & \text{for } s_{dt} < s < s_c, \\ -2\pi \frac{\sigma(s)}{k(s)} \left(\arctan \frac{|k(s)|}{Y(s)} + \pi \right) & \text{for } s_c < s < s_Y, \\ -2\pi \frac{\sigma(s)}{k(s)} \left(\arctan \frac{|k(s)|}{Y(s)} \right) & \text{for } s_Y < s < s_{st}, \\ -\pi \frac{\sigma(s)}{k(s)} \left(\log \frac{Y(s)+k(s)}{Y(s)-k(s)} \right) & \text{for } s_{st} < s. \end{cases} \quad (2.36)$$

Omitting the Θ -function, the discontinuity on the real axis along the unitarity cut becomes then,

$$\text{disc } C_3(s) = -2\pi i \frac{\sigma(s)}{k(s)} \log \frac{Y(s)+k(s)}{Y(s)-k(s)} = 2i\sigma(s)f(s), \quad (2.37)$$

with $\sigma(s) = \sqrt{1 - \frac{4m_{\pi}^2}{s}}$, $f(s) = -\frac{\pi}{k(s)} \log \frac{k(s)+Y(s)}{k(s)-Y(s)}.$

Later, we will compute the unitarity integration of the scalar triangle diagram together with all these intervals above. What is truly interesting here is that the logarithm of the analytic function $f(s)$ is totally complex around the unitarity cut in the complex domain, so we can quick-check it analytically. There is no pole in the function $f(s)$ when the component of logarithm $k(s)$ is taken to zero at the certain threshold two pions $s = 4m_{\pi}^2$, and therefore $f(s)$ is analytically continuous everywhere in the vicinity of unitarity as a result.

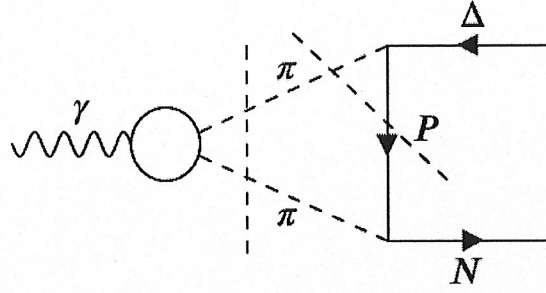


Figure 2.7 One-loop triangle contribution diagram of the anomalous threshold cut and the unitarity cut of the $\Delta-N$ TFFs.

2.5 Dispersive expansions to anomalous discontinuity

We present here the dispersion representations of the unitarity cut with the emphasis on the anomalous contributions for the baryon transition form factors. The anomalous contribution describes the motion of the branch point of the integrand from the unphysical sheet onto the physical sheet (Lucha et al., 2007). Likewise, the anomalous threshold cut will lie on the first Riemann sheet in our case, i.e. physical sheet. In the following, we explain technically how the appearance of the anomalous threshold cut beside the unitarity cut in the three-point triangle diagram as shown in Figure 2.7 based on (Barvinsky and Vilkovisky, 1990; Junker et al., 2020). The mass of the exchange particles m_{ex}^2 caused by lighter baryon state is

$$m_{ex}^2 < \frac{1}{2} (m_{\Delta}^2 + m_n^2 - 2m_{\pi}^2). \quad (2.38)$$

It means that there might be an anomalous threshold cut in case a nucleon is exchanged. Note that for the exchange of heavy baryons like Δ , it does not need a new cut for the dispersion relation. In addition, the amplitude with only the unitarity cut will lead to purely real below the branch point of the threshold on the real positive axis. Suppose that the delta can totally decay into the pion-proton (about 99%) as a particular contribution cut, the discontinuity of the anomalous will lead to the imaginary part of the triangle diagram. Subsequently, it provides to consider one additional anomalous discontinuity in the dispersive integrals of the TFFs. Thus, we need to modify the trajectory of the unitarity and anomalous cut lie on the first Riemann sheet in the complex domain for an analytic function $f(z)$.

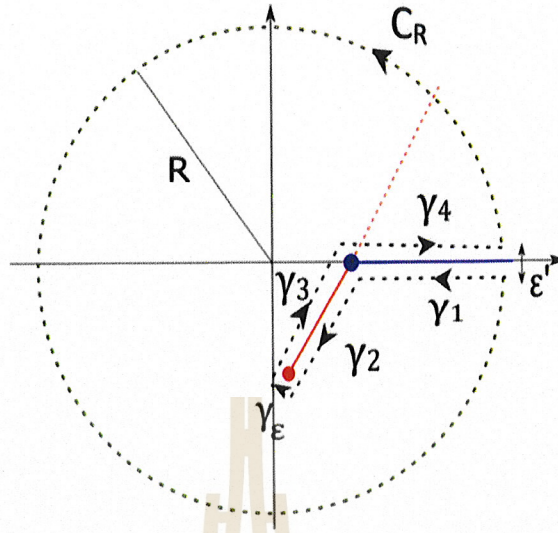


Figure 2.8 Graphic representation of a new integration contour in the complex plane. The trajectory of unitarity cut along the real axis is shown in blue line and the path of branch point through the anomalous threshold cut onto the physical sheet is shown in red.

As shown in Figure 2.8, the blue line on the real axis in the closed contouring represents for the unitarity cut denoted by

$$\gamma_{unit} = [4m_{\pi}^2, \infty), \quad (2.39)$$

and the red line, i.e the so-called the anomalous cut, is parameterized simply as

$$\gamma(x) = s(1-x) + 4m_{\pi}^2 x, \quad (2.40)$$

with $x = [0, 1]$ and s being the branch point of the discontinuity, however, we use slightly different value for the path of branch point $5m_{\pi}^2$ instead of $4m_{\pi}^2$ in reality computation of $\Delta-N$ case. As a consequence, considering a contour $\Gamma = C_R + \gamma_1 + \gamma_2 + \gamma_3 + \gamma_4$ along the closed domain in the z plane, the particular configuration of analytic function $f(z)$ at anywhere of points z except for the two lines has the following form with respect to the cutting rules.

$$f(z) = \frac{1}{2\pi i} \oint_{\Gamma} dz' \frac{f(z')}{z' - z}. \quad (2.41)$$

In what follows we find an integral representation summing all of the segment lines. It is

$$f(z) = \frac{1}{2\pi i} \left(\int_{C_R} + \int_{\gamma_1} + \int_{\gamma_2} + \int_{\gamma_\varepsilon} + \int_{\gamma_3} + \int_{\gamma_4} \right) dz' \frac{f(z')}{z' - z}. \quad (2.42)$$

Let us the integral on the contour γ_ε choose as a reducing point $\varepsilon \rightarrow 0$ and then one becomes

$$\int_{\gamma_\varepsilon} dz' \frac{f(z')}{z' - z} \rightarrow 0. \quad (2.43)$$

By theorem, it is of interest to observe that the radius of circular arch refer to C_R in the relation of Eq. (2.42) and the correlated length of this arch is then equivalent to $2\pi R$ as $\varepsilon \rightarrow 0$. The integral on the circular arch may be chosen as an upper boundary based on the estimation of the *ML* equality:

$$\left| \int_{C_R} dz' \frac{f(z')}{z' - z} \right| \leq \sum_{z' \in C_R} \left| \frac{f(z')}{z' - z} \right| l(C_R). \quad (2.44)$$

According to the properties of reverse triangle inequality, the absolute value of any all three points on $z' \in C_R$ satisfies

$$\frac{1}{|z' - z|} \leq \frac{1}{R + |z|}. \quad (2.45)$$

Which gives rise to write the following integrable function

$$\left| \int_{C_R} dz' \frac{f(z')}{z' - z} \right| \leq \frac{1}{R + |z|} \sum_{z' \in C_R} |f(z')|. \quad (2.46)$$

The integrand on the circular arch C_R must vanish in the way of boundary when the absolute $|z|$ goes to complex ∞ as $|f(z) \rightarrow 0|$. This is now given by

$$\lim_{R \rightarrow \infty} \int_{C_R} dz' \frac{f(z')}{z' - z} = 0. \quad (2.47)$$

We now pick up the two integrations on the segment lines γ_2 and γ_3 as an necessary parameterization curve of $\gamma(x)$ at a certain boundary $\varepsilon \rightarrow 0$. Note however that these two integrals stand in the opposite direction caused by the chosen left and

right side of the segments. These integrals present that

$$\begin{aligned}\lim_{\varepsilon \rightarrow 0} \int_{\gamma_2} dz' \frac{f(z')}{z' - z} &= - \int_{\gamma} \frac{d\gamma}{dx} dx \frac{f_-(\gamma(x))}{\gamma(x) - z}, \\ \lim_{\varepsilon \rightarrow 0} \int_{\gamma_3} dz' \frac{f(z')}{z' - z} &= \int_{\gamma} \frac{d\gamma}{dx} dx \frac{f_+(\gamma(x))}{\gamma(x) - z}.\end{aligned}\tag{2.48}$$

This leads to a representation of the anomalous discontinuity function together with the combination of two integrals above on the parametrization cut γ as a function of x in the plane if complex.

$$\begin{aligned}\lim_{\varepsilon \rightarrow 0} \left(\int_{\gamma_2} + \int_{\gamma_3} \right) &= \int_{\gamma} \frac{d\gamma}{dx} dx \frac{f_+(\gamma(x)) - f_-(\gamma(x))}{\gamma(x) - z}, \\ &= \int_{\gamma} \frac{d\gamma}{dx} dx \frac{\text{disc}_{\text{anom}} f(\gamma(x))}{\gamma(x) - z}.\end{aligned}\tag{2.49}$$

With these similar procedures above, we write a single representation for the unitarity cut on the real axis with the use of two integrals, namely the segment lines γ_1 and γ_4 . Thus

$$\begin{aligned}\lim_{\varepsilon \rightarrow 0} \left(\int_{\gamma_1} + \int_{\gamma_4} \right) &= \int_{\gamma} \frac{d\gamma}{dx} dx \frac{f_+(\gamma_{\text{unit}}) - f_-(\gamma_{\text{unit}})}{\gamma_{\text{unit}} - z}, \\ &= \int_{\gamma} \frac{d\gamma}{dx} dx \frac{\text{disc}_{\text{unit}} f(\gamma_{\text{unit}})}{\gamma_{\text{unit}} - z}.\end{aligned}\tag{2.50}$$

To simplify the notation, we introduce the unitarity relation of Eq. (2.50) in terms of the two pions threshold point $4m_\pi^2$ as:

$$\int_{\gamma} \frac{d\gamma}{dx} dx \frac{\text{disc}_{\text{unit}} f(\gamma_{\text{unit}})}{\gamma_{\text{unit}} - z} = \int_{4m_\pi^2}^{\infty} dz' \frac{\text{disc}_{\text{unit}} f(z')}{z' - z}.\tag{2.51}$$

The argument of the integrand dependence on the z is rearranged into $z + i\varepsilon$ by setting with the infinitesimal epsilon in the unitarity integral in order to avoid the singularities since the discontinuous function along the real axis itself is straight away to define as the boundary value evaluated in the upper complex half plane;

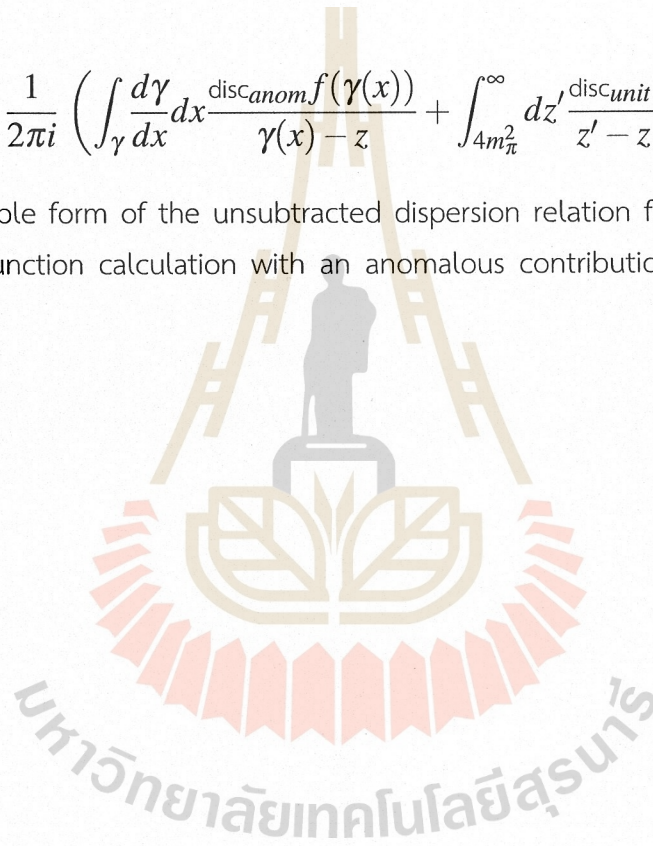
$f(z) = \lim_{\varepsilon \rightarrow 0} f(z + i\varepsilon)$ for $z \in R$. Such a form has

$$\int_{\gamma} \frac{d\gamma}{dx} dx \frac{\text{disc}_{unit} f(\gamma_{unit})}{\gamma_{unit} - z} = \int_{4m_{\pi}^2}^{\infty} dz' \frac{\text{disc}_{unit} f(z')}{z' - z - i\varepsilon}. \quad (2.52)$$

However, it may satisfy only for the unitarity case (right-hand cut) especially when we don't concern ourselves with a new cut in the physical Riemann sheet. Inserting the relations Eq. (2.49) and Eq. (2.52) into the Eq. (2.42), the discontinuity function of the form factors $f(z)$ on the unitarity part and anomalous part may then be written

$$f(z) = \frac{1}{2\pi i} \left(\int_{\gamma} \frac{d\gamma}{dx} dx \frac{\text{disc}_{anom} f(\gamma(x))}{\gamma(x) - z} + \int_{4m_{\pi}^2}^{\infty} dz' \frac{\text{disc}_{unit} f(z')}{z' - z - i\varepsilon} \right). \quad (2.53)$$

It is an example form of the unsubtracted dispersion relation for dealing the scalar three-point function calculation with an anomalous contribution.



CHAPTER III

DISPERSIVE REPRESENTATION TO TRANSITION FORM FACTORS

In the present chapter, we provide the main picture of the dispersive formalism for $N-\Delta$ transition form factors. We give also the relations of the Jone-Scadron form factors to helicity TFF G_m derived in the unsubtracted and subtracted dispersion relations. For the sake of completeness, input structures such as the pion-baryon scattering amplitude T_m and Omnès function $\Omega(s)$ are described following the general framework of Uppsala Group.

3.1 Dispersion relations for the transition form factors

These generic formula of TFFs with the three helicity configuration $m \equiv \sigma - \lambda = \pm 1, 0$ is completely analogy to the work of (Granados et al., 2017; Junker et al., 2020):

$$G_m(s) = \frac{1}{12\pi} \int_{4m_\pi^2}^{\infty} \frac{ds}{\pi} \frac{T_m(s') p_{c.m}^3(s') F_\pi^{V*}(s')}{s'^{1/2}(s' - s - i\epsilon)} + G_m^{anom}(s) + \dots, \quad (3.1)$$

with $p_{c.m}$ is the pion center of mass momentum, $T_m(s)$ is the pion-baryon scattering amplitude and $F_\pi^{V*}(s)$ is the pion vector form factors. In the ΔN transition, there are four possible spin projections for the Δ spin 3/2 particle, denoted by σ and two possible spin projections for the nucleon N particle, denoted by λ . For spin polarization, only the helicity $m \equiv \sigma - \lambda = \pm 1, 0$ is allowed to couple surely with the real photon state in the $N\gamma \rightarrow \Delta$ transition. The anomalous piece of TFFs obtained from the left-hand side of cut structure connecting the branch point of the logarithm is taken into account directly by the provided relation of (Junker et al., 2020):

$$G_m^{anom}(s) = \frac{1}{12\pi} \int_0^1 dx \frac{ds'(x)}{dx} \frac{1}{s'(x) - s} \times \frac{f_m(s'(x)) s'(x) F_\pi^V(s'(x))}{-4[-\lambda(s'(x), m_{\Delta 0}^2, m_n^2)]^{3/2}}, \quad (3.2)$$

with the källén function $\lambda(a, b, c) := a^2 + b^2 + c^2 - 2(ab + bc + ac)$. The pion vector form factors $F_\pi^{V*}(s)$ which has to include the excellent description of the pion physics for energies below 1 GeV is taken from (Leupold, 2018; Hoferichter et al., 2016a). Thus the $F_\pi^{V*}(s)$ for the first order polynomial reads:

$$F_\pi^V = (1 + \alpha_{V_s}) \Omega(s). \quad (3.3)$$

The parameter α_{V_s} can be determined by fitting to the data of the tau decays (Fujikawa et al., 2008) at low energy dynamics. Note that one should not expect the Omnès function $\Omega(s)$ as a good approximation at higher energies where other intermediate states (four pions, six pions,...) may contribute (see more in (Leupold, 2018)). The Omnès function smoothly proportional to the ρ meson contribution is then defined phenomenologically as follow:

$$\Omega(s) = \exp \left(s \int_{4m_\pi^2}^{\infty} \frac{ds'}{\pi} \frac{\delta(s')}{s'(s' - s - i\varepsilon)} \right) \approx F_\pi^{V*}(s), \quad (3.4)$$

with δ referring to the pion p-wave phase shift (Colangelo et al., 2001; Garcia-Martin et al., 2011). The corresponding radii of the three different types of TFFs are calculated

$$\langle r^2 \rangle_m = \frac{6}{G_m(0)} \left. \frac{dG_m(q^2)}{dq^2} \right|_{q^2=0}. \quad (3.5)$$

in terms of the Jone-Scadron FFs at the photon point $q^2 = 0$.

3.1.1 Unsubtracted dispersion relations

In this section, we introduce the unsubtracted dispersion of the TFFs following the general formula of Eq. (3.1). The amplitude $T_m(s)$ for the $\Delta^0 \bar{n} \rightarrow \pi^+ \pi^-$ process will be derived, too. The discontinuous function based on only the unitarity cut is given in (Leupold, 2018)

$$\text{disc}_{unit} G_m(s) = i \frac{T_m(s) p_{cm}^3(s) F_\pi^V(s)^*}{6\pi\sqrt{s}}, \quad (3.6)$$

where $p_{cm}^3(s)$ is the pion momentum in the two-pion center of mass frame, taking the form, $p_{cm}(s) = \frac{1}{2\sqrt{s}} \sqrt{\lambda(s, m_\pi^2, m_\pi^2)} = \frac{1}{2} \sqrt{s - 4m_\pi^2}$. Then, the unsubtracted version of

dispersion relation of TFFs for three helicities $m = \pm 1, 0$ reads in general,

$$G_m(s) = \frac{1}{12\pi} \int_{4m_\pi^2}^{\Lambda^2} \frac{ds'}{\pi} \frac{T_m(s') p_{c.m}^3(s') F_\pi^{V*}(s')}{s'^{1/2}(s' - s - i\epsilon)} + G_m^{anom}(s) + c_m \frac{M_V^2}{M_V^2 - s}, \quad (3.7)$$

with the satisfaction range of the vector-meson mass M_V being $1.4 \text{ GeV} < M_V < 1.7 \text{ GeV}$ (Patrignani et al., 2016). In our numerical calculation we take the mass of the excited vector mesons $M_V = 1.55 \text{ GeV}$ which has been adjusted such as to explore the uncertainties of the effective pole of the p-wave projection on the physical Riemann sheet. The unsubtracted anomalous piece is presented in Eq. (3.2). The form factors $G_m(s)$ at the infinite energy satisfy the condition below,

$$\begin{aligned} sG_m(-s) &= \frac{s}{12\pi^2} \int_{4m_\pi^2}^{\Lambda^2} ds' \frac{T_m(s') p_{c.m}^3(s') F_\pi^{V*}(s')}{s'^{1/2}(s' + s)} \\ &\quad + sG_m^{anom}(-s) + c_m s \frac{M_V^2}{M_V^2 + s}, \\ \lim_{s \rightarrow \infty} sG_m(-s) &= \frac{1}{12\pi^2} \int_{4m_\pi^2}^{\Lambda^2} ds' \frac{T_m(s') p_{c.m}^3(s') F_\pi^{V*}(s')}{s'^{1/2}} \\ &\quad + G_m^{anom}(-s) + c_m M_V^2 = 0. \end{aligned} \quad (3.8)$$

With this condition, the adjusted dimensionless constant parameter c_m in order to improve the dynamics of higher-energy regime can be written as:

$$\begin{aligned} c_m &= -\frac{1}{M_V^2} \left(\frac{1}{12\pi^2} \int_{4m_\pi^2}^{\Lambda^2} ds' \frac{T_m(s') p_{c.m}^3(s') F_\pi^{V*}(s')}{s'^{1/2}} \right. \\ &\quad \left. + \frac{1}{12\pi} \int_0^1 dx \frac{ds'(x)}{dx} \frac{f_m(s'(x)) s'(x) F_\pi^V(s'(x))}{-4(-\lambda(s'(x), m_\Delta^2, m_n^2))^{3/2}} \right). \end{aligned} \quad (3.9)$$

From this, c_m is determined by fitting the theoretical results to the data in this unsubtracted dispersion relation. The numerical parameters of c_m for each polarization are produced by the chosen NLO parameters c_f or the polynomial parameters P_m . In this investigation, c_f is the only free parameter determined by fitting to the experimental data at the real point photon, $\text{Re}G_M^*(0)$. It is interesting to see to what extent our theoretical results of the form factors with

this formula of unsubtracted dispersion relation agree with the data at the specific cutoff $\Lambda = 2 \text{ GeV}$.

3.1.2 Subtracted dispersion relations

Suppressing the large energy contributions at low energy TFFs, we introduce a way to consider the once-subtraction term as a parameter relative to available data in the dispersive integral. This dispersive representation approach especially for low energy dynamics aspects, i.e subtracted dispersion relation, has already been developed in the Uppsala group (Granados et al., 2017). A subtracted dispersion relation for three different helicities $m = \pm 1, 0$ reads:

$$G_m(s) = G_m(0) + \frac{s}{12\pi} \int_{4m_\pi^2}^{\Lambda^2} \frac{ds'}{\pi} \frac{T_m(s') p_{c.m}^3(s') F_\pi^{V*}(s')}{s'^{3/2}(s' - s - i\epsilon)} + G_m^{anom}(s), \quad (3.10)$$

where $G_m(0)$ are three complex-valued subtraction constants at the photon point $q^2 = 0$, which are fixed by fitting to the experimental data when the cutoff energy Λ is set. The anomalous piece of the subtracted integral takes the form (Junker et al., 2020),

$$G_m^{anom}(s) = \frac{s}{12\pi} \int_0^1 dx \frac{ds'(x)}{dx} \frac{1}{s'(x) - s} \times \frac{f_m(s'(x)) F_\pi^V(s'(x))}{-4(-\lambda(s'(x), m_\Delta^2, m_n^2))^{3/2}}, \quad (3.11)$$

with the källén function defined as $\lambda(a, b, c) = a^2 + b^2 + c^2 - 2(ab + bc + ac)$.

3.2 Jone-Scadron form factors

The Jones-Scadron form factors G_M^* , G_E^* , and G_C^* , namely the magnetic dipole, the electric quadrupole and the coulomb quadrupole form factors are related to the three TFFs of different helicity $(G_{\pm 1}, G_0)$,

$$\begin{aligned} G_M^* &= -\frac{1}{\sqrt{6}} \frac{m_n}{m_n + m_\Delta} (G_{-1} - 3G_{+1}), \\ G_E^* &= \frac{1}{\sqrt{6}} \frac{m_n}{m_n + m_\Delta} (G_{-1} + G_{+1}), \\ G_C^* &= \frac{4}{\sqrt{6}} \frac{m_n}{m_n + m_\Delta} G_0. \end{aligned} \quad (3.12)$$

The helicity form factors, G_m are calculated in the unsubtracted and subtracted dispersion relations mentioned in Section 3.1. Note that it is necessary to consider all constituent terms consistent with the baseline of the formula Eq. (3.12) in the dispersive integral.

The electroproduction multipoles obtained from the imaginary parts of the resonant multipoles at the resonance position $W = M_\Delta$ are also denoted by $M_{1+}^{3/2}$, $E_{1+}^{3/2}$ and $S_{1+}^{3/2}$ (The superscript (3/2) in the multipoles refers to the total isospin 3/2, 1 refers to the partial wave $l=1$, + indicate that the total angular momentum is $J=l+1/2$, being 3/2.) are related to the helicity amplitudes $A_{1/2}$, $A_{3/2}$, and $S_{1/2}$ in Ref. (Pascalutsa et al., 2007):

$$\begin{aligned} M_{1+}^{3/2} &= A_{1/2} + \sqrt{3}A_{3/2}, \\ E_{1+}^{3/2} &= A_{1/2} - \frac{1}{\sqrt{3}}A_{3/2}, \\ S_{1+}^{3/2} &= \sqrt{2}S_{1/2}. \end{aligned} \tag{3.13}$$

Following the literature of (Pascalutsa et al., 2007), the helicity transition amplitudes are defined via the matrix elements of the electromagnetic current J_μ between the nucleon and the delta states as:

$$\begin{aligned} A_{3/2} &\equiv -\frac{e}{\sqrt{2}q_\Delta} \frac{1}{(4m_n m_\Delta)^{1/2}} \langle \Delta(\vec{0}, +3/2) | \mathbf{J} \cdot \boldsymbol{\varepsilon}_{\lambda=+1} | N(-\vec{q}, +1/2) \rangle, \\ A_{1/2} &\equiv -\frac{e}{\sqrt{2}q_\Delta} \frac{1}{(4m_n m_\Delta)^{1/2}} \langle \Delta(\vec{0}, +1/2) | \mathbf{J} \cdot \boldsymbol{\varepsilon}_{\lambda=+1} | N(-\vec{q}, -1/2) \rangle, \\ S_{1/2} &\equiv \frac{e}{\sqrt{2}q_\Delta} \frac{1}{(4m_n m_\Delta)^{1/2}} \langle \Delta(\vec{0}, +1/2) | J^0 | N(-\vec{q}, +1/2) \rangle, \end{aligned} \tag{3.14}$$

where $q_\Delta \equiv |\vec{q}| = \frac{Q_+ Q_-}{2m_\Delta}$ is the three-momentum of virtual photon at the rest frame of Δ , and the inside polarization vector of $A_{1/2}$ and $A_{3/2}$ is given by $\boldsymbol{\varepsilon}_{\lambda=+1} = \frac{-1}{\sqrt{2}}(0, 1, i, 0)$. And Q_\pm is defined as $Q_\pm = \sqrt{Q^2 + (m_\Delta \pm m_n)^2}$. The relations between the Jones-Scadron form factors and the helicity transition amplitudes are

expressed via (Pascalutsa et al., 2007):

$$\begin{aligned}
 A_{3/2} &= -N \frac{\sqrt{3}}{2} \{G_M^* + G_E^*\}, \\
 A_{1/2} &= -N \frac{1}{2} \{G_M^* - 3G_E^*\}, \\
 S_{1/2} &= N \frac{q_\Delta}{\sqrt{2}m_\Delta} G_C^*.
 \end{aligned} \tag{3.15}$$

Combining Eq. (3.13) and Eq. (3.15), we obtain

$$\begin{aligned}
 M_{1+}^{3/2} &= N G_M^*, \\
 E_{1+}^{3/2} &= -N G_E^*, \\
 S_{1+}^{3/2} &= -N \frac{q_\Delta}{2m_\Delta} G_C^*,
 \end{aligned} \tag{3.16}$$

where q_Δ is the magnitude of the virtual photon three-momentum in the Δ rest frame: $q_\Delta = \frac{Q_+ Q_-}{2m_\Delta} \approx 0.259$ GeV and N is defined as:

$$N \equiv \frac{e}{2} \sqrt{\frac{Q_+ Q_-}{2m_n^3} \frac{(m_n + m_\Delta)}{Q_+}}. \tag{3.17}$$

The electromagnetic properties of the $N - \Delta(1232)$ transition and the helicity amplitudes $A_{1/2}$, $A_{3/2}$, and $S_{1/2}$ are both described by Jones-Scadron form factors, magnetic dipole (G_M^*), electric quadrupole (G_E^*), and Coulomb quadrupole (G_C^*).

The experimental data shown in Figure 1.2 are the Q^2 dependence of $N\Delta(1232)$ transition magnetic dipole $\text{Im}M_{1+}^{3/2}$, the electric quadrupole ratio R_{EM} and the scalar quadrupole ratio R_{SM} . It is found that the magnetic dipole form factor G_M^* is much larger than the other two form factors G_E^* and G_C^* . The relations between the conventional magnetic dipole form factor $M_{1+}^{3/2}$, the two ratios R_{EM} , R_{SM} with the Jones-Scadron form factors are shown as below,

$$\text{Re}G_M^*(-Q^2) = \frac{8m_n m_\Delta}{e(m_n + m_\Delta)Q_-} \sqrt{\frac{2\pi k_\Delta \Gamma_\Delta}{3}} \text{Im}M_{1+}^{3/2}(Q^2), \tag{3.18}$$

$$R_{EM} = -\frac{\text{Re}G_E^*}{\text{Re}G_M^*}, \quad R_{SM} = -\frac{Q_+Q_-}{4m_\Delta^2} \frac{\text{Re}G_C^*}{\text{Re}G_M^*}. \quad (3.19)$$

with $\text{Im}M_{1+}^{3/2}$ being the imaginary part of the resonant multipoles at the resonance position taken from experimental data, the electric charge $e = \sqrt{4\pi\alpha} \approx 0.303$, the delta decay width $\Gamma_\Delta \approx 0.117$ GeV, and the momentum of the pion as produced in the Δ rest frame, $k_\Delta = \lambda^{1/2}(m_\Delta^2, m_n^2, m_\pi^2)/(2m_\Delta)$. Here, the Q^2 in the conventional relation is $Q^2 = -q^2$. To avoid confusion, let us note that our form factors G_M^* , G_E^* , and G_C^* are dependent on q^2 . At the real photon point $Q^2 = 0$, the available experimental values are provided by (Pascalutsa et al., 2007)

$$\begin{aligned} \text{Re}G_M^*(0) &= 3.02, \\ \text{Re}G_E^*(0) &= 0.075, \\ R_{EM}(0) &= -0.025. \end{aligned} \quad (3.20)$$

In the present work, we are only interested in the $\Delta^0 \bar{n} \rightarrow \pi^+ \pi^-$ process as the input of the dispersive representation at the time-like region. The kinematical point of virtual photon γ is physically located outside the low energy region, $q^2 = (m_\Delta + m_n)^2$. Therefore, we can correlate the second kinematical constraint to the point at the end of the Dalitz decay region, where $q^2 = (m_\Delta - m_n)^2$.

The fixed helicity amplitudes TFFs G_m can be written in terms of form factors, F_1 , F_2 and F_3 (Carlson, 1986; Granados et al., 2017; Junker et al., 2020),

$$\begin{aligned} G_{-1}(q^2) &= (-m_n(m_n + m_\Delta) + q^2) F_1(q^2) + \frac{1}{2}(m_\Delta^2 - m_n^2 + q^2) F_2(q^2) \\ &\quad + q^2 F_3(q^2), \end{aligned} \quad (3.21)$$

$$G_0(q^2) = m_\Delta^2 F_1(q^2) + m_\Delta^2 F_2(q^2) + \frac{1}{2}(m_\Delta^2 - m_n^2 + q^2) F_3(q^2),$$

$$G_{+1}(q^2) = m_\Delta(m_n + m_\Delta) F_1(q^2) + \frac{1}{2}(m_\Delta^2 - m_n^2 + q^2) F_2(q^2) + q^2 F_3(q^2).$$

When the TFFs satisfy with the kinematical constraints $q^2 = (m_\Delta - m_n)^2$ and

$q^2 = (m_\Delta + m_n)^2$, the helicity amplitudes have

$$\begin{aligned} G_{-1}((m_\Delta - m_n)^2) &= G_{+1}((m_\Delta - m_n)^2) = G_0((m_\Delta - m_n)^2), \\ G_{-1}((m_\Delta + m_n)^2) &= G_{+1}((m_\Delta + m_n)^2) = \frac{m_\Delta + m_n}{m_\Delta} G_0((m_\Delta + m_n)^2), \end{aligned} \quad (3.22)$$

and the very useful inverted version of the relations Eq. (3.21) are

$$\begin{aligned} F_1(q^2) &= \frac{G_{+1}(q^2) - G_{-1}(q^2)}{((m_\Delta + m_n)^2 - q^2)}, \\ F_2(q^2) &= \frac{2}{\lambda(q^2, m_\Delta^2, m_n^2)} [-2q^2 G_0(q^2) + (m_\Delta m_n - m_n^2 + q^2) G_{+1}(q^2) + \\ &\quad + (m_\Delta^2 - m_\Delta m_n) G_{-1}(q^2)], \\ F_3(q^2) &= \frac{2}{\lambda(q^2, m_\Delta^2, m_n^2)} [(m_\Delta^2 - m_n^2 + q^2) G_0(q^2) \\ &\quad - m_\Delta^2 (G_{+1}(q^2) + G_{-1}(q^2))]. \end{aligned} \quad (3.23)$$

According the Siegert theorem (Salone and Leupold, 2021; Ramalho, 2016), the electric and charge form factors: G_E^* and G_C^* can be connected in a direct way using the definition of Eq. (3.21) at the chosen threshold region. Then,

$$G_C^*((m_\Delta - m_n)^2) = -\frac{2m_\Delta}{m_\Delta - m_n} G_E^*((m_\Delta - m_n)^2). \quad (3.24)$$

Due to the lack of experimental data for $\text{Re}G_C^*(0)$ at the zero point, we find the subtraction constant G_C^* in accordance with the dispersive integrals. It is expressed in general form

$$G(q^2) = G(0) + q^2 \Delta g(q^2). \quad (3.25)$$

This supports to obtain

$$\begin{aligned} G_C^*(0) &= -(m_\Delta - m_n)^2 \Delta g_C^*((m_\Delta - m_n)^2) \\ &\quad + \frac{2m_\Delta}{m_\Delta - m_n} (G_E^*(0) + (m_\Delta - m_n)^2 \Delta g_E^*((m_\Delta - m_n)^2)), \end{aligned} \quad (3.26)$$

with Δg is given by the dispersive integrals and $\text{Re}G_E^*(0)$ is taken from the data. Then the numerical values for G_C^* at zero point $Q^2=0$ we get

$$\begin{aligned}\text{Re}G_C^*(0) &= 0.678, \\ R_{SM}(0) &= -0.023.\end{aligned}\tag{3.27}$$

In this setting, we explore that the predictions of multipole form factors for $\Delta-N$ transition: G_M^* , G_E^* and G_C^* are fitted to the experimental data with both subtracted and unsubtracted dispersion relations. As well as the two ratios R_{EM} and R_{SM} are determined and compared to the data. For the case of these transitions, a simple choice of physical range is to take into account the cutoff energy at $\Lambda=1$ GeV and $\Lambda=2$ GeV. The interest of other quantities are the differential decay rate of $\Delta^0 \rightarrow Ne^+e^-$ and the two-body decay rate of $\Delta^0 \rightarrow N\gamma$, see more discussion in the Chapter (V).

3.3 Pion-baryon scattering amplitude $T_m(s)$

Having briefly introducing function $T_m(s)$ as a crucial input in the dispersive representation Eq. (3.1), let us now study the derivation of amplitude $T_m(s)$ based on the cut structure of pion-baryon interaction according to the Figure 3.1. The formal amplitude of the $\Delta^0 \bar{n} \rightarrow \pi^+ \pi^-$ process are decomposed into two cut structure, namely a left-hand cut $K_L(s)$ and a right-hand cut $K_R(s)$. That is

$$T(s) = K_L(s) + K_R(s).\tag{3.28}$$

The red blob of the left-hand cut relative to the internal baryon propagator makes it possible to consider as a direct way of connection between the scalar triangle diagram and the baryon exchanged diagram, i.e the amplitude $K_L(s)$. Following the (Leupold, 2018), now we deal with the right-hand cut structure continue to the discontinuity along the unitarity cut via the homogeneous MO equation

$$\text{Im}(T(s) - K_L(s)) = T(s)e^{-i\delta(s)} \sin \delta(s),\tag{3.29}$$

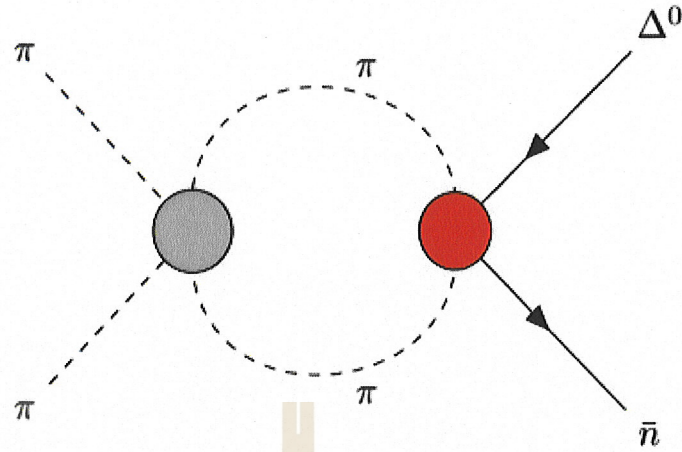


Figure 3.1 Sketch of the Feynman diagram of $\Delta^0 \bar{n}$ interaction in the Lowest order approximation (red blob), including the $\pi\pi$ rescattering consideration (gray blob).

with the pion p-wave phase shift δ . By applying the ansatz with an auxiliary function $H(s)$,

$$T(s) - K_L(s) = H(s)\Omega(s), \quad (3.30)$$

we get,

$$\text{Im}(H(s)\Omega(s)) = (K_L(s) + H(s)\Omega(s))e^{-i\delta(s)} \sin \delta(s). \quad (3.31)$$

Focusing on the product of the imaginary part in above Eq. (3.31), we write

$$\begin{aligned} \text{Im}H(s)\text{Re}\Omega(s) + \text{Re}H(s)\text{Im}\Omega(s) \\ = K_L(s)e^{-i\delta(s)} \sin \delta(s) + H(s)\Omega(s)e^{-i\delta(s)} \sin \delta(s). \end{aligned} \quad (3.32)$$

Recalling the homogeneous version of Eq. (3.29), i.e

$$\text{Im}\Omega(s) = \Omega(s)e^{-i\delta} \sin \delta, \quad (3.33)$$

we rewrite the homogeneous equation

$$\text{Im}H(s)\text{Re}\Omega(s) + \text{Re}H(s)\text{Im}\Omega(s) = K_L(s)e^{-i\delta(s)} \sin \delta(s) + H(s)\text{Im}\Omega(s), \quad (3.34)$$

$$\begin{aligned}
\text{Im}H(s)\text{Re}\Omega(s) + \text{Im}\Omega(s)(\text{Re}H(s) - H(s)) &= K_L(s)e^{-i\delta(s)}\sin\delta(s), \\
\text{Im}H(s)\text{Re}\Omega(s) - i\text{Im}H(s)\text{Im}\Omega(s) &= K_L(s)e^{-i\delta(s)}\sin\delta(s), \\
\text{Im}H(s)(\text{Re}\Omega(s) - i\text{Im}\Omega(s)) &= K_L(s)e^{-i\delta(s)}\sin\delta(s), \\
\text{Im}H(s)|\Omega(s)|e^{-i\delta(s)} &= K_L(s)e^{-i\delta(s)}\sin\delta(s), \\
\text{Im}H(s) &= \frac{K_L(s)\sin\delta(s)}{|\Omega(s)|} \equiv \frac{K(s)\sin\delta(s)}{|\Omega(s)|}.
\end{aligned} \tag{3.35}$$

Having the discontinuity relation,

$$\text{disc}H(s) = 2i\text{Im}H(s). \tag{3.36}$$

and the expression of the once-subtracted dispersion relation, we have,

$$H(s) = \underbrace{H(0)}_{\text{real polynomial}} + \frac{s}{\pi} \int_{4m_\pi^2}^{\infty} ds' \frac{\text{Im}H(s')}{s'(s' - s - i\varepsilon)}, \tag{3.37}$$

$$H(s) = P_{n-1}(s) + \frac{s^n}{\pi} \int_{4m_\pi^2}^{\infty} ds' \frac{K(s')\sin\delta(s')}{|\Omega(s')|s'^n(s' - s - i\varepsilon)}, \quad \text{for the order of } n,$$

with the $n-1$ order of real polynomial terms denote $P_{n-1}(s)$. The dispersion relation of the $T_m(s)$ amplitude can then be formulated in line with the substitution of Eq. (3.30) into Eq. (3.37).

$$T(s) = K(s) + \Omega(s)P_{n-1}(s) + \frac{s^n\Omega(s)}{\pi} \int_{4m_\pi^2}^{\infty} ds' \frac{K(s')\sin\delta(s')}{|\Omega(s')|s'^n(s' - s - i\varepsilon)}, \tag{3.38}$$

This is a familiar dispersive integral form of the pion-baryon scattering amplitude related to only the unitarity cut consideration. However, notice that there is no any polynomial $P_{n-1}(s)$ contribution for higher order terms since the Omnès function in the integral Eq. (3.38) diverges as s tend to infinity. To avoid the problem, one may express the input structure of amplitude function $T_m(s)$ for the TFFs representation $G_m(s)$ in terms of the extra anomalous threshold cut caused by the light exchanged baryon state p . One therefore can write the once-subtracted dispersion relations

of the amplitude $T_m(s)$ for three helicity configurations $m = \pm 1, 0$ finally,

$$T_m(s) = K_m(s) + \Omega(s) \left(P_m(s) + \frac{s}{\pi} \int_{4m_\pi^2}^{\infty} ds' \frac{K_m(s') \sin \delta(s')}{|\Omega(s')| s'(s' - s - i\epsilon)} \right) + \Omega(s) T_m^{\text{anom}}(s). \quad (3.39)$$

The anomalous contribution $T_m^{\text{anom}}(s)$ is given by (Junker et al., 2020)

$$T^{\text{anom}}(s) = s \int_0^1 dx \frac{ds'(x)}{dx} \frac{1}{s'(x) - s} \times \frac{t_{IAM}(s'(x))}{\Omega(s'(x)) s'(x)} \times \frac{2f(s'(x))}{(-\lambda(s'(x), m_\Delta^2, m_n^2))^{1/2} k^2(s'(x))}, \quad (3.40)$$

with the straight-line path of the anomalous branch cut which is similar to the structure of the branch point and branch cut for the scalar triangle definition Eq. (2.40),

$$s'(x) = (1-x)s_+ + x4m_\pi^2. \quad (3.41)$$

Additionally, we also need to consider the analytic continuation of amplitude $t_{IAM}(s)$ in order to be the true scattering amplitude at the two-pion threshold in the complex plane. For our case, this unitarized version of $t_{IAM}(s)$ can be taken directly from approximation of ChPT derived by the inverse amplitude method (Junker et al., 2020);

$$t_{IAM} = \frac{t_2^2(s)}{t_2(s) - t_4(s)}, \quad (3.42)$$

with the components of amplitude

$$t_2(s) = \frac{s\sigma^2(s)}{96\pi F^2},$$

$$t_4(s) = i\sigma(s)t_2(s)^2 + \frac{t_2(s)}{48\pi^2 F^2} \left[s \left(\bar{l} + \frac{1}{3} \right) - \frac{15}{2}m_\pi^2 - \frac{1}{2s}m_\pi^4 \right. \\ \left. (41 - 2L_s(s)(73 - 24\sigma(s)^2) + 3L_s(s)^2(5 - 32\sigma(s)^2 + 3\sigma(s)^4)) \right], \quad (3.43)$$

$$L_s(s) = \frac{1}{\sigma^2(s)} \left(\frac{1}{2\sigma(s)} \log \frac{1+\sigma(s)}{1-\sigma(s)} - 1 \right), \quad (3.44)$$

where the pion decay constant, $F = 0.0868$ GeV. The helicity amplitude $K_m(s)$ in terms of all possible parameters can be obtained numerically in the chiral perturbation theory Eq. (4.43). Recalling that the structure of the helicity amplitudes $K_m(s)$,

$$\begin{aligned} K_{+1} &= C_{oct} (C_{+1} + D_{+1} R_s^{\text{oct}}) + C_{dec} (E_{+1} + F_{+1} R_s^{\text{dec}}), \\ K_{-1} &= C_{oct} (C_{-1} + D_{-1} R_s^{\text{oct}}) + C_{dec} (E_{-1} + F_{-1} R_s^{\text{dec}}), \\ K_0 &= C_{oct} (C_0 + D_0 R_d^{\text{oct}}) + C_{dec} (E_0 + F_0 R_d^{\text{dec}}), \end{aligned} \quad (3.45)$$

with the constant parameters defined,

$$C_{oct} = -\frac{g_A h_A}{4\sqrt{6}F_\pi^2}, C_{dec} = -\frac{5h_A H_A}{12\sqrt{6}F_\pi^2}. \quad (3.46)$$

The numerical code for the partial-wave projection of the reduced amplitude $K_m(s)$ produces

$$K_m(s) = g_m(s) - \frac{2f_m(s)}{Y(s)k^2(s)} + \frac{f_m(s)}{k^3(s)} \log \frac{Y(s) + k(s)}{Y(s) - k(s)}. \quad (3.47)$$

Here, there is no cut structure in the introduced functions $f_m(s)$ and $g_m(s)$ above. The other functions, $Y(s)$ and $k(s)$ are described in Appendix (D). $f_m(s)$ take the explicit form from the definition of Eq. (3.45),

$$\begin{aligned} f_{+1}(s) &= -C_{oct} D_{+1}(s) (k^2(s) - Y(s)), \\ f_0(s) &= -C_{oct} D_0(s) 2Y(s), \\ f_{-1}(s) &= -C_{oct} D_{-1}(s) (k^2(s) - Y(s)). \end{aligned} \quad (3.48)$$

with regard to the inside parameters of the chiral Lagrangian. The polynomial contribution terms, P_m from the NLO contact diagram for numerical computation

are introduced as

$$\begin{aligned}
 P_+ &= 2C_{oct} + C_{dec} \frac{5(m_\Delta + m_n)}{6m_\Delta} - c_F \frac{m_\Delta + m_n}{\sqrt{3}F_\pi^2}, \\
 P_0 &= C_{oct} + C_{dec} \frac{3m_\Delta - m_n}{6m_\Delta} + c_F \frac{m_n(m_\Delta + m_n)}{\sqrt{3}F_\pi^2 m_\Delta}, \\
 P_- &= C_{oct} \frac{2(m_\Delta - m_n - m_p)}{m_\Delta} - C_{dec} \frac{(m_\Delta + m_n)(6m_\Delta - m_n)}{6m_\Delta^2} \\
 &\quad - c_F \frac{m_n(m_\Delta + m_n)}{\sqrt{3}F_\pi^2 m_\Delta}.
 \end{aligned} \tag{3.49}$$

The insertion values in Eq. (3.41) for the branch points of the logarithm, when $Y(s) = k(s)$, are located at

$$\begin{aligned}
 s_\pm &= -\frac{1}{2}m_{ex}^2 + \frac{1}{2}(m_\Delta^2 + m_n^2 + 2m_\pi^2) \\
 &\quad - \frac{m_\Delta^2 m_n^2 - m_\pi^2(m_\Delta^2 + m_n^2) + m_\pi^4}{2m_{ex}^2} \\
 &\quad \mp \frac{\lambda^{1/2}(m_\Delta^2, m_{ex}^2, m_\pi^2) \lambda^{1/2}(m_{ex}^2, m_n^2, m_\pi^2)}{2m_{ex}^2}.
 \end{aligned} \tag{3.50}$$

We take the trajectory of the branch point s_+ located in the lower half plane on the physical Riemann sheet for the small values of m_Δ^2 . For the case of baryon exchange $m_{ex}^2 = m_p^2$, there is some trajectory as varying the function of the mass $m_\Delta^2 + i\epsilon$ crossing the unitarity cut. Thus the branch point s_+ is written in the form

$$\begin{aligned}
 s_+ &= -\frac{1}{2}m_{ex}^2 + \frac{1}{2}(m_\Delta^2 + m_n^2 + 2m_\pi^2) \\
 &\quad - \frac{m_\Delta^2 m_n^2 - m_\pi^2(m_\Delta^2 + m_n^2) + m_\pi^4}{2m_{ex}^2} \\
 &\quad - i \frac{\lambda^{1/2}(m_\Delta^2, m_{ex}^2, m_\pi^2) (-\lambda(m_{ex}^2, m_n^2, m_\pi^2))^{1/2}}{2m_{ex}^2}.
 \end{aligned} \tag{3.51}$$

The values of the parameters associated with the three point vertex functions are given by the estimation of large- N_c approximation (Pascalutsa et al., 2007; Ledwig et al., 2012)

$$\begin{aligned} F_\pi &= 92.28 \text{ MeV}, g_A = D + F = 1.26, \\ h_A &= \frac{3g_A}{\sqrt{2}} \approx 2.67, H_A = \frac{9g_A}{5} \approx 2.27. \end{aligned} \quad (3.52)$$

The above are the ingredients and finalized expressions for the pion-baryon scattering amplitude. Then the dispersion relations for amplitude $T_m(s)$ can be evaluated at a given cutoff energy up to $\Lambda = 2$ GeV. We will use, as inputs, the results of amplitude $T_m(s)$ arising from the lowest order two pions approximation for the representation of TFFs $G_m(s)$ at low energy regime.

3.4 Omnès function and pion p-wave phase shift

Our aim is to focus on the parameterization of pion vector form factors, based on the discontinuity function that is subjected to the Muskhelishvili-Omnès (MO) relation (Iwamura, 1976) in a given pion p-wave phase shift. Various approaches of the Omnès calculations can be seen in more details in (Anisovich and Leutwyler, 1996; Niecknig et al., 2012). The fundamental expectation quantity of pion vector form factors defines in general via (Hanhart, 2012)

$$\langle 0 | J^\mu | \pi^+(p_+) \pi^-(p_-) \rangle = e(p_+ - p_-)^\mu F_V(s), \quad (3.53)$$

with $s = (p_+ + p_-)^2$. However, we discuss here only the pion form factors F_V solely in terms of the pion p-wave phase shift, i.e Omnès function. It is assumed that the homogeneous MO equation of motion of the function $F(s)$ is given by

$$\text{Im}F(s) = F(s)e^{-i\delta(s)} \sin \delta(s), \quad (3.54)$$

with $\delta(s)$ denoting a general form of the phase shift function and the corresponding general form factors reading as;

$$F(s) = H(s)\Omega(s), \quad (3.55)$$

where $H(s)$ refers to some polynomial function and the Omnès function is equivalent to 1 if the boundary condition $s=0$. The Omnès function is related to the pion phase shift,

$$\Omega(s) = \exp \left(s \int_{4m_\pi^2}^{\infty} \frac{ds'}{\pi} \frac{\delta(s')}{s'(s'-s-i\epsilon)} \right), \quad \text{for } s \in \mathbb{R}. \quad (3.56)$$

Later we calculate the Omnès function in the complex s -plane, so we may eliminate the argument $-i\epsilon$ from the expression of Eq. (3.59), that is,

$$\Omega(s) = \exp \left(s \int_{4m_\pi^2}^{\infty} \frac{ds'}{\pi} \frac{\delta(s')}{s'(s'-s)} \right), \quad \text{for } s \in \mathbb{C}. \quad (3.57)$$

The derivation of the Omnès function is shown in Appendix (F).

As a particular case, we deal with the formalism of the amplitude of $\pi\pi$ scattering in the p-wave projection from the experimental data. The pion phase shift for different wave projections beyond the pion scattering amplitude has been examined in (Garcia-Martin et al., 2011) for each different energy interval. We therefore take into account the parametrization function of the pion phase shift from (Garcia-Martin et al., 2011) for the low $\sqrt{s} \leq 2m_K$ and intermediate energies $2m_K < \sqrt{s} < \sqrt{s_{\text{cut}}}$. The parameterized function for the phase shift in the energy region above $\sqrt{s_{\text{cut}}}$ is taken directly from (Hanhart, 2012) in order to extrapolate smoothly the phase shift to a value as $s \rightarrow \infty$. So there will be a need to consider the following three intervals for the pion p-wave phase shift parameterization function in our process,

$$\begin{aligned} \delta_1(s) = & \cot^{-1} \left(\frac{\sqrt{s}}{2|p_{c.m}|^3} (m_\rho^2 - s) \left(\frac{2m_\pi^3}{m_\rho^2 \sqrt{s}} + b_0 + b_1 w(s) \right) \right) \text{ for } \sqrt{s} \leq 2m_K, \\ & \delta_1(2m_K) + \lambda_1 \left(\frac{\sqrt{s}}{2m_K} - 1 \right) + \lambda_2 \left(\frac{\sqrt{s}}{2m_K} - 1 \right)^2 \text{ for } 2m_K < \sqrt{s} < \sqrt{s_{\text{cut}}}, \\ & \pi + \delta_1(s_{\text{cut}}) \left(\frac{\Lambda^2 + s_{\text{cut}}}{\Lambda^2 + s} \right) \text{ for } \sqrt{s_{\text{cut}}} < \sqrt{s}, \end{aligned} \quad (3.58)$$

with the value of energy above the intermediate level, $\sqrt{s_{\text{cut}}} = 1.4$ GeV, the K mass fixed to $m_K = 0.496$ GeV, the ρ mass equal to $m_\rho = 0.7736$ GeV, and the function

$$w(s) = \frac{\sqrt{s} - \sqrt{s_0 - s}}{\sqrt{s} + \sqrt{s_0 - s}} \quad \text{for } \sqrt{s_0} = 1.05 \text{ GeV}. \quad (3.59)$$

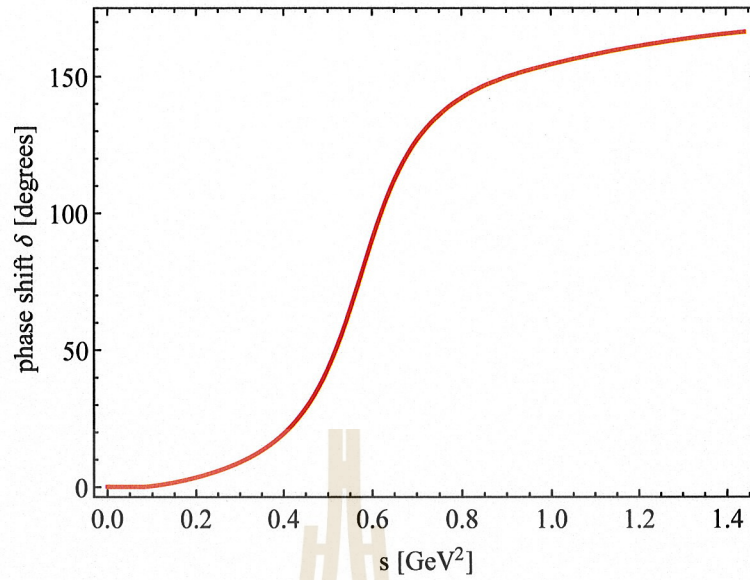


Figure 3.2 Parametrization results of the pion p-wave phase shift in line with (3.58) at the specific range, $0 < s(\text{GeV}^2) < 1.4$. In the plot, we start the energy range from 0 GeV^2 instead of starting at $4m_\pi^2 \text{ GeV}^2$.

The constant values of p-wave parameters from (Garcia-Martin et al., 2011) are introduced as; $b_0 = 1.043$, $b_1 = 0.19$, $\lambda_1 = 1.39$, $\lambda_2 = -1.70$ and $\Lambda = 10 \text{ GeV}$. The numerical results of the Omnès function parameterized in the p-wave phase shifts by using the experimental data are graphically shown in the following Figure 3.2, Figure 3.3 and Figure 3.4.

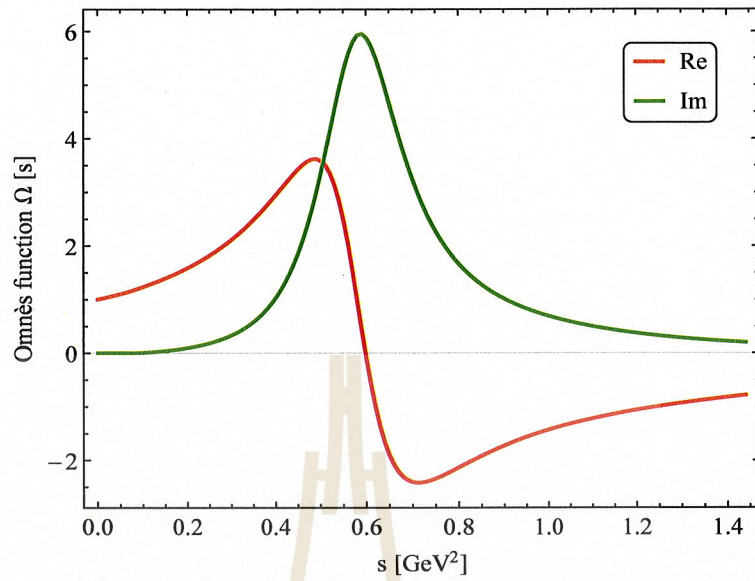


Figure 3.3 Real and imaginary part of the Omnès function as parameterized in the pion p-wave phase shift at a given physical range, $0 < s(\text{GeV}^2) < 1.4$.

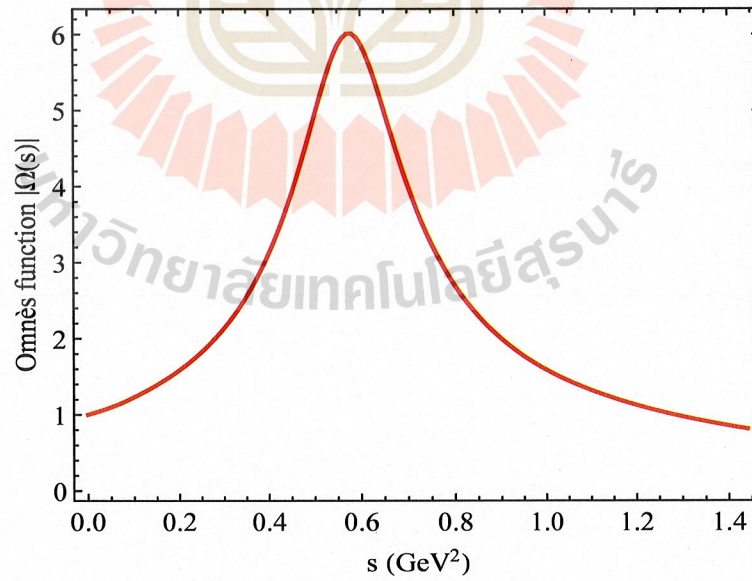


Figure 3.4 The absolute parameterization result of Omnès function in the range, $0 < s(\text{GeV}^2) < 1.4$. All the parameterization results are similar to the works of (Garcia-Martin et al., 2011; Hanhart, 2012).

CHAPTER IV

HELICITY AMPLITUDES OF PROJECTION FORMALISM

This chapter lays the mathematical groundwork necessary to calculate the Feynman matrix elements for the $\Delta-N$ interaction using baryon Chiral Perturbation Theory (ChPT). We address how the amplitude function arises within the projection formalism to obtain explicit expressions for the reduced amplitudes. These reduced amplitudes serve as crucial input for the pion-baryon scattering amplitudes which are ideally determined using the Muskhelishvili-Omnès function (Omnes, 1958). Further theoretical calculations will be presented, following the established principles of Feynman diagrams.

4.1 Baryon chiral perturbation theory

The leading-order (LO) chiral Lagrangian that incorporates decuplet baryon states can be expressed as (Jenkins and Manohar, 1991; Pascalutsa et al., 2007; Ledwig et al., 2014; Holmberg and Leupold, 2018)

$$\begin{aligned}
 \mathcal{L}_{\text{baryon}}^{(1)} = & \text{tr}(\bar{B}(i\not{D} - m_{(8)})B) \\
 & + \bar{T}_{abc}^{\mu}(i\gamma_{\mu\nu\alpha}D^{\alpha} - \gamma_{\mu\nu}m_{(10)})(T^{\nu})^{abc} \\
 & + \frac{D}{2}\text{tr}(\bar{B}\gamma^{\mu}\gamma_5\{u_{\mu}, B\}) + \frac{F}{2}\text{tr}(\bar{B}\gamma^{\mu}\gamma_5[u_{\mu}, B]) \\
 & + \frac{h_A}{2\sqrt{2}}\left(\varepsilon^{ade}\bar{T}_{abc}^{\mu}(u_{\mu})_d^b B_e^c + \varepsilon_{ade}\bar{B}_c^e(u^{\mu})_b^d T_{\mu}^{abc}\right) \\
 & - \frac{H_A}{4m_R}\varepsilon_{\mu\nu\alpha\beta}\left(\bar{T}_{abc}^{\mu}(D^{\nu}T^{\alpha})^{abd}(u^{\beta})_d^c \right. \\
 & \quad \left. + (D^{\nu}\bar{T}^{\alpha})_{abd}(T^{\mu})^{abc}(u^{\beta})_c^d\right), \tag{4.1}
 \end{aligned}$$

where tr denotes the trace over flavor indices, B represents the octet baryon field, T_{abc}^{μ} represents the decuplet baryon field, $\not{D} = \gamma^{\mu}D_{\mu}$ is the covariant derivative,

$m_{(8)}$ and $m_{(10)}$ are the octet and decuplet baryon masses, respectively, u_μ is the pseudoscalar meson field, D , F , h_A , and H_A are low-energy constants (LECs) to be determined phenomenologically, m_R is a reference mass scale, and ε_{ade} and $\varepsilon_{\mu\nu\alpha\beta}$ are the Levi-Civita symbols. The fully antisymmetric products of 2 and 3 gamma matrices are defined as (Peskin and Schroeder, 1995),

$$\gamma^{\mu\nu} = \frac{1}{2}[\gamma^\mu, \gamma^\nu], \quad (4.2)$$

and

$$\begin{aligned} \gamma^{\mu\nu\alpha} &= \frac{1}{6}(\gamma^\mu\gamma^\nu\gamma^\alpha + \gamma^\nu\gamma^\alpha\gamma^\mu + \gamma^\alpha\gamma^\mu\gamma^\nu \\ &\quad - \gamma^\mu\gamma^\alpha\gamma^\nu - \gamma^\alpha\gamma^\nu\gamma^\mu - \gamma^\nu\gamma^\mu\gamma^\alpha), \\ &= \frac{1}{2}\{\gamma^{\mu\nu}, \gamma^\alpha\} = +i\varepsilon^{\mu\nu\alpha\beta}\gamma_\beta\gamma_5, \end{aligned} \quad (4.3)$$

respectively where $\gamma_5 := i\gamma^0\gamma^1\gamma^2\gamma^3$ and $\varepsilon_{0123} = -1$. The baryon octet can be represented by a matrix, B , as

$$B = \begin{pmatrix} \frac{1}{\sqrt{2}}\Sigma^0 + \frac{1}{\sqrt{6}}\Lambda & \Sigma^+ & p \\ \Sigma^- & -\frac{1}{\sqrt{2}}\Sigma^0 + \frac{1}{\sqrt{6}}\Lambda & n \\ \Xi^- & \Xi^0 & -\frac{2}{\sqrt{6}}\Lambda \end{pmatrix}. \quad (4.4)$$

The baryon decuplet is expressed using a fully symmetric flavor tensor, T^{abc} , with specific elements:

$$\begin{aligned} T^{111} &= \Delta^{++}, \quad T^{112} = \frac{1}{\sqrt{3}}\Delta^+, \\ T^{122} &= \frac{1}{\sqrt{3}}\Delta^0, \quad T^{222} = \Delta^-, \\ T^{113} &= \frac{1}{\sqrt{3}}\Sigma^{*+}, \quad T^{123} = \frac{1}{\sqrt{6}}\Sigma^{*0}, \quad T^{223} = \frac{1}{\sqrt{3}}\Sigma^{*-}, \\ T^{133} &= \frac{1}{\sqrt{3}}\Xi^{*0}, \quad T^{233} = \frac{1}{\sqrt{3}}\Xi^{*-}, \quad T^{333} = \Omega. \end{aligned} \quad (4.5)$$

The Goldstone bosons are encoded in

$$\Phi = \begin{pmatrix} \pi^0 + \frac{1}{\sqrt{3}}\eta & \sqrt{2}\pi^+ & \sqrt{2}K^+ \\ \sqrt{2}\pi^- & -\pi^0 + \frac{1}{\sqrt{3}}\eta & \sqrt{2}K^0 \\ \sqrt{2}K^- & \sqrt{2}\bar{K}^0 & -\frac{2}{\sqrt{3}}\eta \end{pmatrix}, \quad (4.6)$$

$$u^2 := U := \exp(i\Phi/F_\pi), \quad u_\mu := iu^\dagger (\nabla_\mu U) u^\dagger = u_\mu^\dagger.$$

Under chiral transformations, the fields transform as (Jenkins and Manohar, 1991; Scherer and Schindler, 2012a):

$$\begin{aligned} U &\rightarrow LUR^\dagger, & u &\rightarrow Lu h^\dagger = huR^\dagger, \\ u_\mu &\rightarrow hu_\mu h^\dagger, & B &\rightarrow hBh^\dagger, \\ T_\mu^{abc} &\rightarrow h_d^a h_e^b h_f^c T_\mu^{def}, & \bar{T}_{abc}^\mu &\rightarrow (h^\dagger)_a^d (h^\dagger)_b^e (h^\dagger)_c^f \bar{T}_{def}^\mu. \end{aligned} \quad (4.7)$$

Specifically, the distinction between upper and lower flavor indices signifies their transformation properties under flavor symmetry. Upper indices transform according to the representation h , while their lower counterparts transform with the conjugate representation h^\dagger . For baryon octet, the chirally covariant derivatives are defined by

$$D^\mu B = \partial^\mu B + [\Gamma^\mu, B], \quad (4.8)$$

for a decuplet T by

$$(D^\mu T)^{abc} = \partial^\mu T^{abc} + (\Gamma^\mu)_a^{a'} T^{a'bc} + (\Gamma^\mu)_{b'}^b T^{ab'c} + (\Gamma^\mu)_c^{c'} T^{abc'}, \quad (4.9)$$

for an anti-decuplet by

$$(D^\mu \bar{T})_{abc} = \partial^\mu \bar{T}_{abc} - (\Gamma^\mu)_a^{a'} \bar{T}_{a'bc} - (\Gamma^\mu)_{b'}^b \bar{T}_{ab'c} - (\Gamma^\mu)_c^{c'} \bar{T}_{abc'}, \quad (4.10)$$

and for the Goldstone boson fields by

$$\nabla_\mu U = \partial_\mu U - i(v_\mu + a_\mu)U + iU(v_\mu - a_\mu), \quad (4.11)$$

with

$$\begin{aligned} \Gamma_\mu = & \frac{1}{2} \left(u^\dagger (\partial_\mu - i(v_\mu + a_\mu)) u \right. \\ & \left. + u (\partial_\mu - i(v_\mu - a_\mu)) u^\dagger \right), \end{aligned} \quad (4.12)$$

where v and a denote external sources. Within our framework, the interaction term proportional to H_A effectively reduces to the following form:

$$+ \frac{H_A}{2m_R F_\pi} \epsilon_{\mu\nu\alpha\beta} \bar{T}_{abc}^\mu \partial^\nu (T^\alpha)^{abd} \partial^\beta \Phi_d^c, \quad (4.13)$$

where m_R denotes the resonance mass, which in this specific case corresponds to m_Δ . While seemingly straightforward, complications arise due to the use of spin-3/2 Rarita-Schwinger fields. These fields inherently contain unphysical spin-1/2 degrees of freedom. Consequently, the interaction term not only describes the desired spin-3/2 resonance exchange but also generates an unwanted contact interaction. To eliminate this unphysical contact term, we employ the Pascalutsa prescription (Pascalutsa and Timmermans, 1999; Pascalutsa and Vanderhaeghen, 2006; Pascalutsa et al., 2007; Ledwig et al., 2012). This approach dictates a specific substitution in Eq. (4.14):

$$T^\mu \rightarrow -\frac{1}{m_\Delta} \epsilon^{\nu\mu\alpha\beta} \gamma_5 \gamma_\nu \partial_\alpha T_\beta. \quad (4.14)$$

This procedure induces an explicit flavor breaking, but such effects are beyond leading order in our calculations. The H_A term in Eq. (4.13) is already constructed such that only the spin-3/2 components contribute. We will explore both the standard interaction term from Eq. (4.1) and the corresponding one obtained by Eq. (4.14). As discussed in (Junker et al., 2020), differences can be accounted for by contact interactions of the chiral Lagrangian at next-to-leading order (NLO) and beyond.

The complete NLO Lagrangian was presented in (Holmberg and Leupold, 2018). We focus on terms lifting mass degeneracies from leading order (LO) and enabling interactions for the reaction $\Delta\pi \rightarrow n\pi$ (formally $\Delta\bar{n} \rightarrow 2\pi$), where the two pions are in a p-wave.

The relevant NLO Lagrangian for the baryon octet sector reads (Oller

et al., 2006; Frink and Meissner, 2006; Holmberg and Leupold, 2018):

$$\mathcal{L}_8^{(2)} = b_{\chi,D} \text{tr}(\bar{B} \{\chi_+, B\}) + b_{\chi,F} \text{tr}(\bar{B} [\chi_+, B]). \quad (4.15)$$

Here, $\chi_{\pm} = u^{\dagger} \chi u^{\dagger} \pm u \chi^{\dagger} u$ and $\chi = 2B_0(s + ip)$ are constructed from the scalar source s and the pseudoscalar source p . The low-energy constant B_0 is related to the light-quark condensate and the pion-decay constant (see, e.g., (Gasser and Leutwyler, 1984; Gasser and Leutwyler, 1985; Scherer, 2003; Scherer and Schindler, 2012a)). While LO baryon octet states are mass-degenerate, the NLO terms in Eq. (4.15) lift this degeneracy, essentially moving masses to their physical values. Technically, this is achieved by replacing the scalar source s with the quark mass matrix. Numerical results for these parameters can be found in (Kubis and Meissner, 2001). In practice, we use physical masses and omit specifying these parameters here.

The relevant NLO Lagrangian for the baryon decuplet sector reads (Holmberg and Leupold, 2018):

$$\mathcal{L}_{10}^{(2)} = -d_{\chi,(8)} \bar{T}_{abc}^{\mu} (\chi_+)_d^c \gamma_{\mu\nu} (T^{\nu})^{abd}. \quad (4.16)$$

This term provides a mass splitting for the decuplet baryons, reproducing the observed relations $m_{\Omega} - m_{\Xi^*} = m_{\Xi^*} - m_{\Sigma^*} = m_{\Sigma^*} - m_{\Delta}$ (Tanabashi et al., 2018). Here, we focus on the Δ resonance.

For the reaction $\Delta \bar{n} \rightarrow 2\pi$, the relevant NLO Lagrangian term is given by (Holmberg and Leupold, 2018):

$$\mathcal{L}_{8-10}^{(2)} \rightarrow -\frac{c_F}{\sqrt{3}F_{\pi}^2} \bar{n} \gamma_{\mu} \gamma_5 \Delta_{\nu}^0 (\partial^{\mu} \pi^{+} \partial^{\nu} \pi^{-} - (\mu \leftrightarrow \nu)). \quad (4.17)$$

A vector-meson-dominance estimate for the contact parameter c_F is provided in Appendix D of (Junker et al., 2020).

4.2 Feynman amplitude of the scattering process $\Delta^0 \bar{n} \rightarrow \pi^+ \pi^-$

We proceed to compute the Feynman amplitude \mathcal{M} for the $\Delta^0 \bar{n} \rightarrow \pi^+ \pi^-$ scattering process using baryon chiral perturbation theory. Here, we utilize the notations T for the decuplet baryons, B for the octet baryons, and ϕ for the scalar mesons. All conceivable Feynman diagrams in our analysis are displayed in Figure 4.1.

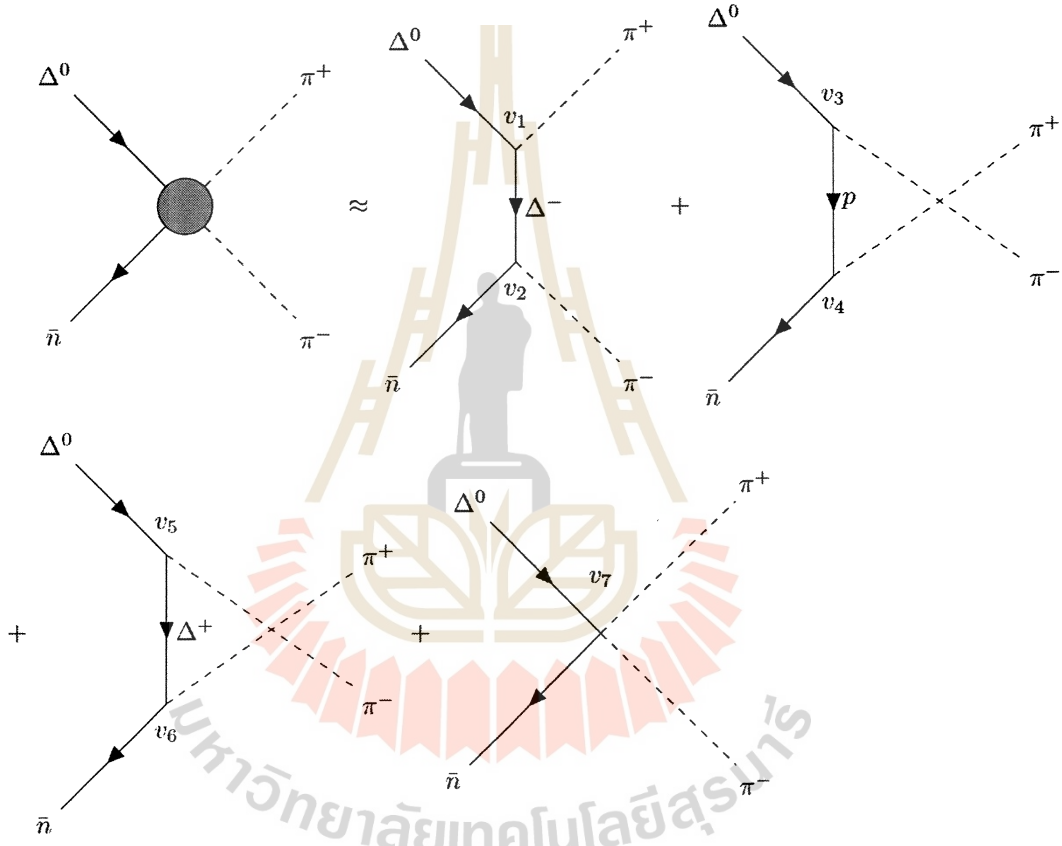


Figure 4.1 Feynman diagrams for the scattering process $\Delta^0 \bar{n} \rightarrow \pi^+ \pi^-$.

Using the Lagrangians introduced in the previous section, the $TT\phi$ vertices are expressed as follows:

$$\begin{aligned}
 v_1 \equiv \mathcal{L}_{\Delta^0 \Delta^- \pi^+} &= -\frac{iH_A}{\sqrt{6}m_\Delta F_\pi} \varepsilon_{\bar{\mu}\nu\alpha\beta} p_{\Delta^0}^\nu p_{\pi^+}^\beta, \\
 v_5 \equiv \mathcal{L}_{\Delta^0 \Delta^+ \pi^-} &= -\frac{2i}{3\sqrt{2}m_\Delta} \frac{H_A}{F_\pi} \varepsilon_{\bar{\mu}\nu\alpha\beta} p_{\Delta^0}^\nu p_{\pi^-}^\beta.
 \end{aligned} \tag{4.18}$$

The $TB\phi$ vertices are given by:

$$\begin{aligned}
 v_2 &\equiv \mathcal{L}_{\Delta^-\bar{n}\pi^-} = \frac{1}{2} \frac{h_A}{F_\pi} p_{\pi^-}^\mu, \\
 v_3 &\equiv \mathcal{L}_{\Delta^0 p \pi^-} = \frac{1}{2\sqrt{3}} \frac{h_A}{F_\pi} p_{\pi^-}^\mu, \\
 v_6 &\equiv \mathcal{L}_{\Delta^+ \bar{n} \pi^+} = -\frac{1}{2\sqrt{3}} \frac{h_A}{F_\pi} p_{\pi^+}^\mu.
 \end{aligned} \tag{4.19}$$

The $BB\phi$ vertex is given by:

$$v_4 \equiv \mathcal{L}_{\bar{n} p \pi^+} = -\frac{1}{\sqrt{2}} \frac{(D+F)}{F_\pi} \not{p}_{\pi^+} \gamma_5. \tag{4.20}$$

Lastly, the NLO vertex is represented as:

$$v_7 \equiv \mathcal{L}_{\text{NLO}} = -\frac{c_F}{\sqrt{3}F_\pi^2} (P_{\pi^+}^\mu p_{\pi^-}^\nu - p_{\pi^+}^\nu p_{\pi^-}^\mu) g_{\nu\alpha} \bar{v}(p_{\bar{n}}) \gamma_\mu \gamma_5 u^\alpha(p_{\Delta^0}). \tag{4.21}$$

The total Feynman amplitude for the scattering process $\Delta^0 \bar{n} \rightarrow \pi^+ \pi^-$ is written in the following form:

$$\begin{aligned}
 \mathcal{M}_{\Delta^0 \bar{n} \rightarrow \pi^+ \pi^-} &= -\frac{g_A h_A}{2\sqrt{6}F_\pi^2} \frac{1}{u - m_p^2 + i\epsilon} p_{\pi^-}^\mu g_{\mu\alpha} \bar{v}_n \not{p}_{\pi^+} \gamma_5 (\not{p}_\Delta - \not{p}_{\pi^-} + m_p) u_\Delta^\alpha \\
 &+ \frac{h_A H_A}{3\sqrt{6}m_\Delta F_\pi^2} i\varepsilon_{\nu\alpha\beta}^\lambda p_\Delta^\nu p_{\pi^-}^\beta p_{\pi^+}^\mu \bar{v}_n S_{\mu\lambda} (p_\Delta - p_{\pi^-}) u_\Delta^\alpha \\
 &- \frac{h_A H_A}{2\sqrt{6}m_\Delta F_\pi^2} i\varepsilon_{\nu\alpha\beta}^\lambda p_\Delta^\nu p_{\pi^+}^\beta p_{\pi^-}^\mu \bar{v}_n S_{\mu\lambda} (p_\Delta - p_{\pi^+}) u_\Delta^\alpha \\
 &- \frac{c_F}{\sqrt{3}F_\pi^2} (p_{\pi^+}^\mu p_{\pi^-}^\alpha - p_{\pi^+}^\alpha p_{\pi^-}^\mu) g_{\alpha\beta} \bar{v}_n \gamma_\mu \gamma_5 u_\Delta^\beta,
 \end{aligned} \tag{4.22}$$

where $g_A = D + F$ and the spin- $\frac{3}{2}$ propagator $S_{\mu\nu}(p)$ is represented as:

$$S_{\mu\nu}(p) = -\frac{\not{p} + m}{p^2 - m^2 + i\epsilon} P_{\mu\nu}^{3/2}(p) + \frac{2}{3m^2} (\not{p} + m) \frac{p_\mu p_\nu}{p^2} - \frac{1}{3m} \frac{p_\mu p^\alpha \gamma_{\alpha\nu} + \gamma_{\mu\alpha} p^\alpha p_\nu}{p^2}. \quad (4.23)$$

4.3 Projection formalism

The entire calculation in this section directly leads to the analytic formula of Feynman matrix elements (\mathcal{M}) from the general spin structure of the pion-induced $\Delta^0 \bar{n} \rightarrow \pi^+ \pi^-$ process. The Feynman matrix elements with a spinor matrix structure is a central concept used to decompose the process into linear combinations of basis amplitudes. The fact that a projection formalism makes sense rests on the scalar quantities a_i being an explicit form of M_μ . That is,

$$\mathcal{M}(s, \theta, \sigma, \lambda = 1/2) = \bar{v}_n(p_{\bar{n}}, 1/2) M_\mu(p_\Delta, p_{\bar{n}}, k_\perp) u_\Delta^\mu(p_\Delta, \sigma), \quad (4.24)$$

$$\bar{v}_n(p_{\bar{n}}, 1/2) M_\mu(p_\Delta, p_{\bar{n}}, k_\perp) u_\Delta^\mu(p_\Delta, \sigma) = \sum_i a_i \bar{v}_n(p_{\bar{n}}, 1/2) M_i^\mu g_{\mu\nu} u_\Delta^\nu(p_\Delta, \sigma).$$

The amplitude M_μ includes the product of gamma matrices γ^μ and one γ_5 ; it can be contracted with p_n , p_Δ and k_\perp to be moved towards the spinor \bar{v}_n or u_Δ into the elements of M_μ . If we eliminate the contraction terms \not{p}_n , \not{p}_Δ and \not{k}_\perp by the equation of motion, there is only one term left, \not{k}_\perp . Supposing there are four possible objects $p_{\bar{n}}^\mu$, p_Δ^μ , k_\perp and γ^μ for the Lorentz index on M_μ that we can also reduce, we can eliminate the momentum p_Δ^μ and matrix γ^μ using the relation of the equation of motion. As a final result, this leaves us with four possible independent structures of the M^μ type;

$$\gamma_5 k_\perp^\mu, \quad \gamma_5 p_n^\mu, \quad \not{k}_\perp \gamma_5 p_n^\mu, \quad \not{k}_\perp \gamma_5 k_\perp^\mu. \quad (4.25)$$

We now describe the simplest form of spin structures (M^μ) with states indexed by ($i = 1, 2, 3, 4$) (Junker et al., 2020):

$$M_1^\mu = [q^2 - (m_\Delta + m_n)^2] \gamma_5 k_\perp^\mu - m_\Delta \not{k}_\perp \gamma_5 p_n^\mu, \quad (4.26)$$

$$\begin{aligned}
M_2^\mu &= \gamma_5 p_n^\mu, \\
M_3^\mu &= \not{k}_\perp \gamma_5 p_n^\mu, \\
M_4^\mu &= [q^2 - (m_\Delta - m_n)^2] \not{k}_\perp \gamma_5 \not{k}_\perp^\mu - m_\Delta \not{k}_\perp^\mu \gamma_5 p_n^\mu.
\end{aligned} \tag{4.27}$$

These four constructed structures of (M^μ) in the center-of-mass frame satisfy $(\bar{v}_n(p_n, +1/2) M_i^\mu g_{\mu\nu} u_\Delta^\nu(p_\Delta, \sigma) \sim \delta_{ii\Delta})$ with $(i_\Delta = 5/2 - \sigma)$. For the remaining task, we find the scalar quantity (a_i) for the amplitude (M^μ) . In general, there is still a need for a 64-basis decomposition of Lorentz-spinor structures since (M^μ) is a type of (4×4) spinor matrix with $(\mu = 1, 2, 3, 4)$. However, 32 basis elements of those are not parity-conserving, so we can restrict ourselves to a basis of 32 spinor structures. The first four terms at this point (Junker et al., 2020):

$$T_\mu^i = P_{on}^n M_i^\nu P_{on}^\Delta P_{\nu\mu}^{3/2} \tag{4.28}$$

with the projection operator ('t Hooft and Veltman, 1979):

$$\begin{aligned}
P_{on}^n &= \frac{1}{2m_n}(m_n - \not{p}_{\bar{n}}), & P_{off}^n &= \frac{1}{2m_n}(m_n + \not{p}_{\bar{n}}), \\
P_{on}^\Delta &= \frac{1}{2m_\Delta}(m_\Delta + \not{p}_\Delta), & P_{off}^\Delta &= \frac{1}{2m_\Delta}(m_\Delta - \not{p}_\Delta), \\
P_{\mu\nu}^{1/2} &= \frac{1}{3}\gamma_\mu\gamma_\nu + \frac{1}{3p_\Delta^2}(\not{p}_\Delta\gamma_\mu g_{\nu\alpha} + g_{\mu\alpha}\gamma_\nu \not{p}_\Delta)p_\Delta^\alpha, \\
P_{\mu\nu}^{3/2} &= g_{\mu\nu} - P_{\mu\nu}^{1/2}.
\end{aligned} \tag{4.29}$$

Throughout this evaluation part of this section, we do not deal with the specification of the other 28 structures from $i = 5$ to $i = 32$ because we do not need it at the end of our calculation. Therefore, we introduce the Dirac adjoint structures directly:

$$\bar{T}_\mu^i = \gamma_0 (T_\mu^i)^\dagger \quad \text{for } i = 1, \dots, 32. \tag{4.30}$$

Having inserted 32 elements of linearly independent structures for T_μ^i , we are now

free to decompose any M_μ via the following relation:

$$M_\mu = \sum_{i=1}^{32} a_i T_\mu^i, \quad \text{with } a_i = \sum_{j=1}^{32} (C^{-1})_{ij} \text{Tr}(\bar{T}_\mu^j M^\mu) \quad (4.31)$$

and the 32×32 matrix elements C represented by the spinor trace:

$$C_{ij} = \text{Tr}(\bar{T}_\mu^i T_\nu^j) g^{\mu\nu}. \quad (4.32)$$

Due to the basis elements C_{ij} themselves as an inner product, we consider them directly from the explicit calculation of $\det(C) \neq 0$, which shows that C is an invertible matrix and the 32 elements T_μ^i are linearly independent. Matrix C_{ij} is actually block diagonal since the different projection operators are zero in the inner product for two basis elements. We are only interested in the first four a_i block diagonal, that is,

$$C_{ij} = C_j \delta_{ji}, \quad \text{for } j, i = 1, 2, 3, 4. \quad (4.33)$$

And the explicit formalism that supports a term to determine the coefficient functions a_i for the complete set of linearly independent structures becomes:

$$a_i = \frac{\text{Tr}(\bar{T}_\mu^i M^\mu)}{C_i}, \quad \text{for } i = 1, 2, 3, 4, \quad (4.34)$$

with the definition of C_i :

$$C_i = \text{Tr}(\bar{T}_\mu^i T_\nu^i g^{\mu\nu}). \quad (4.35)$$

The consequent values for four explicit expressions C_i obtained numerically are

$$\begin{aligned} C_1 &= \frac{k_\perp^2}{4m_\Delta m_n} ((m_\Delta + m_n)^2 - q^2) \lambda(q^2, m_\Delta^2, m_n^2), \\ C_2 &= \frac{-1}{12m_\Delta^3 m_n} ((m_\Delta - m_n)^2 - q^2) \lambda(q^2, m_\Delta^2, m_n^2), \\ C_3 &= \frac{k_\perp^2}{12m_\Delta^3 m_n} ((m_\Delta + m_n)^2 - q^2) \lambda(q^2, m_\Delta^2, m_n^2), \end{aligned} \quad (4.36)$$

$$C_4 = \frac{-(k_\perp^2)^2}{4m_\Delta m_n} ((m_\Delta - m_n)^2 - q^2) \lambda(q^2, m_\Delta^2, m_n^2), \quad (4.37)$$

with the Källén function

$$\lambda(a, b, c) = a^2 + b^2 + c^2 - 2(ab + bc + ac) \quad (4.38)$$

and $k_\perp^2 = -4p_{c.m}^2 \sin^2 \theta$, where the center of mass momentum of the pions is $p_{c.m} = \sqrt{q^2 - 4m_\pi^2}/2$, and θ denotes the angle between the three momenta of Δ^0 and π^+ . As a summary, we find the general amplitude structure of M_μ with the best choice of the helicity amplitude σ :

$$\begin{aligned} \mathcal{M}(s, \theta, \sigma, \lambda = 1/2) &= \bar{v}_n(p_{\bar{n}}, 1/2) M_\mu(p_\Delta, p_{\bar{n}}, k_\perp) u_\Delta^\mu(p_\Delta, \sigma), \\ &= \frac{\text{Tr}(\bar{T}_\alpha^i M^\alpha)}{C_i} \bar{v}_n(p_{\bar{n}}, 1/2) M_i^\mu g_{\mu\nu} u_\Delta^\mu(p_\Delta, \sigma), \end{aligned} \quad (4.39)$$

where $i = 5/2 - \sigma$. The reduced amplitude dealing with Feynman scattering amplitude in the basis elements $\bar{v}_n M_i^\mu g_{\mu\nu} u_\Delta^\mu$ for the dispersive representation;

$$\begin{aligned} \frac{\bar{v}_n(-p_z, +1/2) M_1^\mu g_{\mu\nu} u_\Delta^\mu(p_z, +3/2)}{\bar{v}_n(-p_z, +1/2) \gamma_5 u_\Delta^1(p_z, +3/2) p_{c.m}} &= 2 \sin \theta (q^2 - (m_\Delta + m_n)^2), \\ \frac{\bar{v}_n(-p_z, +1/2) M_2^\mu g_{\mu\nu} u_\Delta^\mu(p_z, +1/2)}{\bar{v}_n(-p_z, +1/2) \gamma_5 u_\Delta^3(p_z, +3/2) p_{c.m}} &= \frac{2q^2 p_z}{(m_\Delta^2 - m_n^2 + q^2) p_{c.m}}, \\ \frac{\bar{v}_n(-p_z, +1/2) M_3^\mu g_{\mu\nu} u_\Delta^\mu(p_z, -1/2)}{\bar{v}_n(-p_z, +1/2) \gamma_5 u_\Delta^1(p_z, +3/2) p_{c.m}} &= \frac{-2 \sin \theta (q^2 - (m_\Delta + m_n)^2)}{m_\Delta}, \end{aligned} \quad (4.40)$$

with $p_z = \lambda^{1/2}(q^2, m_\Delta^2, m_n^2)/(2\sqrt{q^2})$ in the z direction. As a next task, we find the values of helicity amplitudes using the mathematical expression of reduced amplitudes formulated by the spinor coefficient.

4.4 Helicity amplitudes

In dispersion theory for form factors, the two-step procedure is used to evaluate the structure of pion-baryon amplitudes. One of the formal inputs to this procedure is a set of helicity amplitudes. A detailed evaluation of all

dispersion integral formulations related to the pion rescattering contribution has been carried out (Granados et al., 2017). Therefore, we can directly include the helicity amplitudes of the reaction $\Delta^0 \bar{n} \rightarrow \pi^+ \pi^-$, which excludes the effects of two-pion rescattering in the center-of-mass frame.

$$\begin{aligned}
 K_{\pm 1}(s) &= -\frac{3}{4} \int_0^\pi d\theta \sin^2 \theta \frac{\mathcal{M}(s, \theta, 1/2 \pm 1, 1/2)}{\bar{v}_n(-p_z, +1/2) \gamma_5 u_\Delta^1(p_z, 1/2 \pm 1) p_{c.m.}}, \\
 K_0(s) &= -\frac{3}{2} \frac{m_\Delta^2 - m_n^2 + s}{2s} \int_0^\pi d\theta \sin \theta \cos \theta \\
 &\quad \frac{\mathcal{M}(s, \theta, 1/2, 1/2)}{\bar{v}_n(-p_z, +1/2) \gamma_5 u_\Delta^3(p_z, 1/2) p_{c.m.}}.
 \end{aligned} \tag{4.41}$$

Substituting Eq. (4.39) and Eq. (4.40) into the above Eq. (4.41), the helicity amplitudes become:

$$\begin{aligned}
 K_{+1}(s) &= \frac{3}{2} \int_\pi^0 d(\cos \theta) (1 - \cos^2 \theta) \frac{\text{Tr}(\bar{T}_v^1 M^\nu)}{C_1} (s - (m_\Delta + m_n)^2), \\
 K_{-1}(s) &= \frac{3}{2} \int_\pi^0 d(\cos \theta) (1 - \cos^2 \theta) \frac{\text{Tr}(\bar{T}_v^3 M^\nu)}{C_3} \frac{(s - (m_\Delta + m_n)^2)}{m_\Delta}, \\
 K_0(s) &= -\frac{3}{2} \int_\pi^0 d(\cos \theta) \cos \theta \frac{\text{Tr}(\bar{T}_v^2 M^\nu)}{C_2} \frac{p_z}{p_{c.m.}}.
 \end{aligned} \tag{4.42}$$

Projector formalism simplifies the evaluation of helicity amplitudes involving delta and proton exchange. This formalism allows us to separate and identify the contributions from left-hand cuts (represented by coefficient functions) and purely polynomial terms (denoted by P). Explicit expressions for the helicity amplitudes obtained from the left-hand-cut structures are:

$$\begin{aligned}
 K_{+1} &= -\frac{g_A h_A}{4\sqrt{6}F_\pi^2} (C_{+1} + D_{+1} R_s^{\text{oct}}) - \frac{5h_A H_A}{12\sqrt{6}F_\pi^2} (E_{+1} + F_{+1} R_s^{\text{dec}}), \\
 K_{-1} &= -\frac{g_A h_A}{4\sqrt{6}F_\pi^2} (C_{-1} + D_{-1} R_s^{\text{oct}}) - \frac{5h_A H_A}{12\sqrt{6}F_\pi^2} (E_{-1} + F_{-1} R_s^{\text{dec}}), \\
 K_0 &= -\frac{g_A h_A}{4\sqrt{6}F_\pi^2} (C_0 + D_0 R_d^{\text{oct}}) - \frac{5h_A H_A}{12\sqrt{6}F_\pi^2} (E_0 + F_0 R_d^{\text{dec}}).
 \end{aligned} \tag{4.43}$$

All constant parameters, including the contact polynomial subtraction term (P_m), are listed in Appendix (D).



CHAPTER V

DIFFERENTIAL DALITZ DECAY OF BARYONS

In this section, the decay rates and differential cross-sections for the transition form factors in the processes: $\Delta^0 \rightarrow N\gamma$, Dalitz decay $\Delta^0 \rightarrow Ne^+e^-$, and $e^+e^- \rightarrow \bar{\Delta}^0 N$ scattering are presented. The primary objective is to extract the fundamental intrinsic properties of baryons and measure the precision of the q^2 dependence of form factors in the time-like region with respect to the Dalitz decay distribution. To ensure comprehensive coverage, we present the complete expression of the decay rate Γ for the process $\Delta^0 \rightarrow N\gamma \rightarrow Ne^+e^-$, as well as for the process $e^+e^- \rightarrow \bar{\Delta}^0 N$. These expressions are derived according to the Feynman rules of QED (Peskin and Schroeder, 1995), and with additional insights drawn from lecture notes authored by Stefan Leupold on EFT (Leupold and Terschlusen, 2012) and QCD (Scherer and Schindler, 2012b).

5.1 Decay width of Dalitz decay $\Delta^0 \rightarrow Ne^+e^-$

Both decay rate and differential decay rate lie in the evaluation of the Feynman matrix element for the two processes under the one-photon approximation. The decay rate for the delta particle, taking the form,

$$d\Gamma = \frac{1}{2M} |m_{1 \rightarrow n}|^2 \underbrace{(2\pi)^4 \delta^{(4)} \left(P - \sum_{j=1}^n p_j \right) \prod_{j=1}^n \frac{d^3 p_j}{(2\pi)^3 2E_j}}_{\text{Phasespace}}, \quad (5.1)$$

where M measured in its rest frame $P = (M, \vec{0})$. This particle decays into n particles with masses m_j and momenta q_i , where $i = 1, \dots, n$, and $d^3 p_j$ denotes the volume elements, as outlined in the reference by Peskin and Schroeder (Peskin and Schroeder, 1995).

A Lorentz-invariant quantity known as the spin-averaged amplitude is

defined as follows:

$$\langle |m|^2 \rangle = \frac{1}{D} \sum_{s_i, s_f} |m|^2, \quad (5.2)$$

$$D = \prod_{i=1}^N (2s_i + 1),$$

with spins of the incoming particle N , $i = 1, \dots, N$. The general form of the electromagnetic current expectation value for the transition between initial and final baryon states is expressed as follows:

$$\langle B(p_{out}) | j^\mu(0) | B(p_{in}) \rangle = e \bar{u}(p_{out}) \Gamma^\mu u(p_{in}), \quad (5.3)$$

with Γ^μ being the vertex function for all possible independent Lorentz covariant interaction terms:

$$\begin{aligned} \Gamma^{\mu\nu}(p_\Delta, q) = & -(\gamma^\mu q^\nu - \not{q} g^{\mu\nu}) m_\Delta \gamma_5 F_1(q^2) \\ & + (p_\Delta^\mu q^\nu - p_\Delta \cdot q g^{\mu\nu}) \gamma_5 F_2(q^2) \\ & + (q^\mu q^\nu - q^2 g^{\mu\nu}) \gamma_5 F_3(q^2). \end{aligned} \quad (5.4)$$

Similarly, the complex conjugate values of the vertex function takes the form:

$$\begin{aligned} \bar{\Gamma}^{\mu\nu}(p_\Delta, q) = & (\gamma^\mu q^\nu - \not{q} g^{\mu\nu}) m_\Delta \gamma_5 F_1^*(q^2) \\ & - (p_\Delta^\mu q^\nu - p_\Delta \cdot q g^{\mu\nu}) \gamma_5 F_2^*(q^2) \\ & - (q^\mu q^\nu - q^2 g^{\mu\nu}) \gamma_5 F_3^*(q^2). \end{aligned} \quad (5.5)$$

To obtain a simpler form, the Mandelstam variables is specified in terms of the basic kinematics of the decay, such as the energy and momentum of the particles being considered, at a particular reference frame, which takes the form:

$$\begin{aligned} s &= (p_\Delta + p_n)^2 = (p_{e^+} + p_{e^-})^2 = m_{12}^2 = q^2, \\ t &= (p_\Delta - p_{e^+})^2 = (p_{e^-} + p_n)^2 = m_{23}^2, \end{aligned} \quad (5.6)$$

$$u = (p_\Delta - p_{e^-})^2 = (p_{e^+} + p_n)^2, \quad (5.7)$$

with the identity relation of the Mandelstam variables,

$$s + t + u = m_e^2 + m_e^2 + m_\Delta^2 + m_n^2. \quad (5.8)$$

The Dalitz process $\Delta^0 \rightarrow Ne^+e^-$ is straightforwardly written to the Feynman matrix element by applying the Feynman rules of spinors, vertex functions, and the propagating photon fields mentioned above. As shown in Figure 5.1, the general form of amplitude reads

$$\begin{aligned} \mathcal{M} &= \bar{u}_{e^-}(p_{e^-}, s_{e^-}) (-ie\gamma_\mu) v_{e^+}(p_{e^+}, s_{e^+}) \left(-i\frac{g^{\mu\nu}}{q^2}\right) e\bar{u}_n(p_n, s_n) \Gamma^\nu u^\Delta(p_\Delta, s_\Delta), \\ &= -\frac{e^2}{q^2} \bar{u}_{e^-}(p_{e^-}, s_{e^-}) \gamma_\mu v_{e^+}(p_{e^+}, s_{e^+}) \bar{u}_n(p_n, s_n) \Gamma^{\mu\nu} u_\nu^\Delta(p_\Delta, s_\Delta), \end{aligned} \quad (5.9)$$

with the corresponding hermitian conjugate being represented by

$$\mathcal{M}^\dagger = -\frac{e^2}{q^2} \bar{u}_\beta^\Delta(p_\Delta, s_\Delta) \bar{\Gamma}^{\alpha\beta} u_n(p_n, s_n) \bar{v}_{e^+}(p_{e^+}, s_{e^+}) \gamma_\alpha u_{e^-}(p_{e^-}, s_{e^-}). \quad (5.10)$$

Assuming there are four possible orientations for the incoming spin 3/2 particle, i.e., the factor $D = 2 \times \frac{3}{2} + 1 = 4$, we will aggregate all possibilities below to obtain the average amplitude for the desired decay $\Delta^0 \rightarrow Ne^+e^-$, which takes the form:

$$\begin{aligned} \langle |\mathcal{M}_{\Delta \rightarrow Ne^+e^-}|^2 \rangle &= \frac{e^4}{4q^4} \sum_{s_{e^-}, s_{e^+}, s_\Delta, s_n} \\ &\times \left(\bar{u}_{e^-}(p_{e^-}, s_{e^-}) \gamma_\mu v_{e^+}(p_{e^+}, s_{e^+}) \bar{u}_n(p_n, s_n) \Gamma^{\mu\nu} u_\nu^\Delta(p_\Delta, s_\Delta) \right) \\ &\times \left(\bar{u}_\beta^\Delta(p_\Delta, s_\Delta) \bar{\Gamma}^{\alpha\beta} u_n(p_n, s_n) \bar{v}_{e^+}(p_{e^+}, s_{e^+}) \gamma_\alpha u_{e^-}(p_{e^-}, s_{e^-}) \right), \quad (5.11) \\ &= \frac{e^4}{4q^4} \sum_{s_{e^-}, s_{e^+}, s_\Delta, s_n} (\bar{u}_{e^-})_i (\gamma_\mu)_{ij} (v_{e^+})_j (\bar{v}_{e^+})_k (\gamma_\alpha)_{kl} (u_{e^-})_l \\ &\quad (\bar{u}_n)_a (\Gamma^{\mu\nu})_{ab} (u_\nu^\Delta)_b (\bar{u}_\beta^\Delta)_c (\bar{\Gamma}^{\alpha\beta})_{cd} (u_n)_d, \end{aligned}$$

$$\begin{aligned}
\langle |m_{\Delta \rightarrow Ne^+e^-}|^2 \rangle &= \frac{e^4}{4q^4} \sum_{s_{e^-}} (u_{e^-})_l (\bar{u}_{e^-})_i (\gamma_\mu)_{ij} \sum_{s_{e^+}} (v_{e^+})_j (\bar{v}_{e^+})_k (\gamma_\alpha)_{kl} \\
&\quad \sum_{s_n} (u_n)_d (\bar{u}_n)_a (\Gamma^{\mu\nu})_{ab} \sum_{s_\Delta} (u_\nu^\Delta)_b (\bar{u}_\beta^\Delta)_c (\bar{\Gamma}^{\alpha\beta})_{cd}, \\
&= -\frac{e^4}{4q^4} (\not{p}_{e^-} + m_{e^-})_{li} (\gamma_\mu)_{ij} (\not{p}_{e^+} - m_{e^+})_{jk} (\gamma_\alpha)_{kl} \\
&\quad (\not{p}_n + m_n)_{da} (\Gamma^{\mu\nu})_{ab} (\not{p}_\Delta + m_\Delta)_{bc} P_{\nu\beta} (\bar{\Gamma}^{\alpha\beta})_{cd}, \\
&= -\frac{e^4}{4q^4} \text{Tr} \left[(\not{p}_{e^-} + m_{e^-}) \gamma_\mu (\not{p}_{e^+} - m_{e^+}) \gamma_\alpha \right] \\
&\quad \text{Tr} \left[(\not{p}_n + m_n) \Gamma^{\mu\nu} (\not{p}_\Delta + m_\Delta) P_{\nu\beta} \bar{\Gamma}^{\alpha\beta} \right].
\end{aligned} \tag{5.12}$$

This is a full expression of the spin-average amplitude in terms of the variables s , t and u . Later, as a result, it will actually contain the mixing terms of constrained form factors $G_m(q^2)$. However, we make it clear that we intend to eliminate all mixing FF terms from the amplitude by substituting u with the help of relation in Eq. (5.8). The numerical method for the double differential decay rate, as outlined in Junker's thesis (Junker et al., 2020), is initiated in the center-of-mass frame and expressed using a bilinear form, which takes the following form:

$$\left(\frac{d\Gamma}{dm_{12}^2 dm_{23}^2} \right) (q^2, t) = F^\dagger(q^2) A(q^2, t) F(q^2). \tag{5.13}$$

Here, the matrix representation of $A(q^2, t)$ obtains from the spin-averaged amplitude, and the representations of form factors $F^\dagger(q^2)$ and $F(q^2)$ take the form:

$$F(q^2) = \begin{pmatrix} F_1(q^2) \\ F_2(q^2) \\ F_3(q^2) \end{pmatrix}, \quad F^\dagger(q^2) = (F_1^*(q^2), F_2^*(q^2), F_3^*(q^2)). \tag{5.14}$$

Note that it is still mixing form factors when we calculate the amplitude terms with respect to form factors definition. Thus, a new quadratic relation is defined below based on the bilinear form in order to get only the diagonalization terms

via

$$\left(\frac{d\Gamma}{dm_{12}^2 dm_{23}^2} \right) (q^2, t) = G^\dagger(q^2) D(q^2, t) G(q^2), \quad (5.15)$$

with the new representation of form factors,

$$G(q^2) = \begin{pmatrix} G_1(q^2) \\ G_2(q^2) \\ G_3(q^2) \end{pmatrix}, \quad G^\dagger(q^2) = (G_1^*(q^2), G_2^*(q^2), G_3^*(q^2)), \quad (5.16)$$

which can be transformed as

$$G(q^2) = T(q^2) \cdot F(q^2), \quad F(q^2) = T^{-1}(q^2) G(q^2). \quad (5.17)$$

It is implied a diagonalize matrix for the argument of $D(q^2, t)$, so we can rewrite it as the following form:

$$\left(\frac{d\Gamma}{dm_{12}^2 dm_{23}^2} \right) (q^2, t) = G^\dagger(q^2) (T^{-1}(q^2))^\dagger A(q^2, t) T(q^2) G(q^2), \quad (5.18)$$

with the transformation matrix being defined by the fixed helicity amplitudes Eq. (3.21) and Eq. (3.23)

$$T(q^2) = \begin{pmatrix} m_\Delta(m_\Delta + m_n) & \frac{1}{2}(m_\Delta^2 - m_n^2 + q^2) & q^2 \\ m_\Delta^2 & m_\Delta^2 & \frac{1}{2}(m_\Delta^2 - m_n^2 + q^2) \\ -m_n(m_\Delta + m_n) + q^2 & \frac{1}{2}(m_\Delta^2 - m_n^2 + q^2) & q^2 \end{pmatrix}, \quad (5.19)$$

where the inverse matrix takes the form

$$T^{-1}(q^2) = \begin{pmatrix} \frac{1}{((m_\Delta + m_n)^2 - q^2)} & 0 & \frac{-1}{((m_\Delta + m_n)^2 - q^2)} \\ \frac{2(-m_n^2 + m_\Delta m_n + q^2)}{\lambda(q^2, m_\Delta^2, m_n^2)} & \frac{-4q^2}{\lambda(q^2, m_\Delta^2, m_n^2)} & \frac{2(m_\Delta^2 - m_\Delta m_n)}{\lambda(q^2, m_\Delta^2, m_n^2)} \\ \frac{-2m_\Delta^2}{\lambda(q^2, m_\Delta^2, m_n^2)} & \frac{2(-m_n^2 + m_\Delta^2 + q^2)}{\lambda(q^2, m_\Delta^2, m_n^2)} & \frac{-2m_\Delta^2}{\lambda(q^2, m_\Delta^2, m_n^2)} \end{pmatrix}, \quad (5.20)$$

with the Källén function

$$\lambda(x, y, z) = x^2 + y^2 + z^2 - 2(xy + yz + zx). \quad (5.21)$$

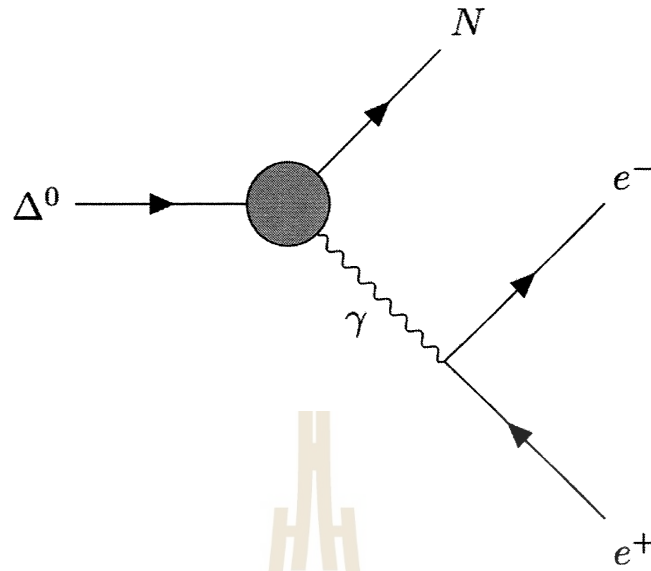


Figure 5.1 Sketch of Feynman of Dalitz decay $\Delta^0 \rightarrow Ne^+e^-$ with respect to the one-photon approximation. Here, the baryon vertex is represented by a gray blob and the QED vertex is denoted with $e^-e^+\gamma$.

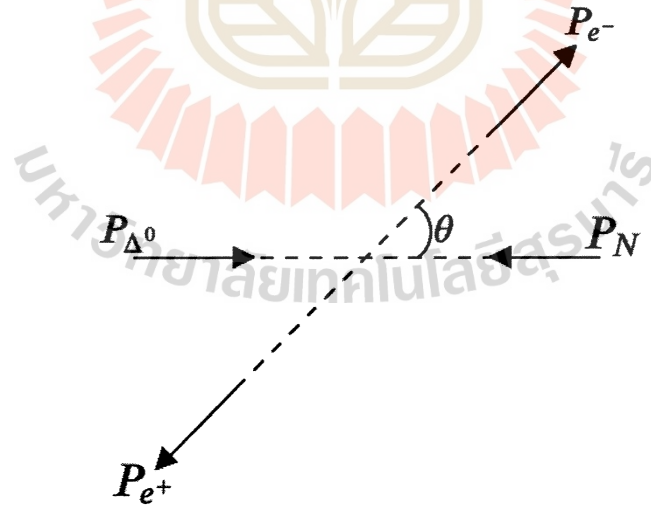


Figure 5.2 Graphic representation of the Dalitz decay $\Delta^0 \rightarrow Ne^-e^+$ in the C-M frame.

For Dalitz case, we may define the coordinate system of particles in alignment with the trajectory of polar angle θ between the direction of electron and nucleon at the center of mass frame. All observables of Feynman matrix

elements for decay are dependent of Lorentz invariant, so that it is convenient to assign the Lorentz scalar quantities in the center of mass frame, see in Figure 5.2. From now on, the kinematic t will be replaced by the choice of definition Eq. (5.22) in the numerical calculation.

$$t = m_{23}^2 = m_e^2 + m_n^2 + 2E_e E_n - 2|\vec{p}_e| |\vec{p}_n| \cos \theta. \quad (5.22)$$

As a next step, we carry out the phase space integration for the Dalitz decay by setting the momentum of mother particle P with the corresponding mass m_Δ and energy E , while the outgoing momenta refer to the symbols p_1, p_2, p_3 instead of p_{e^+}, p_{e^-}, p_n . The masses of decay particles refer to m_1, m_2, m_3 and the energies of each state is represented by E_1, E_2, E_3 . The whole double differential decay rate in the rest frame reads

$$\begin{aligned} \frac{d\Gamma}{dm_{12}^2 dm_{23}^2} &= \frac{\langle |m_{\Delta \rightarrow Ne^+e^-}|^2 \rangle}{2m_\Delta} \int \prod_{i=1}^3 \frac{dp_i (2\pi)^4}{(2\pi)^3 2E_i} \delta^{(4)}(P - p_1 - p_2 - p_3) \\ &\quad \times \delta(m_{12}^2 - (p_1 + p_2)^2) \delta(m_{23}^2 - (p_2 + p_3)^2), \\ &= \frac{\langle |m_{\Delta \rightarrow Ne^+e^-}|^2 \rangle}{2m_\Delta} \underbrace{\int \frac{dp_1}{(2\pi)^3 2E_1} \frac{dp_2}{(2\pi)^3 2E_2} \frac{dp_3}{(2\pi)^3 2E_3} (2\pi)^4}_{\text{Phasespace}} \\ &\quad \times \underbrace{\delta^{(4)}(P - p_1 - p_2 - p_3) \delta(m_{12}^2 - (p_1 + p_2)^2) \delta(m_{23}^2 - (p_2 + p_3)^2)}_{\text{Phasespace}}. \end{aligned} \quad (5.23)$$

The detail calculation of the phase space intergration for the double differential decay rate is provided in the Appendix (H). Thus, the final expression of the double differential decay rate for Dalitz decay $\Delta^0 \rightarrow Ne^+e^-$ in a given frame can be written in the form

$$\frac{d\Gamma}{dm_{12}^2 dm_{23}^2} = \frac{1}{32m_\Delta^3 (2\pi)^3} \langle |m_{\Delta \rightarrow Ne^+e^-}|^2 \rangle. \quad (5.24)$$

In the fixed photon approximation, one can express the differentials for the

observable momenta $|\vec{p}_\Delta|$ and $|\vec{p}_{e^-}|$ as:

$$\begin{aligned} dm_{23}^2 &= -2|\vec{p}_{e^-}||\vec{p}_\Delta|d\cos\theta, \quad (\because |\vec{p}_\Delta| = |\vec{p}_n|) \\ dm_{12}^2 &= dq^2. \end{aligned} \quad (5.25)$$

Inserting Eq. (5.25) into Eq. (5.24), it supports us to get the final simplest form

$$\frac{d\Gamma}{dq^2 d\cos\theta} = \frac{-2|\vec{p}_{e^-}||\vec{p}_\Delta|}{32(p_\Delta^2)^{3/2}(2\pi)^3} \langle |m_{\Delta \rightarrow Ne^+e^-}|^2(q^2, \theta) \rangle. \quad (5.26)$$

When the results of the amplitude obtained from using the FeynCalc package in Mathematica, with the replacement of the variables s and t by the definition in Eq. (5.22), and the angle θ is substituted into Eq. (5.24), we get

$$\begin{aligned} \frac{d\Gamma}{dq^2 d\cos\theta} &= \frac{1}{(2\pi)^3} \frac{e^4 |\vec{p}_\Delta| |\vec{p}_{e^-}|}{96m_\Delta^3 q^2} (q^2 - (m_\Delta - m_n)^2) \\ &\times \left[\left(1 + \cos^2\theta + \frac{4m_e^2}{q^2} \sin^2\theta \right) \right. \\ &\times (3|G_{+1}(q^2)|^2 + |G_{-1}(q^2)|^2) \\ &\left. + 4 \left(\sin^2\theta + \frac{4m_e^2}{q^2} \cos^2\theta \right) \frac{q^2}{m_\Delta^2} |G_0(q^2)|^2 \right], \end{aligned} \quad (5.27)$$

with the momenta of the Δ and e being evaluated in the rest frame at $\vec{q}=0$;

$$|\vec{p}_{e^-}| = \sqrt{\frac{q^2}{4} - m_e^2}, \quad p_z \equiv |\vec{p}_\Delta| = \frac{\lambda^{1/2}(q^2, m_\Delta^2, m_n^2)}{2\sqrt{q^2}}. \quad (5.28)$$

As a remarkable feature, the kinematic boundaries for the Dalitz decay allow exploration up to the range of the timelike region.

$$4m_e^2 \leq q^2 \leq (m_\Delta - m_n)^2, \quad (5.29)$$

and the factor values of $q^2 - (m_\Delta + m_n)^2$ and $q^2 - (m_\Delta - m_n)^2$ are always non-positive. However, if one integrates the scattering angle θ over the range from 0 to π , the total decay rate is indeed positive physically, as this θ integration gives an essential

minus sign for the decay process. Again, assuming that the kinematical boundaries for $m_e^2 \ll q^2$ and $m_e^2 \ll m_\Delta^2$ in the fixed photon approximation, the θ -dependence of the double-differential decay width is expressed:

$$\begin{aligned} \frac{d\Gamma}{dq^2 d\cos\theta} &= \frac{1}{(2\pi)^3} \frac{e^4 p_z}{96m_\Delta^3 q^2} \frac{\sqrt{q^2}}{2} \beta_e (q^2 - (m_\Delta - m_n)^2) \\ &\times [(1 + \cos^2\theta) (3|G_{+1}(q^2)|^2 + |G_{-1}(q^2)|^2) \\ &+ \frac{4q^2}{m_\Delta^2} \sin^2\theta |G_0(q^2)|^2], \end{aligned} \quad (5.30)$$

with the kinematical electron velocity being presented by

$$\beta_e = \sqrt{1 - \frac{4m_e^2}{q^2}}. \quad (5.31)$$

The electromagnetic Dalitz decay, which explores the strong interaction dynamics at a given kinetic energy of 1.2 GeV, has been successfully studied through proton-proton collisions at the HADES collaboration with GSI (Adamczewski-Musch et al., 2017). With the described electromagnetic transition form factors (eTFFs) yielding $G_M^* \approx 3$, $G_E^* \approx 0$, and $G_C^* \approx 0$, and the provided decay width $\Gamma_{\Delta \rightarrow N\gamma} = 0.66$ MeV, we now derive the generic formula for $\Gamma_{\Delta \rightarrow Ne^+e^-}$ in terms of the Jone-Scadron FFs as a function of q^2 . It is convenient to introduce with our FFs $G_{\pm 1,0}$ correlated to Jone-Scadron FFs through the translational relations:

$$\begin{aligned} (3|G_{+1}(q^2)|^2 + |G_{-1}(q^2)|^2) &= \frac{3}{2} \left(\frac{m_\Delta + m_n}{m_n} \right)^2 (3|G_E^*(q^2)|^2 + |G_M^*(q^2)|^2), \\ |G_0(q^2)|^2 &= \frac{3}{8} \left(\frac{m_\Delta + m_n}{m_n} \right)^2 |G_C^*(q^2)|^2. \end{aligned} \quad (5.32)$$

Since we focus on the angular θ intergration from π to 0 in the given relation

Eq. (5.30) analytically, we can get:

$$\begin{aligned} \frac{d\Gamma}{dq^2} &= \frac{e^4}{(2\pi)^3 96m_\Delta^3 q^2} p_z \frac{\sqrt{q^2}}{2} \beta_e ((m_\Delta - m_n)^2 - q^2) \\ &\times \int_{-1}^1 dx \left[(1+x^2) (3|G_{+1}(q^2)|^2 + |G_{-1}(q^2)|^2) \right. \\ &\quad \left. + \frac{4q^2}{m_\Delta^2} (1-x^2) |G_0(q^2)|^2 \right]. \end{aligned} \quad (5.33)$$

With the substitution of formula Eq. (5.32), the decay width can be reduced to the simplest form

$$\begin{aligned} \frac{d\Gamma}{dq^2} &= \frac{e^4}{(2\pi)^3 96m_\Delta^3 q^2} p_z \frac{\sqrt{q^2}}{2} \beta_e ((m_\Delta - m_n)^2 - q^2) \times \frac{3}{2} \left(\frac{m_\Delta + m_n}{m_n} \right)^2 \\ &\times \int_{-1}^1 dx \left[\left((3|G_E^*(q^2)|^2 + |G_M^*(q^2)|^2) + \frac{q^2}{m_\Delta^2} |G_C^*(q^2)|^2 \right) \right. \\ &\quad \left. + x^2 \left((3|G_E^*(q^2)|^2 + |G_M^*(q^2)|^2) - \frac{q^2}{m_\Delta^2} |G_C^*(q^2)|^2 \right) \right], \\ &= \frac{e^4}{(2\pi)^3 64m_\Delta^3 q^2} p_z \frac{\sqrt{q^2}}{2} \beta_e ((m_\Delta - m_n)^2 - q^2) \left(\frac{m_\Delta + m_n}{m_n} \right)^2 \\ &\times \left[2 \left((3|G_E^*(q^2)|^2 + |G_M^*(q^2)|^2) + \frac{q^2}{m_\Delta^2} |G_C^*(q^2)|^2 \right) \right. \\ &\quad \left. + \frac{2}{3} \left((3|G_E^*(q^2)|^2 + |G_M^*(q^2)|^2) - \frac{q^2}{m_\Delta^2} |G_C^*(q^2)|^2 \right) \right], \\ \frac{d\Gamma}{dq^2} &= a(q^2) \left(2 + \frac{2}{3} b(q^2) \right), \end{aligned} \quad (5.34)$$

where the two parameters $a(q^2)$ and $b(q^2)$ are defined in accordance with (Bratkovskaya et al., 1995) for a comparison to the QED-type case, taking

the form

$$a(q^2) = \frac{e^4}{(2\pi)^3 64 m_\Delta^3 q^2} p_z \frac{\sqrt{q^2}}{2} \beta_e ((m_\Delta - m_n)^2 - q^2) \left(\frac{m_\Delta + m_n}{m_n} \right)^2 \times \left((3|G_E^*(q^2)|^2 + |G_M^*(q^2)|^2) + \frac{q^2}{m_\Delta^2} |G_C^*(q^2)|^2 \right), \quad (5.35)$$

$$b(q^2) = \frac{(3|G_E^*(q^2)|^2 + |G_M^*(q^2)|^2) - \frac{q^2}{m_\Delta^2} |G_C^*(q^2)|^2}{(3|G_E^*(q^2)|^2 + |G_M^*(q^2)|^2) + \frac{q^2}{m_\Delta^2} |G_C^*(q^2)|^2}.$$

For more convenience, we define new parameters based on the two q^2 -dependent parameters by

$$A = \int dq^2 a(q^2), \quad B = \int dq^2 b(q^2). \quad (5.36)$$

In the time-like eTFFs, a QED type determination of the Dalitz decay can be related to the intrinsic structure of baryon coupling by a virtual photon. Such a type of QED version of the Dalitz width in the one-photon approximation introduces

$$\frac{d\Gamma_{\text{QED}}}{dq^2 d\cos\theta} = \frac{e^4}{(2\pi)^3 96 m_\Delta^3 q^2} p_z \frac{\sqrt{q^2}}{2} \beta_e ((m_\Delta - m_n)^2 - q^2) \times \left(1 + \cos^2\theta + \frac{4m_e^2}{q^2} \sin^2\theta \right) (3|G_{+1}(0)|^2 + |G_{-1}(0)|^2). \quad (5.37)$$

In this case, we replace Jones-Scadron TFFs combinations described in the relation of Eq. (5.32) so as to compare with the parameter results in the width $\Gamma_{\Delta \rightarrow Ne^+e^-}$. The newly modified formula is then given by

$$\frac{d\Gamma_{\text{QED}}}{dq^2 d\cos\theta} = \frac{e^4}{(2\pi)^3 96 m_\Delta^3 q^2} p_z \frac{\sqrt{q^2}}{2} \beta_e ((m_\Delta - m_n)^2 - q^2) \times \left(1 + \cos^2\theta + \frac{4m_e^2}{q^2} - \frac{4m_e^2}{q^2} \cos^2\theta \right) \times \frac{3}{2} \left(\frac{m_\Delta + m_n}{m_n} \right)^2 (3|G_E^*(0)|^2 + |G_M^*(0)|^2), \quad (5.38)$$

$$\begin{aligned}
\frac{d\Gamma_{\text{QED}}}{dq^2 d\cos\theta} &= \frac{e^4}{(2\pi)^3 64m_\Delta^3 q^2} p_z \frac{\sqrt{q^2}}{2} \beta_e \frac{((m_\Delta - m_n)^2 - q^2)}{q^2} \\
&\times ((q^2 + 4m_e^2) + (q^2 - 4m_e^2) \cos^2 \theta) \\
&\times \left(\frac{m_\Delta + m_n}{m_n} \right)^2 (3|G_E^*(0)|^2 + |G_M^*(0)|^2).
\end{aligned} \tag{5.39}$$

Noticeably, this expression no longer depends on the electric and magnetic form factors when we set it equal to the real photon case $q^2 = 0$. From Eq. (5.39), the two quantities which have a similar type to our Dalitz case are identified smoothly as:

$$\begin{aligned}
\frac{d\Gamma_{\text{QED}}}{dq^2 d\cos\theta} &= a(q^2) (1 + b(q^2) \cos^2 \theta), \\
\frac{d\Gamma_{\text{QED}}}{dq^2} &= a(q^2) \left(2 + \frac{2}{3} b(q^2) \right),
\end{aligned} \tag{5.40}$$

with the identified parameters being referred to

$$\begin{aligned}
a(q^2) &= \frac{e^4 p_z}{(2\pi)^2 64m_\Delta^3 q^2} \frac{\sqrt{q^2}}{2} \beta_e \frac{((m_\Delta - m_n)^2 - q^2)}{q^2} \left(\frac{m_\Delta + m_n}{m_n} \right)^2 \\
&\times (q^2 + 4m_e^2) (3|G_E^*(0)|^2 + |G_M^*(0)|^2), \\
b(q^2) &= \frac{(q^2 - 4m_e^2)}{(q^2 + 4m_e^2)}.
\end{aligned} \tag{5.41}$$

5.2 Decay width of two-body decay $\Delta^0 \rightarrow N\gamma$

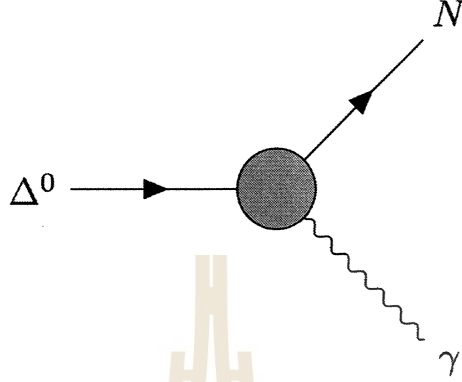


Figure 5.3 Sketch of Feynman diagram for the two-body decay $\Delta^0 \rightarrow N\gamma$.

We will now focus solely on evaluating the matrix element for the specific scenario of the two-body decay width of $\Delta^0 \rightarrow n\gamma$, shown in Figure 5.3. However, the particular process does not involve the decay of particles from a real photon to an electron-positron pair. Thus, all of the Feynman matrix elements, including their conjugates, can be derived by applying the Feynman rules as follows:

$$\begin{aligned}
 \mathcal{M} &= -ie \bar{u}_n(p_n, s_n) \epsilon_\mu^*(q, s_\gamma) \Gamma^{\mu\nu} u_\nu^\Delta(p_\Delta, s_\Delta), \\
 &= -ie \bar{u}_n(p_n, s_n) \Gamma^{\mu\nu} u_\nu^\Delta(p_\Delta, s_\Delta) \epsilon_\mu^*(q, s_\gamma), \\
 \mathcal{M}^\dagger &= ie \epsilon_\alpha(q, s_\gamma) \bar{u}_\beta^\Delta(p_\Delta, s_\Delta) \bar{\Gamma}^{\alpha\beta} u_n(p_n, s_n).
 \end{aligned} \tag{5.42}$$

Here, $\Gamma^{\mu\nu}$ is the vertex function, and $\epsilon_\alpha(q, s_\gamma)$ is the transverse polarization vector of photon. Since there are four possibility states for the incoming particle Δ ($D=4$), the spin-averaged amplitude of the two-body decay takes the form:

$$\begin{aligned}
 \langle |m_{\Delta \rightarrow n\gamma}|^2 \rangle &= \frac{e^2}{4} \sum_{s_\Delta, s_n, s_\gamma} \left[\bar{u}_n(p_n, s_n) \Gamma^{\mu\nu} u_\nu^\Delta(p_\Delta, s_\Delta) \epsilon_\mu^*(q, s_\gamma) \right] \\
 &\quad \times \left[\epsilon_\alpha(q, s_\gamma) \bar{u}_\beta^\Delta(p_\Delta, s_\Delta) \bar{\Gamma}^{\alpha\beta} u_n(p_n, s_n) \right],
 \end{aligned} \tag{5.43}$$

$$\begin{aligned}
\langle |m_{\Delta \rightarrow n\gamma}|^2 \rangle &= \frac{e^2}{4} \sum_{s_\gamma} \epsilon_\mu^*(q, s_\gamma) \epsilon_\alpha(q, s_\gamma) \sum_{s_n} u_n(p_n, s_n) \bar{u}_n(p_n, s_n) \Gamma^{\mu\nu} \\
&\quad \times \sum_{s_\Delta} u_v^\Delta(p_\Delta, s_\Delta) \bar{u}_\beta^\Delta(p_\Delta, s_\Delta) \bar{\Gamma}^{\alpha\beta}, \\
&= \frac{e^2}{4} \text{Tr} \left[g_{\mu\alpha} (\not{p}_n + m_n) \Gamma^{\mu\nu} (\not{p}_\Delta + m_\Delta) P_{\nu\beta} \bar{\Gamma}^{\alpha\beta} \right],
\end{aligned} \tag{5.44}$$

with the spin sum rules for vector-spinors and the polarization vectors being introduced in Appendix (E). Since these matrix elements are independent of the momentum variable integration, we can separately determine the integral part of the two-body phase space as follows:

$$\Gamma = \frac{1}{2m_\Delta} \langle |m_{\Delta \rightarrow n\gamma}|^2 \rangle \underbrace{\int \frac{d^3 p_1}{(2\pi)^3 2E_1} \frac{d^3 p_2}{(2\pi)^3 2E_2} (2\pi)^4 \delta^{(4)}(P - p_1 - p_2)}_{I_{PS}}. \tag{5.45}$$

The detailed integration over momentum for the underbrace part of the two-body phase space is provided in Appendix (G). As a consequence, the formula can explicitly yield the final form of the differential decay rate for the two-body decay in the center-of-mass frame, which is given by

$$\Gamma = \frac{|\vec{p}_{cm}|}{8\pi m_\Delta^2} \langle |m_{\Delta \rightarrow n\gamma}|^2 \rangle \Theta(m_\Delta - m_n), \tag{5.46}$$

with the CM momentum being $|\vec{p}_{cm}| = \frac{1}{2m_\Delta} (m_\Delta^2 - m_n^2)$. The final decay width of $\Delta \rightarrow n\gamma$, in terms of the transition form factors $G_{\pm 1}$ for on-shell condition at a real photon point $q^2 = 0$, simplified by (Junker et al., 2020), takes the form

$$\Gamma = \frac{e^2 (m_\Delta^2 - m_n^2)}{96\pi m_\Delta^3} (m_\Delta - m_n)^2 (3|G_{+1}(0)|^2 + |G_{-1}(0)|^2). \tag{5.47}$$

The correct experimental data of the total width for the electromagnetic decay channel $\Delta \rightarrow n\gamma$ is provided $\Gamma_{\Delta \rightarrow n\gamma} = 0.66$ MeV from the HADES collaboration (Adamczewski-Musch et al., 2017). It is important to verify the fundamental parameters before proceeding with the calculation of form factors for the three-body decay. Based on the numerical value, our calculated decay width result of $\Gamma_{\Delta \rightarrow n\gamma} = 0.65$ MeV demonstrates excellent agreement with the available

HADES data. This agreement holds when considering the input parameters of form factors as $G_M^*(0) = 3.02$ and $G_E^*(0) = 0.075$ at the exact energy value $q^2 = 0$, as reported in (Pascalutsa et al., 2007). Therefore, the impact of changing for $\Delta \rightarrow n\gamma$ is acceptable around 1%.

5.3 Differential cross section of $e^+e^- \rightarrow \bar{\Delta}^0 N$ scattering

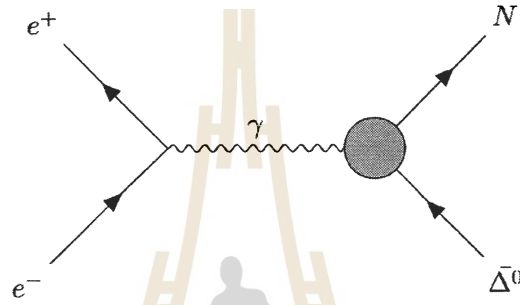


Figure 5.4 Sketch of Feynman diagram for the 2 to 2 scattering $e^-e^+ \rightarrow \bar{\Delta}^0 N$.

To complete our theoretical investigation of the eTFFs for the entire time-like region q^2 , we also need to analytically simplify the differential cross-section for electron-positron annihilation to antibaryon-baryon scattering with respect to the Feynman rules. By analogy with this principle, the Feynman amplitude of the formalism for the $e^-e^+ \rightarrow \bar{\Delta}^0 n$ reaction in Figure 5.4, and its corresponding Hermitian conjugate, are nicely introduced through the contraction of indices for each particle, taking the form,

$$\begin{aligned}
 \mathcal{M} &= e \bar{u}_n(p_n, s_n) \bar{\Gamma}^\nu v_\Delta^\Delta(p_\Delta, s_\Delta) \left(\frac{-ig_{\mu\nu}}{q^2} \right) \bar{v}_{e^+}(p_{e^+}, s_{e^+}) (ie\gamma^\mu) u_{e^-}(p_{e^-}, s_{e^-}), \\
 &= \frac{e^2}{q^2} \bar{u}_n(p_n, s_n) \bar{\Gamma}^{\mu\nu} v_\Delta^\Delta(p_\Delta, s_\Delta) \bar{v}_{e^+}(p_{e^+}, s_{e^+}) \gamma_\mu u_{e^-}(p_{e^-}, s_{e^-}), \\
 \mathcal{M}^\dagger &= \frac{e^2}{q^2} \bar{u}_{e^-}(p_{e^-}, s_{e^-}) \gamma_\alpha v_{e^+}(p_{e^+}, s_{e^+}) \bar{v}_\beta^\Delta(p_\Delta, s_\Delta) \Gamma^{\alpha\beta} u_n(p_n, s_n).
 \end{aligned} \tag{5.48}$$

The average value of the amplitude in the entire system of $e^-e^+ \rightarrow \bar{\Delta}n$ scattering, obtained by directly multiplying matrix elements, takes the form:

$$\begin{aligned}
 \langle |m_{e^-e^+ \rightarrow \bar{\Delta}n}|^2 \rangle &= \frac{e^4}{4q^4} \sum_{s_{e^-}, s_{e^+}, s_{\Delta}, s_n} (\bar{u}_n)_i (\bar{\Gamma}^{\mu\nu})_{ij} (v_{\Delta}^\Delta)_j (\bar{v}_{e^+})_k (\gamma_\mu)_{kl} (u_{e^-})_l \\
 &\quad \times (\bar{u}_{e^-})_a (\gamma_\alpha)_{ab} (v_{e^+})_b (\bar{v}_{\Delta}^\Delta)_c (\Gamma^{\alpha\beta})_{cd} (u_n)_d, \\
 &= \frac{e^4}{4q^4} \sum_{s_{e^-}} ((u_{e^-})_l (\bar{u}_{e^-})_a) (\gamma_\alpha)_{ab} \sum_{s_{e^+}} ((v_{e^+})_b (\bar{v}_{e^+})_k) (\gamma_\mu)_{kl} \\
 &\quad \times \sum_{s_{\Delta}} ((v_{\Delta}^\Delta)_j (\bar{v}_{\Delta}^\Delta)_c) (\Gamma^{\alpha\beta})_{cd} \sum_{s_n} ((u_n)_d (\bar{u}_n)_i) (\bar{\Gamma}^{\mu\nu})_{ij}, \\
 &= \frac{-e^4}{4q^4} (\not{p}_{e^-} + m_e)_{la} (\gamma_\alpha)_{ab} (\not{p}_{e^+} - m_e)_{bk} (\gamma_\mu)_{kl} \\
 &\quad \times ((\not{p}_{\Delta} - m_{\Delta}) P_{\nu\beta})_{jc} (\Gamma^{\alpha\beta})_{cd} (\not{p}_n + m_n)_{di} (\bar{\Gamma}^{\mu\nu})_{ij}, \\
 &= \frac{-e^4}{4q^4} \text{Tr} \left[(\not{p}_{e^-} + m_e) \gamma_\alpha (\not{p}_{e^+} - m_e) \gamma_\mu \right] \\
 &\quad \times \text{Tr} \left[(\not{p}_{\Delta} - m_{\Delta}) P_{\nu\beta} \Gamma^{\alpha\beta} (\not{p}_n + m_n) \bar{\Gamma}^{\mu\nu} \right],
 \end{aligned} \tag{5.49}$$

with the necessary input vertex function being given by (Junker et al., 2020),

$$\begin{aligned}
 \Gamma^{\mu\nu}(p_{\Delta}, q) &= (\gamma^\mu q^\nu - \not{q} g^{\mu\nu}) m_{\Delta} \gamma_5 F_1(q^2) \\
 &\quad + (p_{\Delta}^\mu q^\nu - p_{\Delta} \cdot q g^{\mu\nu}) \gamma_5 F_2(q^2) \\
 &\quad + (q^\mu q^\nu - q^2 g^{\mu\nu}) \gamma_5 F_3(q^2),
 \end{aligned} \tag{5.50}$$

and their relative conjugate function refers to

$$\begin{aligned}
 \bar{\Gamma}^{\mu\nu}(p_{\Delta}, q) &= -(\gamma^\mu q^\nu - \not{q} g^{\mu\nu}) m_{\Delta} \gamma_5 F_1^*(q^2) \\
 &\quad - (p_{\Delta}^\mu q^\nu - p_{\Delta} \cdot q g^{\mu\nu}) \gamma_5 F_2^*(q^2) \\
 &\quad - (q^\mu q^\nu - q^2 g^{\mu\nu}) \gamma_5 F_3^*(q^2).
 \end{aligned} \tag{5.51}$$

A fully generic form of the differential cross-section for the average over the spin orientations is conveniently described via

$$d\sigma = \frac{\langle |\mathcal{M}_{e^-e^+ \rightarrow \bar{\Delta}n}|^2 \rangle}{4p_{cm,in} \sqrt{q^2}} (2\pi)^4 \delta^{(4)}(p_1 + p_2 - \sum_{j=3}^n p_j) \prod_{j=3}^n \frac{d^3 p_j}{(2\pi)^3 2E_j}, \quad (5.52)$$

$$\sigma = \frac{1}{\prod_j N_j!} \int d\sigma,$$

with N being the indistinguishable number of the final state particles. Since all observable of $\langle |\mathcal{M}_{e^-e^+ \rightarrow \bar{\Delta}n}|^2 \rangle$ depend on Lorentz invariant quantities, it is allowed to introduce the well-known Mandelstam variables for the 2 to 2 scattering in our process;

$$\begin{aligned} s &= (p_{e^-} + p_{e^+})^2 = (p_{\Delta} + p_n)^2 = q^2, \\ t &= (p_{e^-} - p_{\Delta})^2 = (p_{e^+} - p_n)^2, \\ u &= (p_{e^-} - p_n)^2 = (p_{e^+} - p_{\Delta})^2. \end{aligned} \quad (5.53)$$

Here, we denote the initial states' four momenta as p_{e^-} and p_{e^+} , and the mass value as m_e . The momenta of final scattering states are represented by p_{Δ} and p_n with their masses m_{Δ} and m_n respectively. The total energy of the system is denoted as q^2 . Likewise the previous case, the whole calculation of spin-average differential cross section will be performed in the center of mass frame, defined by $\vec{p}_{e^+} + \vec{p}_{e^-} = 0$. In principle, by setting the kinematical angle trajectory, the observable t relative to the scattering angle θ in the center of mass frame, takes the form

$$\begin{aligned} t &= (p_{e^-} - p_{\Delta})^2 = p_{e^-}^2 + p_{\Delta}^2 - 2E_e E_{\Delta} + 2\vec{p}_{e^-} \cdot \vec{p}_{\Delta}, \\ &= m_e^2 + m_{\Delta}^2 - 2E_e E_{\Delta} + 2|\vec{p}_{e^-}| |\vec{p}_{\Delta}| \cos(\theta), \end{aligned} \quad (5.54)$$

where θ is the angle between the direction of the incoming three-momentum \vec{p}_{e^-} and outgoing three-momentum \vec{p}_{Δ} . One can then continue further computation for

the t -dependence of the momentum integration in this prescription:

$$\begin{aligned} \frac{d\sigma}{dt} = & \frac{1}{4|\vec{p}_e|\sqrt{q^2}} \int \frac{d^3\vec{p}_\Delta}{(2\pi)^3 2E_\Delta} \frac{d^3\vec{p}_n}{(2\pi)^3 2E_\Delta} \langle |m_{e^-e^+ \rightarrow \bar{\Delta}n}|^2 \rangle \\ & \times (2\pi)^4 \delta^{(4)}(p_{e^-} + p_{e^+} - p_\Delta - p_n) \delta(t - (p_{e^-} - p_\Delta)^2). \end{aligned} \quad (5.55)$$

where:

$$\begin{aligned} E_{e^-} &= \frac{1}{2}\sqrt{q^2}, E_\Delta = \frac{q^2 - m_n^2 + m_\Delta^2}{2\sqrt{q^2}}, \\ |\vec{p}_{e^-}| &= \frac{\sqrt{\lambda(q^2, m_e^2, m_e^2)}}{2\sqrt{q^2}} = \sqrt{\frac{q^2}{4} - m_e^2}, \\ |\vec{p}_\Delta| &= \frac{\sqrt{\lambda(q^2, m_n^2, m_\Delta^2)}}{2\sqrt{q^2}}. \end{aligned} \quad (5.56)$$

The spin-averaged differential cross section of 2 to 2 interaction in terms of the variable q^2 and θ takes the form

$$\left(\frac{d\sigma}{d\Omega} \right)_{CM}(q^2, \theta) = \frac{|\vec{p}_\Delta|}{64\pi^2 |\vec{p}_{e^-}| q^2} \langle |m_{e^-e^+ \rightarrow \bar{\Delta}n}|^2 \rangle. \quad (5.57)$$

Finally, the differential cross section for $e^-e^+ \rightarrow \bar{\Delta}n$ scattering can be written as

$$\begin{aligned} \left(\frac{d\sigma}{d\Omega} \right)_{CM}(q^2, \theta) &= \frac{|\vec{p}_\Delta|}{|\vec{p}_{e^-}|} \frac{e^4}{96\pi^2 q^4} (q^2 - (m_\Delta - m_n)^2) \\ &\times \left[\left(1 + \cos^2 \theta + \frac{4m_e^2}{q^2} \sin^2 \theta \right) \right. \\ &\times (3|G_{+1}(q^2)|^2 + |G_{-1}(q^2)|^2) \\ &\left. + 4 \left(\frac{q^2}{m_\Delta^2} \sin^2 \theta + \frac{4m_e^2}{m_\Delta^2} \cos^2 \theta \right) |G_0(q^2)|^2 \right]. \end{aligned} \quad (5.58)$$

In particular, there is a negligible term associated with the electron mass, given its very small value m_e compared to the mass of the baryon decuplet state delta

$m_e^2 \ll m_\Delta^2$. Since m_e is omitted, the differential cross section can be simplified as:

$$\begin{aligned} \left(\frac{d\sigma}{d\Omega} \right)_{CM}(q^2, \theta) &= \frac{e^4 |\vec{p}_\Delta|}{96\pi^2 q^6} \frac{\sqrt{q^2}}{2} (q^2 - (m_\Delta - m_n)^2) \\ &\times \left[(1 + \cos^2 \theta) (3|G_{+1}(q^2)|^2 + |G_{-1}(q^2)|^2) \right. \\ &\left. + \frac{4q^2}{m_\Delta^2} \sin^2 \theta |G_0(q^2)|^2 \right]. \end{aligned} \quad (5.59)$$

The form factors are also substituted accordingly by applying our combinations Eq. (5.32), taking the form

$$\begin{aligned} \left(\frac{d\sigma}{d\Omega} \right)_{CM}(q^2, \theta) &= \frac{e^4 |\vec{p}_\Delta|}{64\pi^2 q^6} \frac{\sqrt{q^2}}{2} (q^2 - (m_\Delta - m_n)^2) \left(\frac{m_\Delta + m_n}{m_n} \right)^2 \\ &\times \left[(1 + \cos^2 \theta) (3|G_E^*(q^2)|^2 + |G_M^*(q^2)|^2) \right. \\ &\left. + \frac{q^2}{m_\Delta^2} \sin^2 \theta |G_C^*(q^2)|^2 \right]. \end{aligned} \quad (5.60)$$

In brief, the behavior of these cross-sections could be comparable to those corresponding to the general relation predicted by the choice of e^+e^- annihilation into Baryon-Antibaryon pairs (Korner and Kuroda, 1977), but it is important to consider the different kinematical regions, particularly at high energies q^2 . For such a prediction in one-photon approximation, it is given by (Korner and Kuroda, 1977)

$$\begin{aligned} \frac{d\sigma}{d\cos\theta} &\propto \sum_\lambda \frac{1}{2} (1 + \cos^2 \theta) \left(|\Gamma^{\lambda+1,\lambda}(q^2)|^2 + |\Gamma^{\lambda-1,\lambda}(q^2)|^2 \right) \\ &+ \sin^2 \theta |\Gamma^{\lambda,\lambda}(q^2)|^2, \end{aligned} \quad (5.61)$$

where the solid angle notation $d\Omega = d\phi d\cos\theta$. According to the formalism (Junker et al., 2020), the helicity amplitudes to the form factors combinations are introduced as follows directly

$$\frac{|G_{-1}(q^2)|^2}{|G_{+1}(q^2)|^2} = 3 \frac{|\Gamma^{\frac{1}{2},-\frac{1}{2}}(q^2)|^2}{|\Gamma^{\frac{3}{2},\frac{1}{2}}(q^2)|^2}, \quad (5.62)$$

$$\frac{|G_0(q^2)|^2}{|G_{+1}(q^2)|^2} = \frac{3}{2} \frac{m_\Delta^2}{q^2} \frac{|\Gamma_{\frac{1}{2},\frac{1}{2}}^{\frac{1}{2},\frac{1}{2}}(q^2)|^2}{|\Gamma_{\frac{3}{2},\frac{1}{2}}^{\frac{3}{2},\frac{1}{2}}(q^2)|^2}. \quad (5.63)$$

The expression of the differential cross-section for e^+e^- annihilation into Baryon-Antibaryon pairs aims solely to verify the correspondence with our kinematical coefficients.



CHAPTER VI

RESULTS AND DISCUSSIONS

In the present chapter, we show the numerical results of the Jone-Scadron $\Delta \rightarrow N\gamma$ transition form factors in both the unsubtracted and subtracted dispersion relations as well as the differential decay width of Dalitz decay $\Delta^0 \rightarrow Ne^+e^-$ resulted from the subtracted transition form factors.

6.1 Results of unsubtracted dispersion relation

We apply the unsubtracted dispersion relation Eq. (3.6) to get the three TFFs ($G_{\pm 1}, G_0$) of different helicity at the real photon point $Q^2 = 0$. The three Jone-Scadron form factors G_M^* , G_E^* and G_C^* are derived via three TFFs $G_{\pm 1}, G_0$ in Eq. (6.1),

$$\begin{aligned} G_M^* &= -\frac{1}{\sqrt{6}} \frac{m_n}{m_n + m_\Delta} (G_{-1} - 3G_{+1}), \\ G_E^* &= \frac{1}{\sqrt{6}} \frac{m_n}{m_n + m_\Delta} (G_{-1} + G_{+1}), \\ G_C^* &= \frac{4}{\sqrt{6}} \frac{m_n}{m_n + m_\Delta} G_0. \end{aligned} \tag{6.1}$$

Both the polynomial subtraction constants $P_{M/E/C}^*$ and three Jone-Scadron form factors depends on the three coupling constants h_A, H_A, g_A and the NLO parameter c_F . In this unsubtracted dispersion relation calculation, Δ -nucleon-pion coupling constant $h_A \approx 3g_A/\sqrt{2} \approx 2.67$, Δ -nucleon-photon coupling constant $H_A \approx 9g_A/5 \approx 2.27$, and $g_A = D + F = 1.26$ are determined in the Large- N_c approximation and chiral perturbation theory, and take the same values as in the previous works (Junker et al., 2020; Pascalutsa et al., 2007; Ledwig et al., 2012; Pascalutsa and Vanderhaeghen,

2006). The model parameters are shown in Eq. (6.2),

$$\begin{aligned} F_\pi &= 92.28 \text{ MeV}, g_A = D + F = 1.26, \\ h_A &= \frac{3g_A}{\sqrt{2}} \approx 2.67, H_A = \frac{9g_A}{5} \approx 2.27. \end{aligned} \quad (6.2)$$

The only free parameter c_F is determined by fitting the magnetic FFs G_M^* to the experimental data $G_M^*(0) = 3.02$ (Pascalutsa et al., 2007). It is found that there are two values of c_F which lead to a good fit to G_M^* , as shown in Table 6.1 with the cutoff $\Lambda = 2 \text{ GeV}$. For both $c_F = 0.57 \text{ GeV}^{-1}$ and $c_F = -7.8 \text{ GeV}^{-1}$, we can get the

Table 6.1 c_F , $G_m(0)$ and $G_M^*(0)$ determined in the unsubtracted dispersion relation with cutoff $\Lambda = 2 \text{ GeV}$.

Quantity	$c_F = 0.57 \text{ GeV}^{-1}$	$c_F = -7.8 \text{ GeV}^{-1}$
$G_{+1}(0)$	$-4.278 + 0.126 i$	$4.823 + 0.126 i$
$G_{-1}(0)$	$4.299 + 0.093 i$	$-2.637 + 0.093 i$
$G_0(0)$	$-0.953 - 0.537 i$	$4.211 - 0.537 i$
$G_M^*(0)$	$3.025 - 0.050 i$	$3.020 + 0.050 i$

perfect fit for $G_M^*(0)$. And we found that the polynomial subtraction constants P_M^* at the photon point are different for these two cases which are shown in Table 6.2. The unsubtracted dispersion relation calculation is not enough to determine the $\Delta \rightarrow N\gamma$ transition form factors, but it provides us the hints about the basic range of c_F , we will carry on subtracted dispersion relation based on it.

Table 6.2 Polynomial constants P_M^* determined in the unsubtracted dispersion relation for different c_F .

Quantity	$P_M^* = 451.15 \text{ GeV}^{-2}$	$P_M^* = 366.92 \text{ GeV}^{-2}$
$G_M^*(0)$	$3.02193 - 0.050 i$	$3.022 + 0.050 i$

6.2 Results of subtracted dispersion relation

The three Jone-Scadron form factors are calculated in the subtracted dispersion relation in the space- and time-like regions $-0.7 \ll q^2(\text{GeV}^2) \ll (m_\Delta - m_n)^2$ and are presented in Figure 6.1. The experimental values of G_M^* , G_E^* and G_C^* at $Q^2 = 0$ are taken from the Ref. (Pascalutsa et al., 2007), as listed in Table 6.3. The polynomial subtraction constants $P_{M/E/C}^*$ and c_F are determined by fitting the theoretical results to the experimental values of the three Jone-Scadron form factors at the photon point and to experimental data of N- $\Delta(1232)$ transition magnetic dipole $\text{Im}M_{1+}^{3/2}$ in Eq. (3.18), the electric quadrupole ratio R_{EM} and the scalar quadrupole ratio R_{SM} . The least squares method is applied to get the best fit, resulting in $P_M^* = 406.12 \text{ GeV}^{-2}$, $P_E^* = 10.24 \text{ GeV}^{-2}$ and $P_C^* = 122.89 \text{ GeV}^{-2}$ for getting the results of $G_M^*(0)$, $G_E^*(0)$ and $G_C^*(0)$ correspondingly. It turns out that we can get a better fit to the experimental data in the subtracted dispersion relation than in the unsubtracted dispersion relation.

Table 6.3 The values of the magnetic, electric and charge form factors at the real photon point in subtracted dispersion relation.

Quantity	Data values
$G_M^*(0)$	3.022
$G_E^*(0)$	0.0755
$G_C^*(0)$	0.6784

Table 6.4 Jones-Scadron form factors G_M^* , G_E^* , G_C^* at the photon point with the cutoff $\Lambda = 1 \text{ GeV}$ and $\Lambda = 2 \text{ GeV}$. Here $h_A = 2.67$ and $H_A = 2.27$.

Quantity	$\Lambda = 1 \text{ GeV}^{-1}$	$\Lambda = 2 \text{ GeV}^{-1}$
$G_M^*(0)$	3.02	3.02
$\langle r^2 \rangle_M^* \text{ GeV}^{-2}$	19.03	18.35
$G_E^*(0)$	0.07	0.07
$\langle r^2 \rangle_E^* \text{ GeV}^{-2}$	- 8.01	- 8.69
$G_C^*(0)$	0.67	0.67
$\langle r^2 \rangle_C^* \text{ GeV}^{-2}$	- 23.51	- 24.33

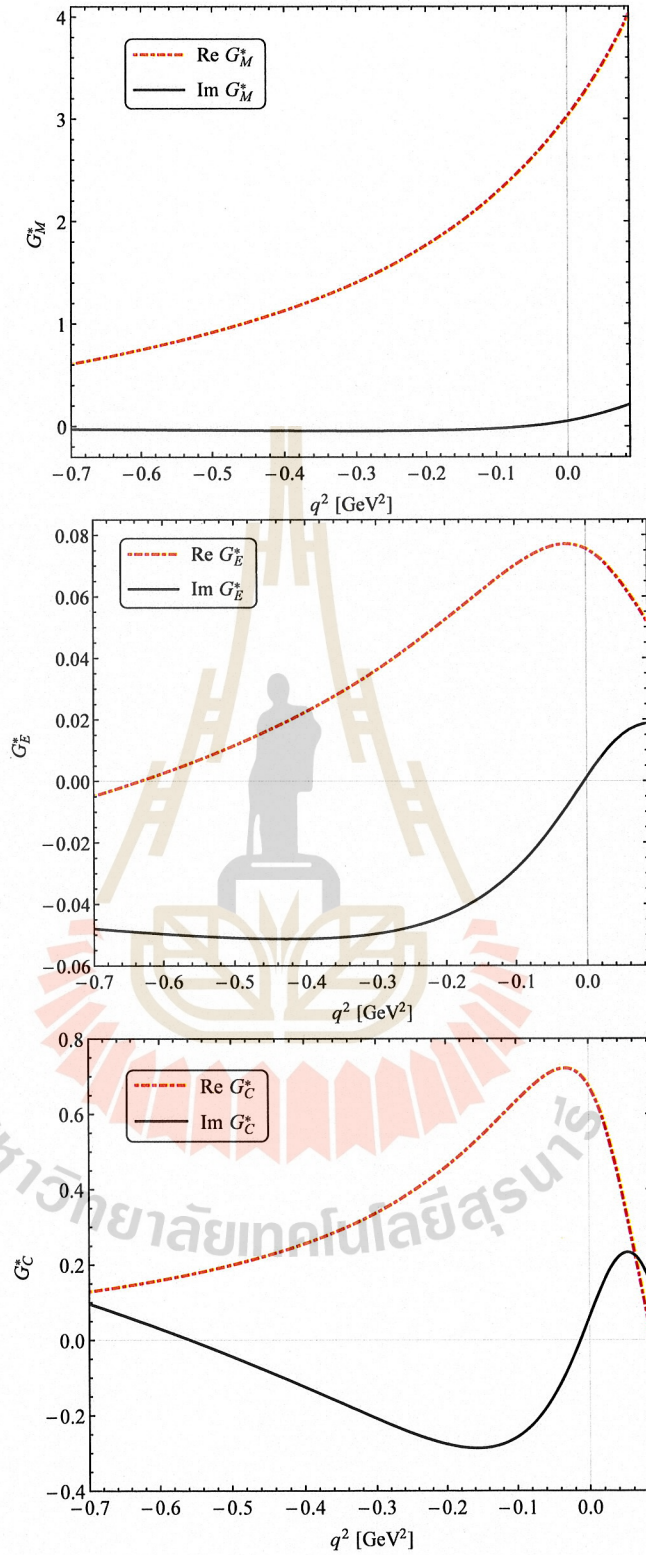


Figure 6.1 Magnetic dipole form factor G_M^* , electric quadrupole form factor G_E^* and Coulomb quadrupole form factor G_C^* in the region, $-0.7 \ll q^2(\text{GeV}^2) \ll (m_\Delta - m_n)^2$. The polynomial constants are fixed to be $P_M^* = 406.12 \text{ GeV}^{-2}$, $P_E^* = 10.24 \text{ GeV}^{-2}$ and $P_C^* = 122.89 \text{ GeV}^{-2}$. The cutoff $\Lambda = 2 \text{ GeV}$.

Table 6.5 Jones-Scadron form factors G_M^* , G_E^* , G_C^* and corresponding radii with different h_A , H_A at the cutoff $\Lambda = 2$ GeV.

Quantity	$h_A \approx 2.9$	$h_A \approx 2.4 \text{ GeV}^{-1}$	$H_A \approx 2.4$	$H_A \approx 2.0$
$G_M^*(0)$	3.02	3.02	3.02	3.02
$\langle r^2 \rangle_M^* \text{ GeV}^{-2}$	18.76	17.95	18.66	18.05
$G_E^*(0)$	0.07	0.07	0.07	0.07
$\langle r^2 \rangle_E^* \text{ GeV}^{-2}$	- 11.01	- 6.38	- 9.18	- 8.21
$G_C^*(0)$	0.67	0.67	0.67	0.67
$\langle r^2 \rangle_C^* \text{ GeV}^{-2}$	- 28.57	- 20.09	- 24.13	- 24.53

Since the h_A and H_A are directly taken from the Large- N_c limit, we verify the theoretical results by systematically adjusting these two coupling constants within a range of $\pm 10\%$ respectively. The theoretical magnetic dipole form factor $\text{Im}M_{1+}^{3/2}$, the two ratios R_{EM} , R_{SM} are compared with experimental data in Figure 6.2, where h_A and H_A are varied. The cutoff is still $\Lambda = 2$ GeV.

As shown in Figure 6.2, the magnetic dipole form factor $\text{Im}M_{1+}^{3/2}$ is well reproduced up to $Q^2 = 0.7 \text{ GeV}^2$, while the ratios R_{EM} is fairly repeated up to $Q^2 = 0.5 \text{ GeV}^2$. The theoretical results of the ratio R_{SM} are globally close to the experimental data except R_{SM} around $Q^2 = 0.12 \text{ GeV}^2$. The theoretical results are quite stable against varying h_A and H_A . We have also calculated the electric and magnetic radii in Eq. (3.5). The radii with different cutoff Λ as well as different coupling constants h_A and H_A are presented in Table 6.4 and Table 6.5, respectively. It is found that all the radii are very stable with changing the cutoff and H_A , but $\langle r^2 \rangle_E^*$ and $\langle r^2 \rangle_C^*$ decrease significantly with a smaller Δ -nucleon-pion coupling constant h_A .

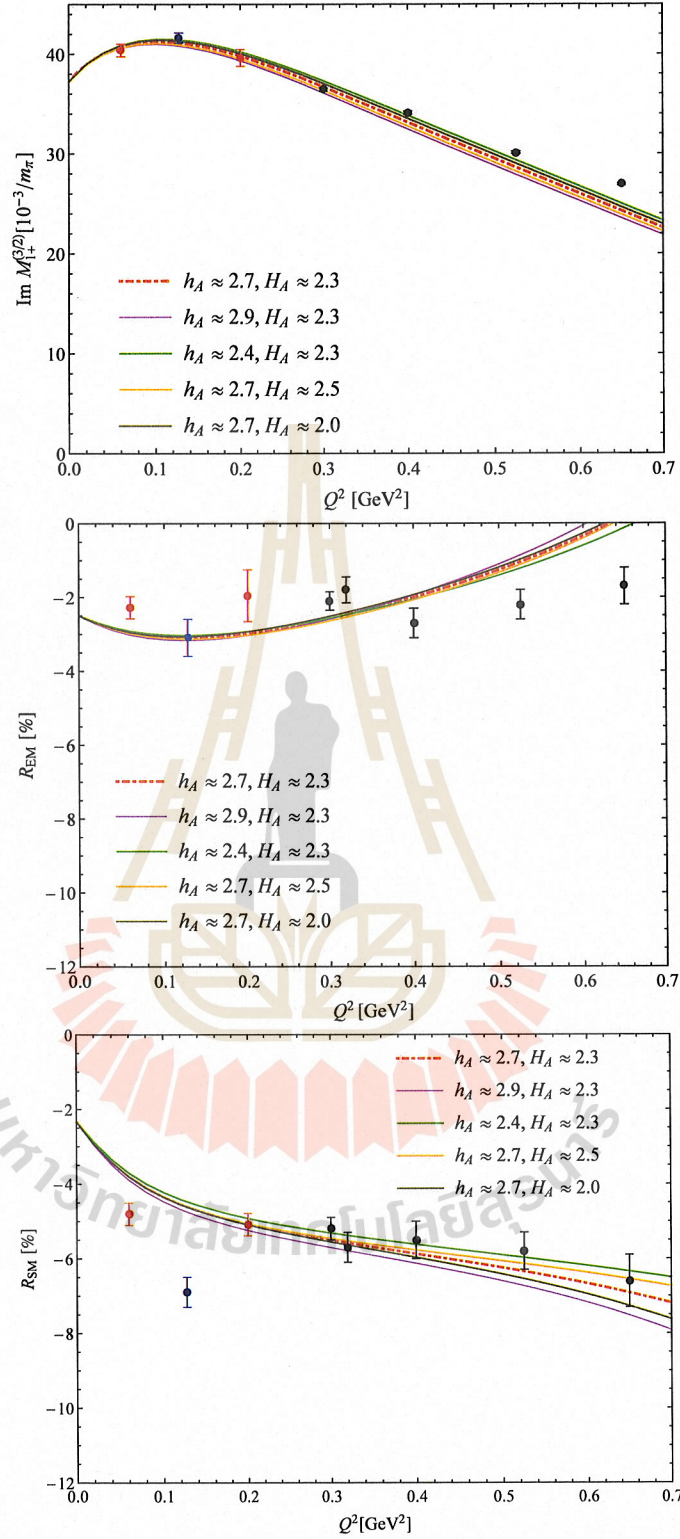


Figure 6.2 Q^2 -dependence of $\text{Im}M_{1+}^{3/2}$, R_{EM} and R_{SM} . Red dot-dashed curve shows the results for the central parameters h_A and H_A , the magenta and green color lines show the results with h_A varied by $\pm 10\%$, and the orange and brown lines for the results with H_A varied by $\pm 10\%$. Data are taken from BATES (blue color) (Sparveris et al., 2005), MAMI (red color) (Sparveris et al., 2007; Stave et al., 2006), and CLAS (black color) (Aznauryan et al., 2009).

6.3 Results of Dalitz decay

In this section, we derived the differential decay width of $\Delta^0 \rightarrow Ne^+e^-$ Dalitz decay with the energy range of $4m_e^2 \leq q^2 (\text{GeV}^2) \leq (m_\Delta - m_n)^2$. The results presented in Figure 6.3, are compared with the QED-type approximation, proposed by HADES collaboration (Adamczewski-Musch et al., 2017). We listed the values of A and B , as defined in the previous Chapter, in Table 6.6, which are derived using the model parameters in our subtracted dispersion relation calculations. Included in Table 6.6 are also the QED analogue results of these two parameters.

Our analysis reveals a remarkable agreement between our single differential decay width and the QED analogue, and the parameters A and B are very close to the QED-type approximation. These findings further corroborate the validity of the coupling constants and model parameters.

Table 6.6 Comparison of the two parameters A and B in the QED approximation and our calculation in $\Delta^0 \rightarrow Ne^+e^-$ Dalitz decay.

Quantity	A	B	$A(2 + \frac{2}{3}B)$
QED analogue	1.90612×10^{-6}	0.0858258	3.92131×10^{-6}
FFs	1.82418×10^{-6}	0.0856501	3.75251×10^{-6}

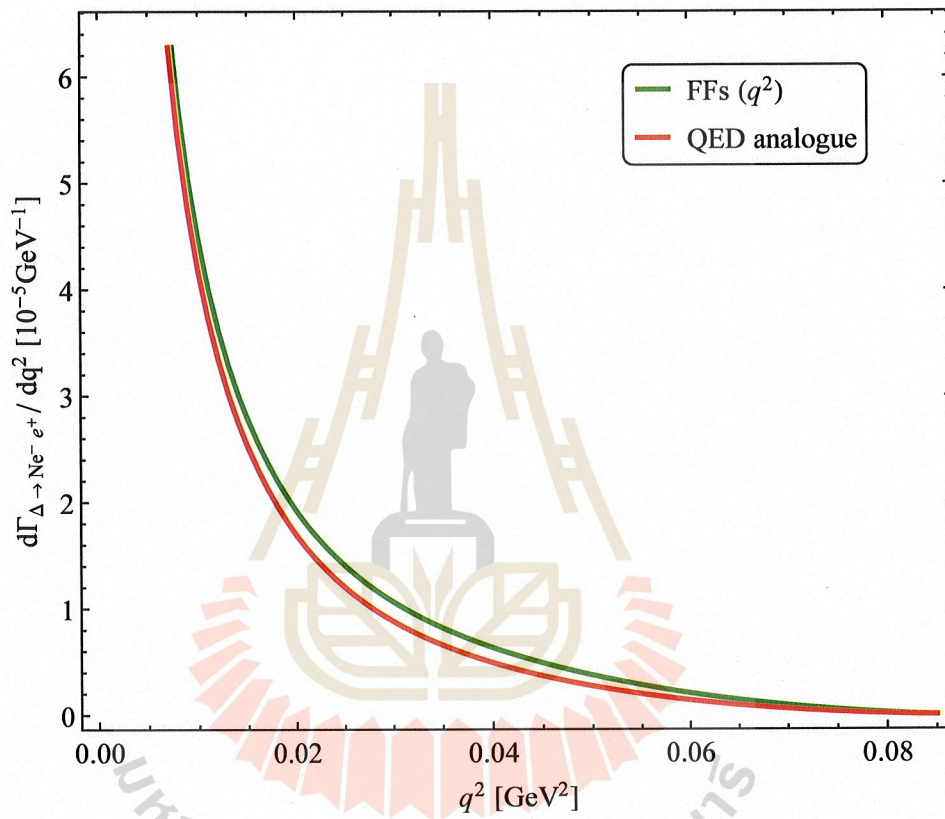


Figure 6.3 Single-differential decay width of the $\Delta^0 \rightarrow Ne^+e^-$ Dalitz decay in comparison with the QED-type approximation in the range, $4m_e^2 \leq q^2 (\text{GeV}^2) \leq (m_\Delta - m_n)^2$. The green line represents the results we calculated using the model parameters fixed in subtracted dispersion relation and red line represents the QED analogue results.

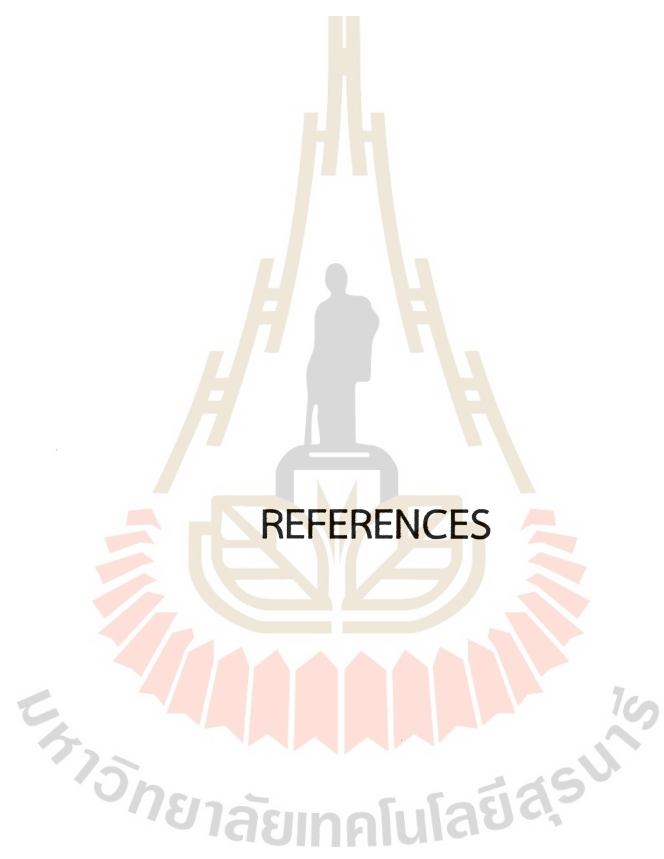
CHAPTER VII

CONCLUSIONS

In this work, we have studied the $\Delta - N$ electromagnetic transition form factors in the dispersion theory and chiral perturbation theory at low Q^2 regions. The three Jone-Scadron multipoles form factors, denoted as G_M^* , G_E^* , and G_C^* , were derived in both the subtracted and unsubtracted dispersion relations with the NLO approximation. Additionally, we have also calculated the differential decay widths of the two-body decay $\Delta^0 \rightarrow N\gamma$ and three-body decay process $\Delta^0 \rightarrow Ne^+e^-$, the cross-section for $e^+e^- \rightarrow \bar{\Delta}^0 N$ has also been derived.

We have determined the NLO parameter c_F to be $c_F = 0.57 \text{ GeV}^{-1}$ or $c_F = -7.8 \text{ GeV}^{-1}$, by fitting $G_M^*(0)$ to 3.02 in the unsubtracted dispersion relation. Then in the subtracted dispersion relation we got the polynomial subtraction constants $P_M^* = 406.12 \text{ GeV}^{-2}$, $P_E^* = 10.24 \text{ GeV}^{-2}$, and $P_C^* = 122.89 \text{ GeV}^{-2}$ by fitting the theoretical results to all experimental data of transition magnetic dipole $\text{Im}M_{1+}^{3/2}$, the electric quadrupole ratio R_{EM} and the scalar quadrupole ratio R_{SM} . We also checked the stability of the theoretical results by varying the coupling constants h_A and H_A within a range of $\pm 10\%$, applying the cutoff $\Lambda = 1 \text{ GeV}$ and $\Lambda = 2 \text{ GeV}$. We have also derived the parameters A and B and differential decay width for the $\Delta^0 \rightarrow Ne^+e^-$ Dalitz decay, all the results are comparable to the direct QED-type approximation from HADES collaboration.

It's found that all numerical results of the multipole FFs exhibit a good agreement with experimental observations overall in the region $-0.7 \text{ GeV}^2 < q^2 \text{ (GeV}^2\text{)} < (m_\Delta - m_n)^2$ including both space-like to time-like regions. The model parameters fixed in subtracted dispersion relation demonstrates coherence in the $\Delta^0 \rightarrow Ne^+e^-$ Dalitz decay calculation. The work shows that coupling constants taken from chiral perturbation theory and Large N_c limits result in a good description of $\Delta - N$ electromagnetic transition form factors. We may apply the method of dispersion relations to other transition form factors in the future.



REFERENCES

- Adamczewski-Musch, J., Arnold, O., Atomssa, E. T., Behnke, C., Belounnas, A., Belyaev, A., Berger-Chen, J. C., Biernat, J., Blanco, A., Blume, C., Böhmer, M., Bordalo, P., Chernenko, S., Chlad, L., Deveau, C., Dreyer, J., Dybczak, A., Eppe, E., Fabbietti, L., Fateev, O., Filip, P., Finocchiaro, P., Fonte, P., Franco, C., Fries, J., Galatyuk, T., Garzón, J. A., Gernhäuser, R., Golubeva, M., Guber, F., Gumberidze, M., Harabasz, S., Hennino, T., Hlavac, S., Holzmann, R., Ierusalimov, A., and Ivashkin, A. (2017). $\Delta(1232)$ Dalitz decay in proton-proton collisions at $T = 1.25$ GeV measured with HADES at GSI. *Phys. Rev. C*, 95(6), 065205.
- Alarcón, J. M., Hiller Blin, A. N., Vicente Vacas, M. J., and Weiss, C. (2017). Peripheral transverse densities of the baryon octet from chiral effective field theory and dispersion analysis. *Nucl. Phys. A*, 964, 18–54.
- Alexandrou, C., de Forcrand, P., Neff, H., Negele, J. W., Schroers, W., and Tsapalis, A. (2005). The N to Delta electromagnetic transition form-factors from lattice QCD. *Phys. Rev. Lett.*, 94, 021601.
- Anisovich, A. V. and Leutwyler, H. (1996). Dispersive analysis of the decay $\eta \rightarrow 3\pi$. *Phys. Lett. B*, 375, 335–342.
- Aznauryan, I. G., Burkert, V., Biselli, A., and Egiyan, H. (2009). Electroexcitation of nucleon resonances from CLAS data on single pion electroproduction. *Phys. Rev. C*, 80, 055203.
- Aznauryan, I. G. and Burkert, V. D. (2012a). Electroexcitation of nucleon resonances. *Prog. Part. Nucl. Phys.*, 67, 1–54.
- Aznauryan, I. G. and Burkert, V. D. (2012b). Nucleon electromagnetic form factors and electroexcitation of low lying nucleon resonances in a light-front relativistic quark model. *Phys. Rev. C*, 85, 055202.
- Aznauryan, I. G. and Burkert, V. D. (2015). Electroexcitation of the $\Delta(1232)_{\frac{3}{2}}^{+}$ and $\Delta(1600)_{\frac{3}{2}}^{+}$ in a light-front relativistic quark model. *Phys. Rev. C*, 92(3), 035211.

- Barvinsky, A. O. and Vilkovisky, G. A. (1990). Covariant perturbation theory. 3: Spectral representations of the third order form-factors. *Nucl. Phys. B*, 333, 512–524.
- Beck, R., Krahn, H., Ahrens, J., Arends, H., Audit, G., Braghieri, A., Drechsel, D., Hanstein, O., McGeorge, J., Owens, R., P. Pedroni, Pinelli, T., Tamas, G., Tiator, L., and Walcher, T. (2000). Determination of the $E2/M1$ ratio in the $\gamma N \rightarrow \Delta(1232)$ transition from a simultaneous measurement of $p(\vec{\gamma}, p)\pi^0$ and $p(\vec{\gamma}, \pi^+)n$. *Phys. Rev. C*, 61, 035204.
- Bissegger, M. and Fuhrer, A. (2007). Chiral logarithms. *Acta Phys. Polon. B*, 38, 2797–2802.
- Blomberg, A., Anez, D., Sparverisa, N., Sarty, A. J., Paolonea, M., Gilad, S. and Hig-
inbothame, D., Ahmed, Z., Albatainehg, H., Alladae, K., Anioli, K., and Annand, J. (2016). Electroexcitation of the $\Delta^+(1232)$ at low momentum transfer. *Phys. Lett. B*, 760, 267–272.
- Bratkovskaya, E. L., Teryaev, O. V., and Toneev, V. D. (1995). Anisotropy of dilepton emission from nuclear collisions. *Phys. Lett. B*, 348, 283–289.
- Brown, G. E. and Weise, W. (1975). Pion Scattering and Isobars in Nuclei. *Phys. Rept.*, 22, 279–337.
- Burkert, V. D. (2018). N^* Experiments and Their Impact on Strong QCD Physics. *Few Body Syst.*, 59(4), 57.
- Burkert, V. D. and Lee, T. S. H. (2004). Electromagnetic meson production in the nucleon resonance region. *Int. J. Mod. Phys. E*, 13, 1035–1112.
- Cardarelli, F., Pace, E., Salme, G., and Simula, S. (1996). Electromagnetic n - delta transition form-factors in a light front constituent quark model. *Phys. Lett. B*, 371, 7–13.
- Carlson, C. E. (1986). ELECTROMAGNETIC $N - \Delta$ TRANSITION AT HIGH Q^2 . *Phys. Rev. D*, 34, 2704.
- Colangelo, G., Gasser, J., and Leutwyler, H. (2001). $\pi\pi$ scattering. *Nucl. Phys. B*, 603, 125–179.

- Cutkosky, R. E. (1960). Singularities and discontinuities of Feynman amplitudes. *J. Math. Phys.*, 1, 429–433.
- Davidson, R. M., Mukhopadhyay, N. C., and Wittman, R. S. (1991). Effective Lagrangian approach to the theory of pion photoproduction in the $\Delta(1232)$ region. *Phys. Rev. D*, 43, 71–94.
- Dong, Y. B., Shimizu, K., and Faessler, A. (2001). Meson cloud and electroproduction of the $\Delta(1232)$ resonance in a relativistic quark model approach. *Nucl. Phys. A*, 689, 889–902.
- Elsner, D., Barneo, P., Bartsch, P., Baumann, D., Bermuth, J., Bosnar, D., Ding, M., M. Distler, Drechsel, D., Ewald, I., Friedrich, J., Friedrich, J., Grzinger, S., Jennewein, P., and Kamalov, S. (2006). Measurement of the LT-asymmetry in π^0 electroproduction at the energy of the $\Delta(1232)$ resonance. *Eur. Phys. J. A*, 27, 91–97.
- Fiolhais, M., Golli, B., and Sirca, S. (1996). The Role of the pion cloud in electroproduction of the $\Delta(1232)$. *Phys. Lett. B*, 373, 229–234.
- Frazer, W. R. and Fulco, J. R. (1960). Effect of a Pion-Pion Scattering Resonance on Nucleon Structure. II. *Phys. Rev.*, 117, 1609–1614.
- Frink, M. and Meissner, U.-G. (2006). On the chiral effective meson-baryon Lagrangian at third order. *Eur. Phys. J. A*, 29, 255–260.
- Frolov, V. V., Adams, G., Ahmidouch, A., Armstrong, C. S., Assamagan, K., Avery, S., Baker, O. K., Bosted, P., Burkert, V., Carlini, R., Davidson, R. M., Dunne, J., Eden, T., Ent, R., Gaskell, D., Geye, P., Hinton, W., Keppel, C., Kim, W., and Klusman, M. (1999). Electroproduction of the $\Delta(1232)$ resonance at high momentum transfer. *Phys. Rev. Lett.*, 82, 45–48.
- Fujikawa, M., Hayashii, H., Eidelman, S., Adachi, I., Aihara, H., Arinstein, K., Aulchenko, V., Aushev, T., Bakich, A. M., Balagura, V., Barberio, E., Bay, A., Bedny, I., Belous, K., Bhardwaj, V., Bitenc, U., Bondar, A., Brodzicka, J., Browder, T. E., Chang, P., Chao, Y., Chen, A., Cheon, B. G., Chistov, R., Cho, S., Choi, Y., Dalseno, J., Dash, M., Epifanov, D., Gabyshev, N., and Golob, B. (2008). High-Statistics Study of the $\tau \rightarrow \pi^- \pi^0 \nu_\tau$ Decay. *Phys. Rev. D*, 78, 072006.

- Garcia-Martin, R., Kaminski, R., Pelaez, J. R., Ruiz de Elvira, J., and Yndurain, F. J. (2011). The Pion-pion scattering amplitude. IV: Improved analysis with once subtracted Roy-like equations up to 1100 MeV. *Phys. Rev. D*, 83, 074004.
- Gasser, J. and Leutwyler, H. (1984). Chiral Perturbation Theory to One Loop. *Annals Phys.*, 158, 142.
- Gasser, J. and Leutwyler, H. (1985). Chiral Perturbation Theory: Expansions in the Mass of the Strange Quark. *Nucl. Phys. B*, 250, 465–516.
- Gellas, G. C., Hemmert, T. R., Ktorides, C. N., and Poulis, G. I. (1999). The Delta nucleon transition form-factors in chiral perturbation theory. *Phys. Rev. D*, 60, 054022.
- Granados, C., Leupold, S., and Perotti, E. (2017). The electromagnetic Sigma-to-Lambda hyperon transition form factors at low energies. *Eur. Phys. J. A*, 53(6), 117.
- Hanhart, C. (2012). A New Parameterization for the Pion Vector Form Factor. *Phys. Lett. B*, 715, 170–177.
- Hanstein, O., Drechsel, D., and Tiator, L. (1996). The Position and the residues of the delta resonance pole in pion photoproduction. *Phys. Lett. B*, 385, 45–51.
- Hoferichter, M., Kubis, B., Ruiz de Elvira, J., Hammer, H. W., and Meißner, U. G. (2016a). On the $\pi\pi$ continuum in the nucleon form factors and the proton radius puzzle. *Eur. Phys. J. A*, 52(11), 331.
- Hoferichter, M., Ruiz de Elvira, J., Kubis, B., and Meißner, U.-G. (2016b). Roy–Steiner-equation analysis of pion–nucleon scattering. *Phys. Rept.*, 625, 1–88.
- Hohler, G., Pietarinen, E., Sabba Stefanescu, I., Borkowski, F., Simon, G. G., Walther, V. H., and Wendling, R. D. (1976). Analysis of Electromagnetic Nucleon Form-Factors. *Nucl. Phys. B*, 114, 505–534.
- Holmberg, M. and Leupold, S. (2018). The relativistic chiral Lagrangian for decuplet and octet baryons at next-to-leading order. *Eur. Phys. J. A*, 54(6), 103.

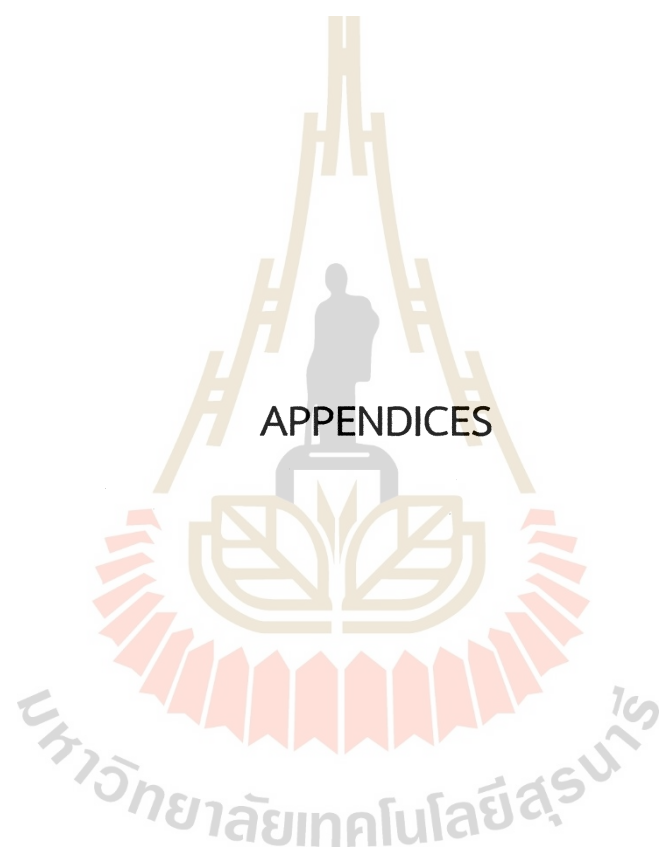
- Iwamura, Y. (1976). A Method of Solution to Muskhelishvili-Omnes Equation in Final State Interaction Model. *Prog. Theor. Phys.*, 56, 1812–1826.
- Jenkins, E. E. and Manohar, A. V. (1991). Chiral corrections to the baryon axial currents. *Phys. Lett. B*, 259, 353–358.
- Jones, H. F. and Scadron, M. D. (1973). Multipole gamma N Delta form-factors and resonant photoproduction and electroproduction. *Annals Phys.*, 81, 1–14.
- Joo, K., Smith, L., Burkert, V., Minehart, R., Aznauryan, I., Elouadrhiri, L., Stepanyan, S., Adams, G., Amarian, M., Anciant, E., Anghinolli, M., Armstrong, D., Asavapibhop, Audit, G., Auger, T., Avakian, H., Barrow, S., Bagdasaryan, H., Battaglieri, M., Beard, K., Bektasoglu, M., Bertozzi, W., Bianchi, N., Biselli, A., Boiarinov, S., and Bonner, B. (2002). Q^2 dependence of quadrupole strength in the $\gamma^* p \rightarrow \Delta^+(1232) \rightarrow p\pi^0$ transition. *Phys. Rev. Lett.*, 88, 122001.
- Junker, O., Leupold, S., Perotti, E., and Vitos, T. (2020). Electromagnetic form factors of the transition from the spin-3/2 Σ to the Λ hyperon. *Phys. Rev. C*, 101(1), 015206.
- Kaewsnod, A., Xu, K., Zhao, Z., Liu, X. Y., Srisuphaphon, S., Limphirat, A., and Yan, Y. (2022). Study of $N(1440)$ structure via $\gamma^* p \rightarrow N(1440)$ transition. *Phys. Rev. D*, 105(1), 016008.
- Kalleicher, F., Dittmayer, U., Gothe, R. W., Putsch, H., Reichelt, T., Schoch, B., and Wilhelm, M. (1997). The determination of $\sigma(\text{LT})/\sigma(\text{TT})$ in electropion production in the Delta resonance region. *Z. Phys. A*, 359, 201–204.
- Kelly, J. J., Roch, R. E., Chai, Z., Jones, M. K., Gayou, O., Sarty, A. J., Frullani, S., Aniol, K., Beise, E. J., Benmokhtar, F., Bertozzi, W., Boeglin, W. U., Botto, T., Brash, E. J., Breuer, H., Brown, E., Burtin, E., Calarco, J. R., Cavata, C., Chang, C. C., Chant, N. S., Chen, J.-P., Coman, M., Crovelli, D., Leo, R. D., Dieterich, S., Escoffier, S., Fissum, K. G., Garde, V., Garibaldi, F., and Georgakopoulos, S. (2005). Recoil polarization for delta excitation in pion electroproduction. *Phys. Rev. Lett.*, 95, 102001.
- Korner, J. G. and Kuroda, M. (1977). e^+e^- Annihilation Into Baryon-anti-Baryon Pairs. *Phys. Rev. D*, 16, 2165.

- Kubis, B. and Meissner, U. G. (2001). Baryon form-factors in chiral perturbation theory. *Eur. Phys. J. C*, 18, 747–756.
- Ledwig, T., Martin Camalich, J., Geng, L. S., and Vicente Vacas, M. J. (2014). Octet-baryon axial-vector charges and SU(3)-breaking effects in the semileptonic hyperon decays. *Phys. Rev. D*, 90(5), 054502.
- Ledwig, T., Martin-Camalich, J., Pascalutsa, V., and Vanderhaeghen, M. (2012). The Nucleon and $\Delta(1232)$ form factors at low momentum-transfer and small pion masses. *Phys. Rev. D*, 85, 034013.
- Leupold, S. (2018). The nucleon as a test case to calculate vector-isovector form factors at low energies. *Eur. Phys. J. A*, 54(1), 1.
- Leupold, S. and Terschlusen, C. (2012). Towards an effective field theory for vector mesons. *PoS, BORMIO2012*, 024.
- Lucha, W., Melikhov, D., and Simula, S. (2007). Dispersion representations and anomalous singularities of the triangle diagram. *Phys. Rev. D*, 75, 016001. [Erratum: *Phys.Rev.D* 92, 019901 (2015)].
- Mergell, P., Meissner, U. G., and Drechsel, D. (1996). Dispersion theoretical analysis of the nucleon electromagnetic form-factors. *Nucl. Phys. A*, 596, 367–396.
- Niecknig, F., Kubis, B., and Schneider, S. P. (2012). Dispersive analysis of $\omega \rightarrow 3\pi$ and $\phi \rightarrow 3\pi$ decays. *Eur. Phys. J. C*, 72, 2014.
- Oller, J. A., Verbeni, M., and Prades, J. (2006). Meson-baryon effective chiral lagrangians to $\mathcal{O}(q^3)$. *JHEP*, 09, 079.
- Omnes, R. (1958). On the Solution of certain singular integral equations of quantum field theory. *Nuovo Cim.*, 8, 316–326.
- Pascalutsa, V. and Timmermans, R. (1999). Field theory of nucleon to higher spin baryon transitions. *Phys. Rev. C*, 60, 042201.
- Pascalutsa, V. and Vanderhaeghen, M. (2006). The Nucleon and delta-resonance masses in relativistic chiral effective-field theory. *Phys. Lett. B*, 636, 31–39.

- Pascalutsa, V., Vanderhaeghen, M., and Yang, S. N. (2007). Electromagnetic excitation of the $\Delta(1232)$ -resonance. *Phys. Rept.*, 437, 125–232.
- Patrignani, C., Agashe, K., Aielli, G., Amsler, C., Antonelli, M., Asner, D., Baer, H., Banerjee, S., Barnett, R., Basaglia, T., Bauer, C., Beatty, J., Belousov, V., Beringer, J., Bethke, S., Bichsel, H., Biebel, O., Blucher, E., Brooijmans, G., Buchmueller, O., Burkert, V., Bychkov, M., Cahn, R., Carena, M., Ceccucci, A., Cerri, A., Chakraborty, D., Chen, M.-C., Chivukula, R., Copic, K., Cowan, G., Dahl, O., D'Ambrosio, G., Damour, T., de Florian, D., DeGrand, T., Dissertori, G., and Gherghetta, T. (2016). Review of Particle Physics. *Chin. Phys. C*, 40(10), 100001.
- Peskin, Michael, E. and Schroeder, Daniel, V. (1995). *An Introduction to quantum field theory*. Addison-Wesley, Reading, USA.
- Phan, K. H. (2017). Scalar one-loop four-point Feynman integrals with complex internal masses. *PTEP*, 2017(6), 063B06.
- Pumsa-ard, K., Lyubovitskij, V. E., Gutsche, T., Faessler, A., and Cheedket, S. (2003). Electromagnetic nucleon delta transition in the perturbative chiral quark model. *Phys. Rev. C*, 68, 015205.
- Ramalho, G. (2016). Improved empirical parametrizations of the $\gamma^*N \rightarrow \Delta(1232)$ and $\gamma^*N \rightarrow N(1520)$ helicity amplitudes and the Siegert's theorem. *Phys. Rev. D*, 93(11), 113012.
- Ramalho, G. and Pena, M. T. (2009). Valence quark contribution for the $\gamma N \rightarrow \Delta$ quadrupole transition extracted from lattice QCD. *Phys. Rev. D*, 80, 013008.
- Ramalho, G. and Pena, M. T. (2012). Timelike $\gamma^*N \rightarrow \Delta$ form factors and Δ Dalitz decay. *Phys. Rev. D*, 85, 113014.
- Rarita, W. and Schwinger, J. (1941). On a theory of particles with half integral spin. *Phys. Rev.*, 60, 61.
- Salone, N. and Leupold, S. (2021). Electromagnetic transition form factors and Dalitz decays of hyperons. *Eur. Phys. J. A*, 57(6), 183.
- Sato, T. and Lee, T. S. H. (2001). Dynamical study of the Δ excitation in $N(e, e'\pi)$ reactions. *Phys. Rev. C*, 63, 055201.

- Scherer, S. (2003). Introduction to chiral perturbation theory. *Adv. Nucl. Phys.*, 27, 277.
- Scherer, S. and Schindler, M. R. (2012a). *A Primer for Chiral Perturbation Theory*. *Lect. Notes Phys.*, 830(2012), pp.1-338.
- Scherer, S. and Schindler, M. R. (2012b). Chiral perturbation theory for mesons. *Lect. Notes Phys.*, 830, 65–144.
- Scherer, S. and Schindler, M. R. (2012c). Quantum chromodynamics and chiral symmetry. *Lect. Notes Phys.*, 830, 1–48.
- Sparveris, N. F., Achenbach, P., Gayoso, C. A., Baumann, D., Bernauer, J., Bernstein, A. M., Bhm, R., Bosnar, D., Botto, T., Christopoulou, A., Dale, D., Ding, M., Distler, M. O., Doria, L., Friedrich, J., Karabarounis, A., Makek, M., Merkel, H., and Mller, U. (2007). Determination of quadrupole strengths in the $\gamma^*p \rightarrow \Delta(1232)$ transition at $Q^2 = 0.20 \text{ (GeV/c)}^2$. *Phys. Lett. B*, 651, 102–107.
- Sparveris, N. F., Alarcon, R., Bernstein, A., Botto, T., Bourgeois, P., Calarco, J., Casagrande, F., Distler, M., Dow, K., Farkondeh, M., Georgakopoulos, S., Gilad, S., Hicks, R., Holtrop, M., Hotta, A., Jiang, X., Karabarounis, A., Kirkpatrick, J., Kowalski, S., and Milner, R. (2005). Investigation of the conjectured nucleon deformation at low momentum transfer. *Phys. Rev. Lett.*, 94, 022003.
- Stave, S., Distler, M. O., Nakagawa, I., Sparveris, N., P.Achenbach, Gayoso, C. A., Baumann, D., Bernauer, J., Bernstein, A. M., Bhm, R., Bosnar, D., Botto, T., Christopoulou, A., Dale, D., Ding, M., Doria, L., Friedrich, J., Karabarounis, A., Makek, M., Merkel, H., Mller, U., and Neuhausen, R. (2006). Lowest Q^2 Measurement of the $\gamma^*p \rightarrow \Delta$ Reaction: Probing the Pionic Contribution. *Eur. Phys. J. A*, 30, 471–476.
- Stave, S., Sparveris, N., Distler, M., Nakagawa, I., Achenbach, P., Gayoso, C. A., Baumann, D., Bernauer, J., Bernstein, A. M., and Botto, T. (2008). Measurements of the $\gamma^*p \rightarrow \Delta$ Reaction At Low Q^2 : Probing the Mesonic Contribution. *Phys. Rev. C*, 78, 025209.
- Stoica, S., Lutz, M. F. M., and Scholten, O. (2011). On kinematical constraints in fermion-antifermion systems. *Phys. Rev. D*, 84, 125001.

- 't Hooft, G. and Veltman, M. J. G. (1979). Scalar One Loop Integrals. *Nucl. Phys. B*, 153, 365–401.
- Tanabashi, M., Hagiwara, K., Hikasa, K., Nakamura, K., Sumino, Y., Takahashi, F., Tanaka, J., Agashe, K., Aielli, G., AMSLER, C., Antonelli, M., Asner, D., Baer, H., Banerjee, S., Barnett, R., Basaglia, T., Bauer, C., Beatty, J., Belousov, V., Beringer, J., Bethke, S., Bettini, A., Bichsel, H., Biebel, O., Black, K., Blucher, E., Buchmuller, O., Burkert, V., Bychkov, M., Cahn, R., Carena, M., Ceccucci, A., Cerri, A., and Chakraborty, D. (2018). Review of Particle Physics. *Phys. Rev. D*, 98(3), 030001.
- Ungaro, M., Stoler, P., Aznauryan, I., Burkert, V., Joo, K., Smith, L., Adams, G., Amarian, M., Ambrozewicz, P., Anghinolfi, M., Asryan, G., Audit, G., Avakian, H., Bagdasaryan, H., Ball, J., Baltzell, N., Barrow, S., Batourine, V., Battaglieri, M., Bedliski, I., Bektasoglu, M., Bellis, M., Benmouna, N., Berman, B., Biselli, A., Bonner, B., Bouchigny, S., Boiarinov, S., and Bradford, R. (2006). Measurement of the $N \rightarrow \Delta^+(1232)$ transition at high momentum transfer by π^0 electroproduction. *Phys. Rev. Lett.*, 97, 112003.
- Zwicky, R. (2017). A brief Introduction to Dispersion Relations and Analyticity. In *Quantum Field Theory at the Limits: from Strong Fields to Heavy Quarks*.



APPENDIX A

DERIVATION OF SCALAR ONE-LOOP FUNCTION

The procedure in this subsequent section is to derive the intermediate steps of scalar direct loop function as mentioned in Eq. (2.23). Recalling that the scalar function correspond to all parameters of the Feynman diagram represented by

$$C_3(s) = \frac{2}{i\pi^2} \int d^4q \int_0^1 dx dy dz \delta(1-x-y-z) \times \frac{1}{[x((q-p_2)^2 - m_\pi^2) + y((q+p_1)^2 - m_\pi^2) + z(q^2 - m_{ex}^2)]^3}, \quad (\text{A.1})$$

$$C_3(s) = \frac{2}{i\pi^2} \int d^4q \int_0^1 dx dy dz \delta(1-x-y-z) \frac{1}{A^3},$$

with $A = z(q^2 - m_{ex}^2) + y((q+p_1)^2 - m_\pi^2) + x((q-p_2)^2 - m_\pi^2)$. In order to evaluate the momentum integration from the relation of Eq. (A.1), it is essential to rewrite the momenta integrant as:

$$\begin{aligned} A &= xq^2 + xp_2^2 - 2qp_2x - xm_\pi^2 + yq^2 + yp_1^2 + 2qp_1y - ym_\pi^2 + zq^2 - zm_{ex}^2, \\ &= (x+y+z)q^2 + 2q(y p_1 - x p_2) - zm_{ex}^2 - ym_\pi^2 - xm_\pi^2 + yp_1^2. \end{aligned} \quad (\text{A.2})$$

Simplifying the denominator A by taking into account $x+y+z=1$ in the equation Eq. (A.2), it's become as:

$$A = q^2 + 2q(y p_1 - x p_2) - zm_{ex}^2 - ym_\pi^2 - xm_\pi^2 + yp_1^2. \quad (\text{A.3})$$

Making a shift of the transformation variable $\hat{q} = q + yp_1 - xp_2$, we get

$$\hat{A} = \hat{q}^2 - (yp_1 - xp_2)^2 - zm_{ex}^2 - ym_\pi^2 - xm_\pi^2 + yp_1^2 + i\epsilon. \quad (\text{A.4})$$

It is straightforward to mention the relation above as:

$$C_3(s) = \frac{2}{i\pi^2} \int_1^0 dx dy dz \int d^4 \hat{q} \quad (A.5)$$

$$(\hat{q}^2 - (yp_1 - xp_2)^2 - zm_{ex}^2 - ym_\pi^2 - xm_\pi^2 + yp_1^2 + xp_2^2 + i\epsilon)^{-3},$$

together with the consideration of $i\epsilon$ for all masses. The d-dimensional integral of the Minkowski space vector l is given by (Peskin and Schroeder, 1995)

$$\int \frac{d^d l}{(2\pi)^d} \frac{1}{(l^2 - \Delta)^n} = \frac{i(-1)^n}{(4\pi)^{d/2}} \frac{\Gamma(n - d/2)}{\Gamma(n)} \left(\frac{1}{\Delta}\right)^{(n-d/2)}. \quad (A.6)$$

The variable numbers in the above must be written in the consideration of $d=4$ and $n=3$ for our calculation.

$$\int \frac{d^4 l}{(2\pi)^4} \frac{1}{(l^2 - \Delta)^3} = \frac{i(-1)^3}{(4\pi)^2} \frac{\Gamma(3-2)}{\Gamma(3)} \left(\frac{1}{\Delta}\right)^{(3-2)}. \quad (A.7)$$

Making the substitution in Eq. (A.5), the result is

$$C_3(s) = \frac{2}{i\pi^2} \int_0^1 dx dy dz \delta(1-x-y-z) \frac{i(-1)^3 (2\pi)^4}{(4\pi)^2} \frac{1}{2} \left(\frac{1}{\Delta}\right), \quad (A.8)$$

$$C_3(s) = - \int_0^1 dx dy dz \delta(1-x-y-z) \left(\frac{1}{\Delta}\right),$$

with the terms

$$\begin{aligned} \Delta &= (yp_1 - xp_2)^2 + zm_{ex}^2 + ym_\pi^2 + xm_\pi^2 - yp_1^2 - xp_2^2, \\ \Delta &= y^2 p_1^2 + x^2 p_2^2 - 2xy p_1 p_2 + zm_{ex}^2 + ym_\pi^2 + xm_\pi^2 \\ &\quad - yp_1^2 - xp_2^2, \end{aligned} \quad (A.9)$$

$$\Delta = y(y-1)p_1^2 + x(x-1)p_2^2 - 2xy p_1 p_2 + zm_{ex}^2 + ym_\pi^2 + xm_\pi^2.$$

Applying the choosen delta functions: $x+y+z=1$, $y-1=-(x+z)$ and $x-1=-(y+z)$ for the integral Eq. (A.8), we have

$$\begin{aligned}\Delta &= -y(x+z)p_1^2 - x(y+z)p_2^2 - 2xyp_1p_2 + zm_{ex}^2 + ym_\pi^2 + xm_\pi^2, \\ \Delta &= -xy(p_1^2 + p_2^2 + 2p_1p_2) - yzp_1^2 - xzp_2^2 + zm_{ex}^2 + ym_\pi^2 + xm_\pi^2, \quad (\text{A.10}) \\ \Delta &= -(yzp_1^2 + xzp_2^2 + xys - zm_{ex}^2 - ym_\pi^2 - xm_\pi^2).\end{aligned}$$

This yields to rewrite the form of Eq. (A.8) as:

$$C_3(s) = \int_0^1 dx dy dz \frac{\delta(1-x-y-z)}{(yzp_1^2 + xzp_2^2 + xys - zm_{ex}^2 - ym_\pi^2 - xm_\pi^2)}. \quad (\text{A.11})$$

In that relation above we perform the integration over the variable number z as follow:

$$C_3(s) = \int_0^1 dx \int_0^{1-x} dy \frac{1}{\Delta_2}, \quad (\text{A.12})$$

with Δ_2 refers to the variable of the integrant:

$$\begin{aligned}\Delta_2 &= yp_1^2 - xyp_1^2 - y^2p_1^2 + xp_2^2 - x^2p_2^2 - xyp_2^2 + xys - m_{ex}^2 + xm_{ex}^2 \\ &\quad + ym_{ex}^2 - ym_\pi^2 - xm_\pi^2, \\ \Delta_2 &= -y^2p_1^2 - x^2p_2^2 + xy(s - p_1^2 - p_2^2) + x(p_2^2 + m_{ex}^2 - m_\pi^2) \\ &\quad + y(p_1^2 + m_{ex}^2 - m_\pi^2) - m_{ex}^2,\end{aligned} \quad (\text{A.13})$$

$$C_3(s) = \int_0^1 dx \int_0^{1-x} dy \frac{1}{\Delta_2}.$$

Performing a shift the integration limits as described above $x=1-x'$, we get:

$$\int_1^0 (-dx) \int_0^x dy = \int_0^1 dx \int_0^x dy, \quad (\text{A.14})$$

The three-piont function integration can then be written as the simple transformation form;

$$C_3(s) = \int_0^1 dx \int_0^x dy \frac{1}{\Delta_3}, \quad (\text{A.15})$$

with an intergrant term in each of the integrals

$$\begin{aligned} \Delta_3 &= -(1-x)^2 p_2^2 - y^2 p_1^2 + (1-x)y (s - p_1^2 - p_2^2) + (1-x) \\ &\quad \times (p_2^2 + m_{ex}^2 - m_\pi^2) + y (p_1^2 + m_{ex}^2 - m_\pi^2) - m_{ex}^2, \\ &= -p_2^2 + 2xp_2^2 - x^2 p_2^2 - y^2 p_1^2 + y(s - p_1^2 - p_2^2) - xy(s - p_1^2 - p_2^2) \\ &\quad + p_2^2 + m_{ex}^2 - m_\pi^2 - x(p_2^2 + m_{ex}^2 - m_\pi^2) - m_{ex}^2 \\ &\quad + y(p_1^2 + m_{ex}^2 - m_\pi^2), \\ &= -x^2 p_2^2 - y^2 p_1^2 - xy(s - p_1^2 - p_2^2) - x(m_{ex}^2 - p_2^2 - m_\pi^2) \\ &\quad + y(m_{ex}^2 - s - m_\pi^2 - p_2^2) - m_\pi^2, \\ \Delta_3 &= -(x^2 p_2^2 + y^2 p_1^2 + xy(s - p_1^2 - p_2^2) + x(m_{ex}^2 - p_2^2 - m_\pi^2) \\ &\quad + y(m_\pi^2 + p_2^2 - m_{ex}^2 - s) + m_\pi^2). \end{aligned} \quad (\text{A.16})$$

Of course the terms in above for the Feynman parameters are identified using the expressions in terms of momenta and masses $p_1^2 = m_\Delta^2$ and $p_2^2 = m_n^2$:

$$\begin{aligned} a &= m_n^2, b = m_\Delta^2, c = s - m_\Delta^2 - m_n^2, \\ d &= m_{ex}^2 - m_n^2 - m_\pi^2, e = m_n^2 + m_\pi^2 - m_{ex}^2 - s, \\ f &= m_\pi^2 + i\varepsilon. \end{aligned} \quad (\text{A.17})$$

Thereafter we must now rewrite the expression of Eq. (A.15) with the use of above Feynman parameters in an easiest ways as:

$$C_3(s) = - \int_0^1 dx \int_0^x dy (ax^2 + by^2 + cxy + dx + ey + f)^{-1}. \quad (\text{A.18})$$

This is a similar expression to a general one-loop scalar three-piont function in a given reference ('t Hooft and Veltman, 1979). With the aim of getting one-dimensional integral from where any integration does not cross any branch cuts, we change the integration boundary limit as $y = y' + \tau x$ in equation above Eq. (A.18).

$$\begin{aligned}
 C_3(s) &= - \int_0^1 dx \int_{-\tau x}^{(1-\tau)x} dy (ax^2 + b(y + \tau x)^2 + cx(y + \tau x) + dx \\
 &\quad + ey + f)^{-1}, \\
 &= - \int_0^1 dx \int_{-\tau x}^{(1-\tau)x} dy (ax^2 + by^2 + b\tau^2 x^2 + 2\tau byx + cxy + c\tau x^2 \\
 &\quad + dx + ey + e\tau x + f)^{-1}, \\
 &= - \int_0^1 dx \int_{-\tau x}^{(1-\tau)x} dy (x^2 (b\tau^2 + c\tau + a) + y^2 b + xy(c + 2\tau b) \\
 &\quad + x(d + e\tau) + ey + f)^{-1}.
 \end{aligned} \tag{A.19}$$

Since the integrant τ satisfies with one of the roots equation $b\tau^2 + c\tau + a = 0$, one can write:

$$\begin{aligned}
 C_3(s) &= - \int_0^1 dx \int_{-\tau x}^{(1-\tau)x} dy \\
 &\quad (y^2 b + xy(c + 2\tau b) + x(d + e\tau) + ey + f)^{-1}.
 \end{aligned} \tag{A.20}$$

From this, it is satisfying to define in the form $f(x, y) = (x((c + 2\tau b)y + e\tau + d) + by^2 + ey + f)^{-1}$. Then it becomes

$$C_3(s) = - \int_0^1 dx \int_{-\tau x}^{(1-\tau)x} dy f(x, y). \tag{A.21}$$

Separating the integration y into the two pieces in order to portray the boundaries based on the specific domain area, assuming that $0 < \tau < 1$ for the sake of graphics, this can be rewritten as:

$$-C_3(s) = \int_0^1 dx \int_0^{(1-\tau)x} dy f(x, y) - \int_0^1 dx \int_0^{-\tau x} dy f(x, y). \tag{A.22}$$

Changing the order of integration quoted in Eq. (A.22) again,

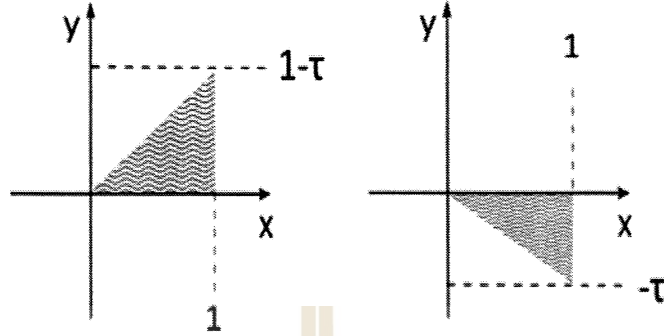


Figure A.1 Two integral triangle boundaries in the step Eq. (A.22).

$$-C_3(s) = \int_0^{(1-\tau)} dy \int_{y/(1-\tau)}^1 dx f(x,y) - \int_0^{-\tau} dy \int_{-y/\tau}^1 dx f(x,y). \quad (\text{A.23})$$

In addition, we insert the integration variable $y = \frac{y'}{1-\tau}$ into the first integral of Eq. (A.23), while the variable $y = -\frac{y''}{\tau}$ puts into the second part of these relation. Then,

$$-C_3(s) = \underbrace{\int_0^1 dy' \int_{y'}^1 dx (1-\tau) f(x,y')}_{:=I} - \underbrace{\int_0^1 dy'' \int_{y''}^1 dx (-\tau) f(x,y'')}_{:=I_1}. \quad (\text{A.24})$$

Solving the first piece I through the integration y , we obtain

$$I = \int_0^1 dy \int_y^1 dx (1-\tau) \quad (\text{A.25})$$

$$\times (x((c+2b\tau)(1-\tau)y + e\tau + d) + b(1-\tau)^2 y^2 + e(1-\tau)y + f)^{-1},$$

$$\begin{aligned} I &= \int_0^1 dy \int_y^1 dx \frac{(1-\tau)}{xM+K} = \int_0^1 dy \int_y^1 dx \frac{(1-\tau)}{M} \frac{1}{x + \frac{K}{M}}, \\ &= \int_0^1 dy \frac{(1-\tau)}{M} \log \frac{M+K}{YM+K}, \end{aligned} \quad (\text{A.26})$$

with the arguments of $M = (c + cb\tau)(1 - \tau)y + e\tau + d$ and $K = b(1 - \tau)^2y^2 + e(1 - \tau)y + f$. Likewise, the result for the second integral I_1 is

$$\begin{aligned}
 I_1 &= \int_0^1 dy \int_y^1 dx \\
 &\quad \frac{(-\tau)}{x((c + 2b\tau)(-\tau)y + e\tau + d) + b(-\tau)^2y^2 + e(-\tau)y + f}, \\
 &= \int_0^1 dy \int_y^1 dx \frac{(-\tau)}{xN + L}, \\
 &= \int_0^1 dy \frac{-\tau}{N} \log \frac{N + L}{yN + L},
 \end{aligned} \tag{A.27}$$

where the substitution arguments $N = (c + 2b\tau)(-\tau)y + e\tau + d$ and $L = b(-\tau)^2y^2 + e(-\tau)y + f$. Combination of all outcoming results from the integrals I and I_1 support to the one has:

$$-C_3(s) = \int_0^1 dy \frac{1 - \tau}{M} \log \frac{M + K}{yM + K} - \int_0^1 dy \frac{(-\tau)}{N} \log \frac{N + K}{yN + K}. \tag{A.28}$$

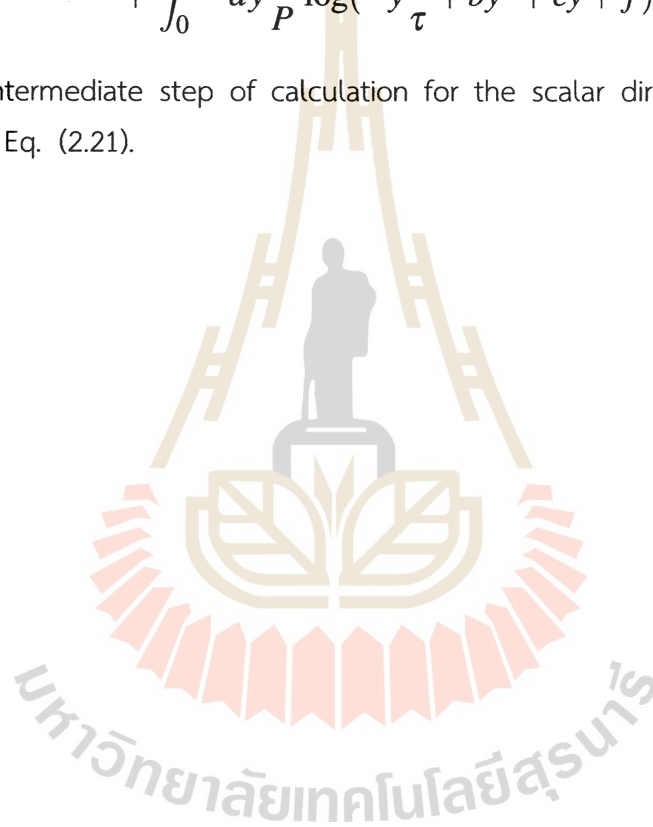
In such a way that making a change of variables $y = \frac{y'}{1 - \tau}$ and $y = -\frac{y''}{\tau}$ in the two integrals, the coefficients of the logarithmic term are obtained as;

$$\begin{aligned}
 -C_3(s) &= \int_0^{(1-\tau)} \frac{dy}{P} \log \frac{P + by^2 + ey + f}{y\frac{P}{1-\tau} + by^2 + ey + f} \\
 &\quad - \int_0^{-\tau} \frac{dy}{P} \log \frac{P + by^2 + ey + f}{-y\frac{P}{\tau} + by^2 + ey + f},
 \end{aligned} \tag{A.29}$$

where $P = (c + 2\tau b)y + e\tau + d$. It can be expanded the sum of the logarithms form explicitly by combining some of the integral terms as

$$\begin{aligned}
 -C_3(s) = & \int_{-\tau}^{(1-\tau)} dy \frac{1}{P} \log(P + by^2 + ey + f) \\
 & - \int_0^{(1-\tau)} dy \frac{1}{P} \log\left(y \frac{P}{1-\tau} + by^2 + ey + f\right) \\
 & + \int_0^{-\tau} dy \frac{1}{P} \log\left(-y \frac{P}{\tau} + by^2 + ey + f\right).
 \end{aligned} \tag{A.30}$$

This is the intermediate step of calculation for the scalar direct loop diagram as presented in Eq. (2.21).



APPENDIX B

STEPS OF DELTA FUNCTION

The following procedure is the derivation steps of the delta function presented in section (3.1.3). Let us recall the smooth functions $f(x,y)$ and $g(x,y)$ which have a common zero are differentiable at least once in the interval of integration. Then

$$\delta(f(x,y))\delta(g(x,y)) = \frac{\delta(x-x_0)\delta(y-y_0)}{\left|\frac{\partial f}{\partial x} \frac{\partial g}{\partial y}\right|_{(x_0,y_0)} - \left|\frac{\partial f}{\partial y} \frac{\partial g}{\partial x}\right|_{(x_0,y_0)}}. \quad (\text{B.1})$$

From the two delta functions $\delta(f(q^0, |\vec{q}|))\delta(g(q^0, |\vec{q}|))$, we derive the zero point of these functions which obey the rules of step Θ -functions according to $f(x_0, y_0) = 0 = g(x_0, y_0)$. Then, we have that zero of both functions

$$\begin{aligned} f(q^0, |\vec{q}|) &= (q^0 + p_1^0)^2 - |\vec{q}|^2 - m_\pi^2, \\ g(q^0, |\vec{q}|) &= (q^0 - p_2^0)^2 - |\vec{q}|^2 - m_\pi^2. \end{aligned} \quad (\text{B.2})$$

with the notation $q^{0*} = -p_1^0 + \sqrt{|\vec{q}|^2 + m_\pi^2}$. Inserting this value of q^{0*} into the function $g(q^0, |\vec{q}|) = 0$, we obtain the value of $|\vec{q}|$. It becomes then

$$(q^0 - p_2^0)^2 - |\vec{q}|^2 - m_\pi^2 = 0, \quad |\vec{q}|^* = \frac{\sqrt{s}}{2} \sqrt{1 - \frac{4m_\pi^2}{s}}. \quad (\text{B.3})$$

Taking the partial derivative at the zero point, we find that

$$\begin{aligned} \frac{\partial f}{\partial q^0} &= \sqrt{s} \quad , \quad \frac{\partial g}{\partial q^0} = -\sqrt{s}, \\ \frac{\partial f}{\partial |\vec{q}|} &= -2|\vec{q}|^* \quad , \quad \frac{\partial g}{\partial |\vec{q}|} = -2|\vec{q}|^*, \end{aligned} \quad (\text{B.4})$$

and

$$\frac{\partial f}{\partial q^0} \frac{\partial g}{\partial |\vec{q}|} \Big|_{(q^{0*}, |\vec{q}|^*)} - \frac{\partial f}{\partial |\vec{q}|} \frac{\partial g}{\partial q^0} \Big|_{(q^{0*}, |\vec{q}|^*)} = 4\sqrt{s}|\vec{q}|^*. \quad (\text{B.5})$$

APPENDIX C

DERIVATION OF JONE-SCADRON FORM FACTORS

Recalling that the definition of the matrix elements of helicity amplitudes introduced in Eq. (3.14)

$$\begin{aligned}
 A_{3/2} &\equiv -\frac{e}{\sqrt{2}q_\Delta} \frac{1}{(4m_n m_\Delta)^{1/2}} \langle \Delta(\vec{0}, +3/2) | \mathbf{J} \cdot \boldsymbol{\varepsilon}_{\lambda=+1} | N(-\vec{q}, +1/2) \rangle, \\
 A_{1/2} &\equiv -\frac{e}{\sqrt{2}q_\Delta} \frac{1}{(4m_n m_\Delta)^{1/2}} \langle \Delta(\vec{0}, +1/2) | \mathbf{J} \cdot \boldsymbol{\varepsilon}_{\lambda=+1} | N(-\vec{q}, -1/2) \rangle, \quad (\text{C.1}) \\
 S_{1/2} &\equiv \frac{e}{\sqrt{2}q_\Delta} \frac{1}{(4m_n m_\Delta)^{1/2}} \langle \Delta(\vec{0}, +1/2) | J^0 | N(-\vec{q}, +1/2) \rangle.
 \end{aligned}$$

From the definition of Eq. (3.15), we derive the charge form factors G_C^* inserting the relation of Eq. (C.1)

$$\begin{aligned}
 G_C^* &= \frac{\sqrt{2}m_\Delta}{Nq_\Delta} S_{1/2} \\
 &= \frac{\sqrt{2}m_\Delta}{Nq_\Delta} \frac{e}{\sqrt{2}q_\Delta} \frac{1}{(4m_n m_\Delta)^{1/2}} \langle \Delta(\vec{0}, +1/2) | J^0 | N(-\vec{q}, +1/2) \rangle, \quad (\text{C.2}) \\
 &= \frac{4m_\Delta^2 m_n}{(m_n + m_\Delta)} \frac{1}{Q_+ Q_-^2} \langle \Delta(\vec{0}, +1/2) | J^0 | N(-\vec{q}, +1/2) \rangle.
 \end{aligned}$$

According to the spin polarization vector in Eq. (E.2), we define the expectation value of electromagnetic current for the zeroth component in the Δ rest frame

$$\langle \Delta | J^0 | N \rangle = \frac{1}{m_\Delta} p_\Delta^\mu \langle \Delta | J^\mu | N \rangle = -\frac{e}{m_\Delta} \underbrace{\bar{u}_\Delta^\nu p_\Delta^\mu \tilde{\Gamma}_{\mu\nu}(p_\Delta, -p_n)} u_n. \quad (\text{C.3})$$

Choosing the selective part of Eq. (C.3) we make it clear to get the simplest form

$$\begin{aligned}
 \bar{u}_\Delta^\nu p_\Delta^\mu \tilde{\Gamma}_{\mu\nu} &= \bar{u}_\Delta^\nu p_\Delta^\mu \left[(\gamma^\mu q^\nu - \not{q} g^{\mu\nu}) m_\Delta \gamma_5 F_1(q^2) \right. \\
 &\quad + (p_\Delta^\mu q^\nu - p_\Delta \cdot q g^{\mu\nu}) \gamma_5 F_2(q^2) \\
 &\quad \left. + (q^\mu q^\nu - q^2 g^{\mu\nu}) \gamma_5 F_3(q^2) \right], \\
 &= \bar{u}_\Delta^\nu \not{p}_\Delta q^\nu m_\Delta \gamma_5 F_1(q^2) + \bar{u}_\Delta^\nu m_\Delta^2 q^\nu m_\Delta \gamma_5 F_2(q^2) \\
 &\quad + \bar{u}_\Delta^\nu p_\Delta \cdot q q^\nu \gamma_5 F_3(q^2), \quad (\because \bar{u}_\Delta^\nu \not{p}_\Delta = \bar{u}_\Delta^\nu m_\Delta), \\
 &= \bar{u}_\Delta^\nu q^\nu \gamma_5 \left[m_\Delta^2 F_1(q^2) + m_\Delta^2 F_2(q^2) + p_\Delta \cdot q F_3(q^2) \right], \\
 &= \bar{u}_\Delta^\nu q^\nu \gamma_5 \underbrace{\left[m_\Delta^2 F_1(q^2) + m_\Delta^2 F_2(q^2) + \frac{1}{2}(q^2 + m_\Delta^2 - m_n^2) F_3(q^2) \right]}_{G_0(q^2)}, \\
 &= \bar{u}_\Delta^\nu q^\nu \gamma_5 G_0(q^2),
 \end{aligned} \tag{C.4}$$

where the three momentum of delta in the z-direction is $p_\Delta \cdot q = \frac{1}{2}(q^2 + m_\Delta^2 - m_n^2)$ and $\bar{u}_\Delta^\nu p_{\Delta\nu} = 0$. Assuming that $\bar{u}_\Delta^\nu q_\nu = -q_\Delta \bar{u}_\Delta^3$ in the rest frame, we write

$$\begin{aligned}
 \langle \Delta | J^0 | N \rangle &= -\frac{e}{m_\Delta} \bar{u}_\Delta^\nu q^\nu \gamma_5 G_0(q^2) u_n, \\
 &= \frac{1}{m_\Delta} q_\Delta G_0(q^2) \underbrace{\bar{u}_\Delta^3 \gamma_5 u_n}_{\text{spinor structure}}.
 \end{aligned} \tag{C.5}$$

In accordance with the properties of the vector spinor (Junker et al., 2020) and gamma matrices of the block-diagonal form, we define the spinor structure explicitly for the spinor component $\bar{u}_\Delta^3(\vec{p}_\Delta = \vec{0}, S_{\Delta_z} = +1/2) \gamma_5 u_n(\vec{p}_N = -\vec{q}, S_{N_z} = +1/2)$

$$\bar{u}_\Delta^3(\vec{p}_\Delta = \vec{0}, S_{\Delta_z} = +1/2) = \begin{pmatrix} \sqrt{m_\Delta} \\ 0 \\ \sqrt{m_\Delta} \\ 0 \end{pmatrix}, \quad \gamma^5 = \begin{pmatrix} -1 & 0 \\ 0 & 1 \end{pmatrix}. \tag{C.6}$$

The spin 1/2 spinor in the same frame has

$$u\left(p_z, s = +\frac{1}{2}\right) = \begin{pmatrix} \sqrt{E-p_z} \\ 0 \\ \sqrt{E+p_z} \\ 0 \end{pmatrix}, u\left(p_z, s = -\frac{1}{2}\right) = \begin{pmatrix} 0 \\ \sqrt{E+p_z} \\ 0 \\ \sqrt{E-p_z} \end{pmatrix}. \quad (\text{C.7})$$

Substituting altogether into the underline part of equation Eq. (C.5), we get

$$\begin{aligned} \bar{u}_\Delta^3 \gamma_5 u_n &= \sqrt{\frac{2}{3}} (\sqrt{m_\Delta}, 0, \sqrt{m_\Delta}, 0) \times \begin{pmatrix} -\sqrt{E_n+p_n} \\ 0 \\ \sqrt{E_n-p_n} \\ 0 \end{pmatrix}, \\ &= -\sqrt{\frac{2}{3}} \sqrt{m_\Delta} \underbrace{(\sqrt{E_n+p_n} - \sqrt{E_n-p_n})}. \end{aligned} \quad (\text{C.8})$$

In addition to the square of the bracket in the underbrace of above Eq. (C.8),

$$\begin{aligned} (\sqrt{E_n+p_n} - \sqrt{E_n-p_n})^2 &= E_n + q_\Delta + E_n - q_\Delta - 2\sqrt{E_n^2 - q_\Delta^2}, \\ &= 2(E_n - m_n) \quad (\because E_n^2 - q_\Delta^2 = E_n^2 - \vec{p}_n^2 = m_n^2), \\ &= 2\left(\frac{m_\Delta^2 + m_n^2 - q^2}{2m_\Delta} - m_n\right), \\ &= \frac{1}{m_\Delta} Q_-^2 \quad (\because Q_\pm = \sqrt{(m_\Delta \pm m_n)^2 + Q^2}). \end{aligned} \quad (\text{C.9})$$

Which yields

$$\bar{u}_\Delta^3 \gamma_5 u_n = -\sqrt{\frac{2}{3}} \sqrt{m_\Delta} \times \frac{Q_-^2}{m_\Delta} \times \frac{\sqrt{m_\Delta}}{Q_-} = -\sqrt{\frac{2}{3}} Q_-. \quad (\text{C.10})$$

Now turning to the form of Eq. (C.5),

$$\begin{aligned}
 \langle \Delta | J^0 | N \rangle &= -\frac{eq_\Delta}{m_\Delta} G_0(q^2) \sqrt{\frac{2}{3}} Q_-, \\
 &\equiv \pm \frac{q_\Delta}{m_\Delta} G_0(q^2) \sqrt{\frac{2}{3}} Q_-, \quad (\because J^0 = \pm e J^0) \\
 &\equiv \pm \frac{Q_+ Q_-}{2m_\Delta^2} \sqrt{\frac{2}{3}} G_0(q^2) Q_-
 \end{aligned} \tag{C.11}$$

The final charge form factors relation can be written by inserting the relation Eq. (C.11) into the Eq. (C.2);

$$\begin{aligned}
 G_C^* &= \frac{4m_\Delta^2 m_n}{(m_n + m_\Delta)} \frac{1}{Q_+ Q_-^2} \langle \Delta(\vec{0}, +1/2) | J^0 | N(-\vec{q}, +1/2) \rangle, \\
 &= \pm \frac{4m_\Delta^2 m_n}{(m_n + m_\Delta)} \frac{1}{Q_+ Q_-^2} \frac{Q_+ Q_-^2}{2m_\Delta^2} \sqrt{\frac{2}{3}} G_0(q^2), \\
 \therefore G_C^* &= -\frac{\zeta^4}{\sqrt{6}} \frac{m_n}{m_n + m_\Delta} G_0(q^2).
 \end{aligned} \tag{C.12}$$

Now we move on the derivation for the helicity amplitude expressed in terms of G_M^* and G_E^* by means of the definition $A_{1/2} = -\frac{N}{2} (G_M^* - 3G_E^*)$

$$\begin{aligned}
 G_M^* - 3G_E^* &= -\frac{2}{N} \frac{-e}{\sqrt{2}q_\Delta} \frac{1}{\sqrt{4m_n m_\Delta}} \\
 &\quad \times \langle \Delta(\vec{0}, +1/2) | \mathbf{J} \cdot \boldsymbol{\varepsilon}_{\lambda=+1} | N(-\vec{q}, -1/2) \rangle, \\
 &= \frac{2(2m_\Delta^2)^{1/2}}{(Q_+ Q_-)^{1/2}} \frac{1}{\sqrt{m_n m_\Delta}} \frac{m_n^{3/2}}{(Q_+ Q_-)^{1/2}} \\
 &\quad \times \frac{Q_+}{m_n + m_\Delta} \langle \Delta(\vec{0}, +1/2) | \mathbf{J} \cdot \boldsymbol{\varepsilon}_{\lambda=+1} | N(-\vec{q}, -1/2) \rangle, \\
 &= \frac{2\sqrt{2}}{Q_-} \frac{m_n}{m_n + m_\Delta} \underbrace{\langle \Delta(\vec{0}, +1/2) | \mathbf{J} \cdot \boldsymbol{\varepsilon}_{\lambda=+1} | N(-\vec{q}, -1/2) \rangle}.
 \end{aligned} \tag{C.13}$$

In a similar way, we firstly focus on the matrix elements of the underbrace in Eq. (C.13) for the Jone-Scadron form factors formulae. Here, only the components of index 1 and 2 will consistent for the state of $\sigma = -\lambda = 1/2$. As mentioned earlier section, to obtain our conventional relation at hand, it is convenient to define the sign for all $m = \pm 1, 0$. One can start

$$\begin{aligned}
 & \langle \Delta(\vec{0}, +1/2) | \mathbf{J} \cdot \boldsymbol{\varepsilon}_{\lambda=+1} | N(-\vec{q}, -1/2) \rangle, \\
 &= \frac{1}{\sqrt{2}} \langle \Delta(\vec{0}, +1/2) | J^\mu | N(-\vec{q}, -1/2) \rangle, \\
 &= \frac{1}{\sqrt{2}} \left[\langle \Delta(\vec{0}, +1/2) | J^1 | N(-\vec{q}, -1/2) \rangle \right. \\
 &\quad \left. - i \langle \Delta(\vec{0}, +1/2) | J^2 | N(-\vec{q}, -1/2) \rangle \right], \\
 &= \frac{1}{\sqrt{2}} \left[-e \bar{u}_\Delta^\nu \tilde{\Gamma}_{1\nu}(p_\Delta, -p_n) u_n + i e \bar{u}_\Delta^\nu \tilde{\Gamma}_{2\nu}(p_\Delta, -p_n) u_n \right], \\
 &= \frac{e}{\sqrt{2}} \left[-\underbrace{\bar{u}_\Delta^\nu \tilde{\Gamma}_{1\nu}(p_\Delta, -p_n)} u_n + i \bar{u}_\Delta^\nu \tilde{\Gamma}_{2\nu}(p_\Delta, -p_n) u_n \right].
 \end{aligned} \tag{C.14}$$

Solving the underlying piece as follow;

$$\begin{aligned}
 \bar{u}_\Delta^\nu \tilde{\Gamma}_{1\nu} &= \bar{u}_\Delta^\nu \left[(\gamma^\mu q^\nu - \not{q} g^{\mu\nu}) m_\Delta \gamma_5 F_1(q^2) \right. \\
 &\quad + (p_\Delta^\mu q^\nu - p_\Delta \cdot q g^{\mu\nu}) \gamma_5 F_2(q^2) \\
 &\quad \left. + (q^\mu q^\nu - q^2 g^{\mu\nu}) \gamma_5 F_3(q^2) \right], \\
 &= -\bar{u}_\Delta^\nu \left[(\not{p}_\Delta - \not{p}_n) m_\Delta \gamma_5 F_1(q^2) + p_\Delta \cdot q \gamma_5 F_2(q^2) + q^2 \gamma_5 F_3(q^2) \right], \\
 &\quad (\because \not{p}_n u_n^\nu = -m_n u_n^\nu)
 \end{aligned} \tag{C.15}$$

$$\bar{u}_\Delta^\nu \tilde{\Gamma}_{1\nu} = -\bar{u}_\Delta^\nu \gamma_5$$

$$\underbrace{\left[(m_\Delta + m_n) m_\Delta F_1(q^2) + \frac{1}{2} (q^2 + m_\Delta^2 - m_n^2) F_2(q^2) + q^2 F_3(q^2) \right]}_{G_{-1}(q^2)}, \quad (\text{C.16})$$

$$= -\bar{u}_\Delta^\nu \gamma_5 G_{-1}(q^2).$$

It allows us to write a form directly as

$$\begin{aligned} & \langle \Delta(\vec{0}, +1/2) | \mathbf{J} \cdot \boldsymbol{\varepsilon}_{\lambda=+1} | N(-\vec{q}, -1/2) \rangle \\ &= \frac{e}{\sqrt{2}} \left[\bar{u}_\Delta^1 \gamma^5 u_n G_{-1}(q^2) - i \bar{u}_\Delta^2 \gamma^5 u_n G_{-1}(q^2) \right]. \end{aligned} \quad (\text{C.17})$$

Let us turn to the explicit derivation of spinor structure $\bar{u}_\Delta^\mu(\vec{p}_\Delta = \vec{0}, S_{\Delta_z} = +1/2) \gamma_5 u_n(\vec{p}_N = -\vec{q}, S_{N_z} = -1/2)$ following the rules of vector spinor in this frame by

$$\begin{aligned} & \bar{u}_\Delta^\mu(\vec{p}_\Delta = \vec{0}, S_{\Delta_z} = +1/2) \\ &= \frac{1}{\sqrt{3}} u(p, -1/2) \varepsilon^\mu(p, +1), \\ &= -\frac{1}{\sqrt{6}} (1+i) \bar{u}_\Delta^\mu(\vec{p}_\Delta = \vec{0}, S_{\Delta_z} = -1/2). \end{aligned} \quad (\text{C.18})$$

Then we calculate

$$\begin{aligned} \bar{u}_\Delta^\mu \gamma^5 u_n &= \frac{-1}{\sqrt{6}} (1+i) (0, \sqrt{m_\Delta}, 0, \sqrt{m_\Delta}) \times \begin{pmatrix} 0 \\ -\sqrt{E_n - p_n} \\ 0 \\ \sqrt{E_n + p_n} \end{pmatrix}, \\ &= \frac{-1}{\sqrt{6}} (1+i) \sqrt{m_\Delta} \left(\sqrt{E_n + p_n} - \sqrt{E_n - p_n} \right), \\ &= \frac{-1}{\sqrt{6}} (1+i) \sqrt{m_\Delta} \times \frac{Q_-^2}{m_\Delta} \times \frac{\sqrt{m_\Delta}}{Q_-}, \\ &= \frac{-1}{\sqrt{6}} (1+i) Q_-. \end{aligned} \quad (\text{C.19})$$

Afterwards the matrix elements term become

$$\begin{aligned}
 \langle \Delta(\vec{0}, +1/2) | \mathbf{J} \cdot \boldsymbol{\varepsilon}_{\lambda=+1} | N(-\vec{q}, -1/2) \rangle &= \frac{-e}{\sqrt{2}} G_{-1}(q^2) \left[\frac{Q_-}{\sqrt{6}} + \frac{Q_-}{\sqrt{6}} \right], \\
 &= -\frac{2}{\sqrt{2}} \frac{Q_-}{\sqrt{6}} G_{-1}(q^2), (\because \mathbf{J} \cdot \boldsymbol{\varepsilon}_{\lambda=+1} = e J^\mu \varepsilon_{\lambda=+1}) \\
 &= \mp \frac{2}{\sqrt{2}} \frac{Q_-}{\sqrt{6}} G_{-1}(q^2).
 \end{aligned} \tag{C.20}$$

Recall that the relation Eq. (C.13);

$$\begin{aligned}
 G_M^* - 3G_E^* &= \frac{m_n}{m_n + m_\Delta} \frac{2\sqrt{2}}{Q_-} \langle \Delta(\vec{0}, +1/2) | \mathbf{J} \cdot \boldsymbol{\varepsilon}_{\lambda=+1} | N(-\vec{q}, -1/2) \rangle, \\
 &= \mp \frac{m_n}{m_n + m_\Delta} \frac{2\sqrt{2}}{Q_-} \frac{2}{\sqrt{2}} \frac{Q_-}{\sqrt{6}} G_{-1}(q^2), \\
 &= \mp \frac{4}{\sqrt{6}} \frac{m_n}{m_n + m_\Delta} G_{-1}(q^2).
 \end{aligned} \tag{C.21}$$

We also derive below that the helicity amplitude for the component $A_{3/2} = -N \frac{\sqrt{3}}{2} [G_M^* + G_E^*]$ as

$$\begin{aligned}
 G_M^* + G_E^* &= -\frac{2}{\sqrt{3}N} A_{3/2}, \\
 &= \frac{2}{\sqrt{3}N} \frac{-e}{2q_\Delta} \frac{1}{(4m_n m_\Delta)^{1/2}} \langle \Delta(\vec{0}, +3/2) | \mathbf{J} \cdot \boldsymbol{\varepsilon}_{\lambda=+1} | N(-\vec{q}, +1/2) \rangle, \\
 &= \frac{e}{\sqrt{6}} \sqrt{\frac{2m_\Delta}{Q_+ Q_-}} \frac{1}{\sqrt{m_n m_\Delta}} \frac{2}{e} \frac{\sqrt{2} m_n^{3/2}}{\sqrt{Q_+ Q_-}} \frac{Q_+}{m_n + m_\Delta} \\
 &\quad \times \langle \Delta(\vec{0}, +3/2) | \mathbf{J} \cdot \boldsymbol{\varepsilon}_{\lambda=+1} | N(-\vec{q}, +1/2) \rangle, \\
 &= \frac{4}{\sqrt{6}} \frac{m_n}{m_n + m_\Delta} \frac{1}{Q_-} \underbrace{\langle \Delta(\vec{0}, +3/2) | \mathbf{J} \cdot \boldsymbol{\varepsilon}_{\lambda=+1} | N(-\vec{q}, +1/2) \rangle}.
 \end{aligned} \tag{C.22}$$

The selective part of the helicity amplitude definition is simplified by

$$\begin{aligned}
& \langle \Delta(\vec{0}, +3/2) | \mathbf{J} \cdot \boldsymbol{\varepsilon}_{\lambda=+1} | N(-\vec{q}, +1/2) \rangle \\
&= \frac{1}{\sqrt{2}} \langle \Delta(\vec{0}, +3/2) | J^\mu | N(-\vec{q}, +1/2) \rangle, \\
&= \frac{1}{\sqrt{2}} \left[\langle \Delta(\vec{0}, +3/2) | J^1 | N(-\vec{q}, +1/2) \rangle \right. \\
&\quad \left. - i \langle \Delta(\vec{0}, +3/2) | J^2 | N(-\vec{q}, +1/2) \rangle \right], \tag{C.23} \\
&= \frac{e}{\sqrt{2}} \left[- \underbrace{\bar{u}_\Delta^1 \tilde{\Gamma}_{\mu\nu}(p_\Delta, -p_n) u_n}_{-\bar{u}_\Delta^1 \gamma_5 G_{+1}(q^2)} + i \underbrace{\bar{u}_\Delta^2 \tilde{\Gamma}_{\mu\nu}(p_\Delta, -p_n) u_n}_{-\bar{u}_\Delta^2 \gamma_5 G_{+1}(q^2)} \right], \\
&= \frac{e}{\sqrt{2}} \left[\bar{u}_\Delta^1 \gamma_5 u_n G_{+1}(q^2) - i \bar{u}_\Delta^2 \gamma_5 u_n G_{+1}(q^2) \right].
\end{aligned}$$

Following to the constructed spinor form for the spin 3/2 state,

$$\begin{aligned}
u^\mu(p, +3/2) &= u(p, +1/2) \varepsilon^\mu(p, +1), \\
&= -\frac{1}{\sqrt{2}} (1+i) \bar{u}_\Delta^\mu(\vec{p}_\Delta = \vec{0}, S_{\Delta_z} = +1/2). \tag{C.24}
\end{aligned}$$

This can be inserted into the equation Eq. (C.23) in order to get the complete expression of the helicity amplitude taking into account the spin 1/2 spinor. Here it is

$$\begin{aligned}
\bar{u}_\Delta^\mu \gamma^5 u_n &= \frac{-1}{\sqrt{2}} (1+i) (\sqrt{m_\Delta}, 0, \sqrt{m_\Delta}, 0) \begin{pmatrix} -\sqrt{E_n + q_\Delta} \\ 0 \\ \sqrt{E_n - q_\Delta} \\ 0 \end{pmatrix}, \\
&= \frac{1}{\sqrt{2}} (1+i) \sqrt{m_\Delta} \left(\sqrt{E_n + q_\Delta} - \sqrt{E_n - q_\Delta} \right), \tag{C.25} \\
&= \frac{1}{\sqrt{2}} (1+i) \sqrt{m_\Delta} \frac{Q_-^2}{m_\Delta} \frac{\sqrt{m_\Delta}}{Q_-} = \frac{1}{\sqrt{2}} (1+i) Q_-.
\end{aligned}$$

It leads to write the matrix element as below

$$\begin{aligned}
 & \langle \Delta(\vec{0}, +3/2) | \mathbf{J} \cdot \boldsymbol{\varepsilon}_{\lambda=+1} | N(-\vec{q}, +1/2) \rangle \\
 &= \frac{e}{\sqrt{2}} \left[\frac{Q_-}{\sqrt{2}} + \frac{Q_-}{\sqrt{2}} \right] G_{+1}(q^2), \\
 &= \frac{2e}{\sqrt{2}} \frac{Q_-}{\sqrt{2}} G_{+1}(q^2), \\
 &= \pm Q_- G_{-1}(q^2).
 \end{aligned} \tag{C.26}$$

Finally the spin 3/2 helicities relation reads as;

$$\begin{aligned}
 G_M^* + G_E^* &= \frac{4}{\sqrt{6}} \frac{m_n}{m_n + m_\Delta} \frac{1}{Q_-} \langle \Delta(\vec{0}, +3/2) | \mathbf{J} \cdot \boldsymbol{\varepsilon}_{\lambda=+1} | N(-\vec{q}, +1/2) \rangle, \\
 &= \pm \frac{4}{\sqrt{6}} \frac{m_n}{m_n + m_\Delta} \frac{1}{Q_-} G_{+1}(q^2) Q_-, \\
 &= \pm \frac{4}{\sqrt{6}} \frac{m_n}{m_n + m_\Delta} G_{+1}(q^2).
 \end{aligned} \tag{C.27}$$

Collecting all the expression Eq. (C.21) and Eq. (C.27) relating the terms of G_M^* and G_E^* , we figure out the Jone-Scadron form factors bmultiplied 3 into the equation Eq. (C.27). Then

$$\begin{aligned}
 G_M^* - 3G_E^* &= \mp \frac{4}{\sqrt{6}} \frac{m_n}{m_n + m_\Delta} G_{-1}(q^2), \\
 3(G_M^* + G_E^*) &= \pm 3 \frac{4}{\sqrt{6}} \frac{m_n}{m_n + m_\Delta} G_{+1}(q^2),
 \end{aligned} \tag{C.28}$$

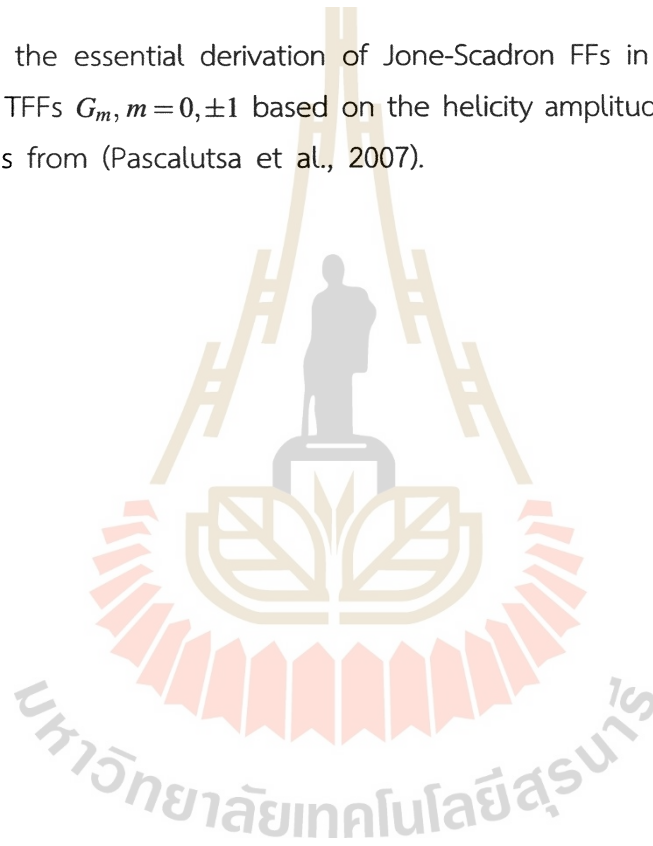
$$\therefore G_M^* = \frac{\zeta}{\sqrt{6}} \frac{m_n}{m_n + m_\Delta} (G_{-1}(q^2) - 3 G_{+1}(q^2)),$$

with the phase factor: $\zeta = -1$. Again we multiply the negative sign into the relation Eq. (C.21) and then take the combination of Eq. (C.21) and Eq. (C.27) as well.

Which gives rise to the final electric form factors relation

$$\begin{aligned}
 -(G_M^* - 3G_E^*) &= \pm \frac{4}{\sqrt{6}} \frac{m_n}{m_n + m_\Delta} G_{-1}(q^2), \\
 G_M^* + G_E^* &= \pm \frac{4}{\sqrt{6}} \frac{m_n}{m_n + m_\Delta} G_{+1}(q^2), \\
 \therefore G_E^* &= -\frac{\zeta}{\sqrt{6}} \frac{m_n}{m_n + m_\Delta} (G_{-1}(q^2) + G_{+1}(q^2)).
 \end{aligned} \tag{C.29}$$

These are all the essential derivation of Jone-Scadron FFs in terms of our linear combinations TFFs $G_m, m=0, \pm 1$ based on the helicity amplitudes of $A_{3/2}$, $A_{1/2}$, and $S_{1/2}$ definitions from (Pascalutsa et al., 2007).



APPENDIX D

COEFFICIENT FUNCTIONS

All necessary input coefficient functions in equation Eq. (4.43) are introduced as follow;

$$\begin{aligned}
 R_s^{\text{oct}}(s) &= \frac{-2Y_p}{\kappa^2} \left(1 - \left(1 - \frac{Y_p^2}{\kappa^2} \right) \frac{|\kappa|}{Y_p} \left(\arctan \left(\frac{|\kappa|}{Y_p} \right) + \pi \Theta(s_Y - s) \right) \right), \\
 R_d^{\text{oct}}(s) &= \frac{4}{\kappa^2} \left(1 - \frac{Y_p}{|\kappa|} \left(\arctan \left(\frac{|\kappa|}{Y_p} \right) + \pi \Theta(s_Y - s) \right) \right), \\
 R_s^{\text{dec}}(s) &= \frac{-2Y_\Delta}{\kappa^2} \left(1 - \left(1 - \frac{Y_\Delta^2}{\kappa^2} \right) \frac{|\kappa|}{Y_\Delta} \arctan \left(\frac{|\kappa|}{Y_\Delta} \right) \right), \\
 R_d^{\text{dec}}(s) &= \frac{4}{\kappa^2} \left(1 - \frac{Y_\Delta}{|\kappa|} \arctan \left(\frac{|\kappa|}{Y_\Delta} \right) \right),
 \end{aligned} \tag{D.1}$$

with

$$\begin{aligned}
 Y_p &= 2m_p^2 - m_\Delta^2 - m_n^2 - 2m_\pi^2 + s, \\
 Y_\Delta &= m_\Delta^2 - m_n^2 - 2m_\pi^2 + s, \\
 \kappa^2 &= \frac{1}{s} (s - 4m_\pi^2) \lambda(s, m_\Delta^2, m_n^2),
 \end{aligned} \tag{D.2}$$

$$s_Y = m_\Delta^2 + m_n^2 + 2m_\pi^2 - 2m_p^2.$$

Note that κ^2 is negative in the range $s_{dt} < s < s_{st}$, i.e. $|\kappa| = \sqrt{-\kappa^2}$. Only for negative κ^2 the expressions equation Eq. (D.1) are correct. For positive κ^2 one has log's instead of arctan's. In practice, however, the integration boundaries of the dispersive integrals run from $4m_\pi^2$ to $\Lambda = 4 \text{ GeV}^2$ which lies below the scattering threshold $s_{st} = (m_\Delta + m_n)^2$. It follows that one has to replace the arctan's with the log's only in the range $4m_\pi^2 < s < s_{dt} = (m_\Delta - m_n)^2$. The coefficient functions in

equation Eq. (D.1) are given by

$$\begin{aligned} C_{+1} &= -\frac{2(m_\Delta - m_n)(m_n + m_p)}{s - (m_\Delta - m_n)^2}, \\ C_{-1} &= -\frac{6(m_\Delta - m_n)(m_n + m_p)}{s - (m_\Delta - m_n)^2}, \end{aligned} \quad (D.3)$$

$$C_0 = \frac{(m_\Delta + m_n)(m_\Delta + m_p)}{s} - \frac{3m_\Delta(m_n + m_p)}{s - (m_\Delta - m_n)^2},$$

$$D_{+1} = 3m_p(m_n + m_p) + \frac{3(m_\Delta - m_n)(m_n + m_p)(m_\pi^2 + m_\Delta m_n - m_p^2)}{s - (m_\Delta - m_n)^2},$$

$$\begin{aligned} D_{-1} &= \frac{3}{m_\Delta}(m_n + m_p)(m_\pi^2 - m_\Delta^2 + m_\Delta m_p - m_p^2) \\ &+ \frac{9(m_\Delta - m_n)(m_n + m_p)(m_\pi^2 + m_\Delta m_n - m_p^2)}{s - (m_\Delta - m_n)^2}, \end{aligned}$$

$$\begin{aligned} D_0 &= 3m_p(m_n + m_p)(m_\Delta^2 - m_\Delta m_p - m_\pi^2 + m_p^2) \\ &- \frac{9m_\Delta(m_n + m_p)(m_\Delta m_n + m_\pi^2 - m_p^2)^2}{s - (m_\Delta - m_n)^2} \\ &+ \frac{3(m_\Delta + m_n)(m_p + m_n)}{s} \left(m_\Delta^3 m_n - m_p(m_\Delta - m_n)(m_\Delta^2 + m_\pi^2) \right. \\ &+ 2m_\Delta^2 m_\pi^2 - m_p^2(m_\Delta(m_\Delta + m_n) + 2m_\pi^2) \\ &\left. + 2m_\Delta m_n m_\pi^2 - m_p^3(m_n - m_\Delta) + m_\pi^4 + m_p^4 \right), \end{aligned} \quad (D.4)$$

$$\begin{aligned}
E_{+1} &= \frac{(m_\Delta - m_n) ((m_\Delta + m_n)^2 - m_\pi^2)}{3m_\Delta (s - (m_\Delta - m_n)^2)}, \\
E_{-1} &= \frac{(m_\Delta - m_n) ((m_\Delta + m_n)^2 - m_\pi^2)}{m_\Delta (s - (m_\Delta - m_n)^2)}, \tag{D.5}
\end{aligned}$$

$$E_0 = -\frac{(m_\Delta + m_n)(2m_\Delta^2 + 2m_\Delta m_n - m_\pi^2)}{6m_\Delta s} + \frac{(m_\Delta + m_n)^2 - m_\pi^2}{2(s - (m_\Delta - m_n)^2)},$$

$$\begin{aligned}
F_{+1} &= -\frac{3s}{2} - \frac{m_\pi^2(2m_\Delta + 3m_n)}{2m_\Delta} + \frac{5(m_\Delta + m_n)^2}{2} \\
&\quad + \frac{(m_\Delta - m_n)((m_\Delta + m_n)^2 - m_\pi^2)(m_\Delta^2 - m_\Delta m_n - m_\pi^2)}{2m_\Delta(s - (m_\Delta - m_n)^2)}, \\
F_{-1} &= \frac{3s}{2} + \frac{m_\pi^2(m_\Delta^2 + m_\Delta m_n - m_n^2) + m_\pi^4}{2m_\Delta^2} - \frac{5(m_\Delta + m_n)^2}{2} \\
&\quad + \frac{3(m_\Delta - m_n)((m_\Delta + m_n)^2 - m_\pi^2)(m_\Delta^2 - m_\Delta m_n - m_\pi^2)}{2m_\Delta(s - (m_\Delta - m_n)^2)}, \tag{D.6} \\
F_0 &= \frac{3m_\Delta^2 s}{2} - \frac{m_\pi^2(7m_\Delta^2 - 2m_\Delta m_n + 2m_n^2) + m_\Delta^2(m_\Delta + m_n)^2}{2} + m_\pi^4 \\
&\quad + \frac{4m_\Delta^2 m_\pi^2(m_\Delta - 2m_n)(m_\Delta + m_n)^2}{2m_\Delta s} \\
&\quad - \frac{m_\pi^4(2m_\Delta^3 + m_\Delta^2 m_n + m_n^3) + m_\pi^6(m_\Delta + m_n)}{2m_\Delta s} \\
&\quad + \frac{3((m_\Delta + m_n)^2 - m_\pi^2)(m_\Delta(m_n - m_\Delta) + m_\pi^2)^2}{2(s - (m_\Delta - m_n)^2)}.
\end{aligned}$$

The explicit expressions for the polynomial terms are

$$\begin{aligned}
 P_{+1} &= -\frac{g_A h_A}{4\sqrt{6}F_\pi^2} 2 - \frac{5h_A H_A}{12\sqrt{6}F_\pi^2} \frac{5(m_\Delta + m_n)}{6m_\Delta}, \\
 P_{-1} &= -\frac{g_A h_A}{4\sqrt{6}F_\pi^2} \frac{2(m_\Delta - m_n - m_p)}{m_\Delta} \\
 &\quad - \frac{5h_A H_A}{12\sqrt{6}F_\pi^2} \frac{s - 2m_\pi^2 - (m_\Delta + m_n)(6m_\Delta - m_n)}{6m_\Delta^2}, \\
 &\approx -\frac{g_A h_A}{4\sqrt{6}F_\pi^2} \frac{2(m_\Delta - m_n - m_p)}{m_\Delta} \\
 &\quad - \frac{5h_A H_A}{12\sqrt{6}F_\pi^2} \frac{-(m_\Delta + m_n)(6m_\Delta - m_n)}{6m_\Delta^2}, \\
 P_0 &= -\frac{g_A h_A}{4\sqrt{6}F_\pi^2} - \frac{5h_A H_A}{12\sqrt{6}F_\pi^2} \frac{3m_\Delta - m_n}{6m_\Delta}.
 \end{aligned} \tag{D.7}$$

The $\Delta\bar{n}\pi^+\pi^-$ contact diagram produces the following polynomials:

$$\begin{aligned}
 P_{+1}^{\text{NLO}\chi\text{PT}} &= -c_F \frac{m_\Delta + m_n}{\sqrt{3}F_\pi^2}, \\
 P_0^{\text{NLO}\chi\text{PT}} &= -c_F \frac{m_\Delta}{\sqrt{3}F_\pi^2}, \\
 P_{-1}^{\text{NLO}\chi\text{PT}} &= c_F \frac{m_n(m_\Delta + m_n) - s}{\sqrt{3}F_\pi^2 m_\Delta}, \\
 &\approx c_F \frac{m_n(m_\Delta + m_n)}{\sqrt{3}F_\pi^2 m_\Delta}.
 \end{aligned} \tag{D.8}$$

APPENDIX E

VECTOR SPINORS

Now we introduce very useful explicit form for the polarization vectors in a given z direction of the center of mass frame. All solutions of the vector-spinors for the spin-3/2 couple to spin-1/2 and spin-1 states are given by (Rarita and Schwinger, 1941; Junker et al., 2020) when it is satisfied the relativistic energy-momentum relation of a particle $E = \sqrt{\vec{p}^2 + m^2}$. The constructed vector-spinor expressed by (Stoica et al., 2011);

$$\begin{aligned}
 u^\mu(p, \pm \frac{3}{2}) &= u(p, \pm \frac{1}{2}) \varepsilon(p, \pm 1), \\
 u^\mu(p, \pm \frac{1}{2}) &= \frac{1}{\sqrt{3}} u(p, \mp \frac{1}{2}) \varepsilon(p, \pm 1), \\
 &\quad + \frac{\sqrt{2}}{\sqrt{3}} u(p, \pm \frac{1}{2}) \varepsilon(p, 0).
 \end{aligned} \tag{E.1}$$

The projections of the particle's spin on the z direction

$$\begin{aligned}
 \varepsilon^\mu(p_z, \pm 1) &= \frac{\mp 1}{\sqrt{2}} (0, 1, \pm i, 0), \\
 \varepsilon^\mu(p_z, 0) &= \frac{1}{m_\Delta} (\vec{p}_z, 0, 0, E),
 \end{aligned} \tag{E.2}$$

and the spin 1/2 spinor in this frame leads to

$$u\left(p_z, s = +\frac{1}{2}\right) = \begin{pmatrix} \sqrt{E - p_z} \\ 0 \\ \sqrt{E + p_z} \\ 0 \end{pmatrix}, \quad u\left(p_z, s = -\frac{1}{2}\right) = \begin{pmatrix} 0 \\ \sqrt{E + p_z} \\ 0 \\ \sqrt{E - p_z} \end{pmatrix}. \tag{E.3}$$

When a particle at rest frame, $p_z=0$, the four-spinors have the form

$$u\left(\vec{p}_z=0, s=+\frac{1}{2}\right)=\begin{pmatrix} \sqrt{m_\Delta} \\ 0 \\ \sqrt{m_\Delta} \\ 0 \end{pmatrix}, u\left(\vec{p}_z=0, s=-\frac{1}{2}\right)=\begin{pmatrix} 0 \\ \sqrt{m_\Delta} \\ 0 \\ \sqrt{m_\Delta} \end{pmatrix}. \quad (\text{E.4})$$



APPENDIX F

SOLUTION OF OMNÈS FUNCTION

The Omnès function above can be analytically solved according to the Schwarz's reflection principle. If a function $F(s) = H(s)\Omega(s)$, then we write it down in terms of the phase shift $\delta(s)$ as;

$$\begin{aligned}\Omega(s + i\varepsilon) &= \Omega(s - i\varepsilon), \\ \Omega(s + i\varepsilon) &= |\Omega(s)|e^{i\delta(s)}, \\ \Omega(s - i\varepsilon) &= |\Omega(s)|e^{-i\delta(s)}.\end{aligned}\tag{F.1}$$

Following the equality of Schwarz's rules, we continue to rewrite it;

$$\begin{aligned}\Omega(s - i\varepsilon) &= \Omega(s + i\varepsilon)e^{-2i\delta(s)}, \\ \log \Omega(s - i\varepsilon) &= \log \Omega(s + i\varepsilon) - 2i\delta(s), \\ \log \Omega(s - i\varepsilon) - \log \Omega(s + i\varepsilon) &= 2i\delta(s), \\ \text{disc } \log \Omega(s) &= 2i\delta(s), \\ \text{Im } \log \Omega(s) &= \delta(s).\end{aligned}\tag{F.2}$$

We now move on to write a dispersion relation for $\log \Omega(s)$ in accordance with the choosen normalization one $\Omega(0) = 1$. That is

$$\log \Omega(s) = \frac{1}{\pi} \int_{4m_\pi^2}^{\infty} \frac{\delta(s')}{s' - s - i\varepsilon} = \frac{1}{\pi} \int_{4m_\pi^2}^{\infty} \frac{\text{Im } \log \Omega(s')}{s' - s - i\varepsilon}, \tag{F.3}$$

Inserting a one subtracted term for the initial condition of $\Omega(0) = 1$ into the relation of Eq. (F.4),

$$\begin{aligned}\log \Omega(s) - \log \Omega(0) &= \frac{1}{\pi} \int_{4m_\pi^2}^{\infty} \left(\frac{\delta(s')}{s' - s - i\varepsilon} - \frac{\delta(s')}{s' - i\varepsilon} \right), \\ \log \Omega(s) &= \frac{s}{\pi} \int_{4m_\pi^2}^{\infty} \frac{\delta(s')}{s'(s' - s - i\varepsilon)}\end{aligned}\tag{F.4}$$

It is a final representation form of the Omnès function mentioned in the relation Eq. (3.59).



APPENDIX G

DERIVATION OF TWO BODY PHASE-SPACE

In this subsequent section, the two body phase-space integral of the differential decay rate is derived as regard to the appropriate rest frame as the same trick parts for three-body. Supposing that

$$\begin{aligned}\Gamma &= \frac{1}{2m_\Delta} \langle |m_{\Delta \rightarrow n\gamma}|^2 \rangle \int \frac{d^3 p_1}{(2\pi)^3 2E_1} \frac{d^3 p_2}{(2\pi)^3 2E_2} (2\pi)^4 \delta^{(4)}(P - p_1 - p_2), \\ &= \frac{1}{8m_\Delta} \langle |m_{\Delta \rightarrow n\gamma}|^2 \rangle \underbrace{\frac{1}{(2\pi)^2} \int \frac{d^3 p_1}{E_1} \frac{d^3 p_2}{E_2} \delta(m_\Delta - E_1 - E_2)}_{I_{PS}}\end{aligned}\quad (G.1)$$

$$\delta^{(3)}(-\vec{p}_1 - \vec{p}_2).$$

To simplify the elimination of component \vec{p}_2 from the delta function of Eq. (G.1), we set the frame where the initial particle is at rest, i.e $P = (E_p, \vec{0}) = (m_\Delta, \vec{0})$. By the momenta of decaying particles $|\vec{p}_2| = |\vec{p}_1|$, the corresponding energy observable write as

$$E_2 = \sqrt{|\vec{p}_2|^2 + m_2^2} = \sqrt{|\vec{p}_1|^2 + m_2^2} = \sqrt{E_1^2 - m_1^2 + m_2^2} = E_2(E_1). \quad (G.2)$$

For the underbrace integral, we obtain

$$\begin{aligned}I_{PS} &= \frac{1}{(2\pi)^2} \int \frac{d^3 p_1}{E_1 E_2(E_1)} \delta(m_\Delta - E_1 - E_2(E_1)), \\ &= \frac{1}{(2\pi)^2} \int_{m_1}^{\infty} d|\vec{p}_1| \frac{|\vec{p}_1|^2}{E_1 E_2(E_1)} \delta(m_\Delta - E_1 - E_2(E_1)) \\ &\quad \int_{-1}^1 d(\cos \theta) \int_0^{2\pi} d\phi, \\ &= \frac{1}{\pi} \int_{m_1}^{\infty} d|\vec{p}_1| \frac{|\vec{p}_1|^2}{E_1 E_2(E_1)} \delta(m_\Delta - E_1 - E_2(E_1)).\end{aligned}\quad (G.3)$$

The above integration is done in the speherical coordinate consideration too. For the remaining part, we change a energy variable from the momentum integrand by $E_1 dE_1 = |\vec{p}_1| d|\vec{p}_1|$. It is written as

$$\begin{aligned} I_{PS} &= \frac{1}{\pi} \int_{m_1}^{\infty} dE_1 \frac{E_1 |\vec{p}_1|}{E_1 E_2(E_1)} \delta(m_{\Delta} - E_1 - E_2(E_1)), \\ &= \frac{1}{\pi} \int_{m_1}^{\infty} dE_1 \frac{|\vec{p}_1|}{E_2(E_1)} \delta(m_{\Delta} - E_1 - E_2(E_1)). \end{aligned} \quad (G.4)$$

In the same frame, let we find the energies in terms of the masses of each decaying particles as below

$$\begin{aligned} m_{\Delta} - E_1 - E_2(E_1) &= 0, \\ E_1 &= \frac{m_{\Delta}^2 + m_1^2 - m_2^2}{2m_{\Delta}}, \quad E_2 = \frac{m_{\Delta}^2 - m_1^2 + m_2^2}{2m_{\Delta}}. \end{aligned} \quad (G.5)$$

With the help of Dirac's property, we calculate the inside of delta function;

$$\begin{aligned} \delta(f(x)) &= \sum_i \frac{1}{|f'(x_i)|} \delta(x - x_i), \quad f(x_i) = 0, \\ \frac{d}{dE_1} (m_{\Delta} - E_1 - E_2(E_1)) &= -1 - \frac{1}{2} \frac{2E_1}{\sqrt{E_1^2 - m_1^2 + m_2^2}}, \\ &= \frac{-m_{\Delta}}{E_2(E_1)}, \end{aligned} \quad (G.6)$$

$$\delta(m_{\Delta} - E_1 - E_2(E_1)) = \frac{E_2(E_1)}{m_{\Delta}} \delta\left(E_1 - \frac{m_{\Delta}^2 + m_1^2 - m_2^2}{2m_{\Delta}}\right).$$

Inserting all together into the relation Eq. (G.1), it is supported us to write a final representation for the two-body decay width as

$$\begin{aligned} \Gamma &= \frac{1}{8\pi m_{\Delta}} \langle |M_{\Delta \rightarrow n\gamma}|^2 \rangle \frac{|\vec{p}_1|}{E_2(E_1)} \frac{E_2(E_1)}{m_{\Delta}}, \\ &= \frac{|\vec{p}_1|}{8\pi m_{\Delta}^2} \langle |M_{\Delta \rightarrow n\gamma}|^2 \rangle \Theta(m_{\Delta} - m_n), \end{aligned} \quad (G.7)$$

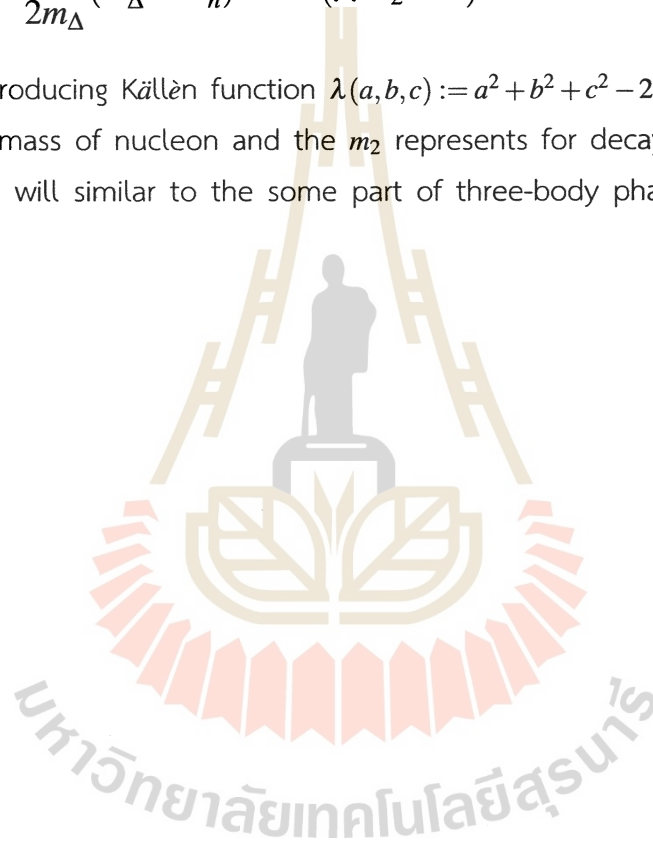
with the center of mass momentum p_1 is given by

$$|\vec{p}_{cm}| = |\vec{p}_1| = \sqrt{E_1^2 - m_1^2} = \left(\left(\frac{m_\Delta^2 + m_1^2 - m_2^2}{2m_\Delta} \right)^2 - m_1^2 \right)^{1/2},$$

$$= \frac{1}{2m_\Delta} \sqrt{\lambda(m_\Delta^2, m_1^2, m_2^2)}, \quad (\text{G.8})$$

$$|\vec{p}_{cm}| = \frac{1}{2m_\Delta} (m_\Delta^2 - m_n^2). \quad (\because m_2 = 0).$$

where the introducing Källén function $\lambda(a, b, c) := a^2 + b^2 + c^2 - 2(ab + bc + ac)$, the m_1 refers to the mass of nucleon and the m_2 represents for decaying particle gamma. All the above will similar to the some part of three-body phase space derivation.



APPENDIX H

DERIVATION OF THREE BODY PHASE-SPACE

Recalling that the double differential decay width relation Eq. (5.23), we now focus on the phase space intergration over the momenta of the considered particles in the following;

$$\begin{aligned} \frac{d\Gamma}{dm_{12}^2 dm_{23}^2} &= \frac{1}{2m_\Delta} \langle |M_{\Delta \rightarrow Ne^+e^-}|^2 \rangle \underbrace{\int \frac{dp_1}{(2\pi)^3 2E_1} \frac{dp_2}{(2\pi)^3 2E_2} \frac{dp_3}{(2\pi)^3 2E_3} (2\pi)^4}_{\text{Phasespace}} \\ &\times \underbrace{\delta^{(4)}(P - p_1 - p_2 - p_3) \delta(m_{12}^2 - (p_1 + p_2)^2) \delta(m_{23}^2 - (p_2 + p_3)^2)}_{\text{Phasespace}}. \end{aligned} \quad (\text{H.1})$$

Note the representation above that the decay paricle of momentum associated with the positron is p_1 , the electron is p_2 , the nucleon is p_2 and all the analogous quantities are defined in the section (6.1). Later, the energy state of a particle related to the zeroth component of q will be used the symbols E_p . To carry out the integration, the property of the delta function introduces

$$\int d^4q \delta^{(4)}(q - p_1 - p_2) = 1. \quad (\text{H.2})$$

Inserting the identity above Eq. (H.2) into Eq. (H.1), the three-body phase space equation become

$$\begin{aligned} \text{Int}_{\text{Phasespace}} &= \int d^4q \int \frac{d^3p_3}{(2\pi)^3 2E_3} \int \frac{d^3p_1}{(2\pi)^3 2E_1} \int \frac{d^3p_2}{(2\pi)^3 2E_2} (2\pi)^4 \\ &\times \delta^{(4)}(P - p_1 - p_2 - p_3) \delta(m_{12}^2 - (p_1 + p_2)^2) \\ &\times \delta(m_{23}^2 - (p_2 + p_3)^2) \delta^{(4)}(q - p_1 - p_2), \end{aligned} \quad (\text{H.3})$$

$$\begin{aligned}
\text{Int}_{\text{phasespace}} &= \int d^4q \int \frac{d^3p_3}{(2\pi)^3 2E_3} (2\pi)^4 \delta^{(4)}(P - q - p_3) \\
&\times \underbrace{\int \frac{d^3p_1}{(2\pi)^3 2E_1} \int \frac{d^3p_2}{(2\pi)^3 2E_2} \delta(m_{23}^2 - (p_2 + p_3)^2) \delta^{(4)}(q - p_1 - p_2)}_{\text{Int}_{\text{new}}}. \tag{H.4}
\end{aligned}$$

Then the momentum integration of Int_{new} of the underlined part for Eq. (H.4)

$$\begin{aligned}
\text{Int}_{\text{new}} &= \int \frac{d^3p_1}{(2\pi)^3 2E_1} \frac{d^3p_2}{(2\pi)^3 2E_2} \delta(m_{23}^2 - (p_2 + p_3)^2) \\
&\times \delta^{(4)}(q - p_1 - p_2), \tag{H.5} \\
&= \int \frac{d^3p_1}{(2\pi)^3 2E_1} \frac{d^3p_2}{(2\pi)^3 2E_2} \delta(m_{23}^2 - (p_2 + p_3)^2) \\
&\times \delta(q - E_1 - E_2) \delta^{(3)}(\vec{q} - \vec{p}_1 - \vec{p}_2).
\end{aligned}$$

Since all inserting integrands inside the equation of Eq. (H.5) are Lorentz invariant quantities, so it is convenient to evaluate it an appropriate frame where the decay particle is at rest, i.e $\vec{q} = 0$. This relation Eq. (H.5) can then be written

$$\begin{aligned}
\text{Int}_{\text{new}} &= \int \frac{d^3p_1}{(2\pi)^3 2E_1} \int \frac{d^3p_2}{(2\pi)^3 2E_2} \delta(m_{23}^2 - (p_2 + p_3)^2) \\
&\times \delta(q - E_1 - E_2) \delta^{(3)}(-\vec{p}_1 - \vec{p}_2). \tag{H.6}
\end{aligned}$$

To eliminate the momentum \vec{p}_2 from the delta function of above $\delta^{(3)}(-\vec{p}_1 - \vec{p}_2)$, we consider $\vec{p}_1 + \vec{p}_2 = 0$ in the CM frame. For this choices $|\vec{p}_2| = |\vec{p}_1|$ due to $\vec{p}_2 = -\vec{p}_1$, the energy of state is

$$E_2 = \sqrt{\vec{p}_2^2 + m_2^2} = \sqrt{|\vec{p}_1|^2 + m_2^2} = \sqrt{E_1^2 - m_1^2 + m_2^2} = E_2(E_1). \tag{H.7}$$

After that it is satisfied to rewrite the momentum integral of Eq. (H.6) as follow:

$$\begin{aligned}
 \text{Int}_{new} &= \frac{1}{4(2\pi)^6} \int \frac{d^3 p_1}{E_1 E_2(E_1)} \delta(m_{12} - E_1 - E_2(E_1)) \\
 &\quad \times \delta(m_{23}^2 - m_2^2 - m_3^2 - 2E_2 E_3 + 2|\vec{p}_2||\vec{p}_3|\cos\theta), \\
 &= \frac{1}{4(2\pi)^6} \int \frac{d^3 p_1}{E_1 E_2(E_1)} \delta(m_{12} - E_1 - E_2(E_1)) \\
 &\quad \times \delta(2|\vec{p}_1||\vec{p}_3|\cos\theta + \dots\dots\dots).
 \end{aligned} \tag{H.8}$$

Setting the momentum integral in the spherical coordinate, we calculate

$$\begin{aligned}
 \text{Int}_{new} &= \frac{1}{4(2\pi)^6} \int_0^{2\pi} d\phi \int_{-1}^1 d(\cos\theta) \int_{m_1}^{\infty} d|\vec{p}_1| \frac{|\vec{p}_1|^2}{E_1 E_2(E_1)} \\
 &\quad \times \delta(m_{12} - E_1 - E_2(E_1)) \frac{1}{2|\vec{p}_1||\vec{p}_3|} \delta(\cos\theta \dots\dots\dots), \\
 &= \frac{1}{8(2\pi)^5} \int_{m_1}^{\infty} d|\vec{p}_1| \frac{|\vec{p}_1|}{E_1 E_2(E_1)} \delta(m_{12} - E_1 - E_2(E_1)) \frac{1}{|\vec{p}_3|}.
 \end{aligned} \tag{H.9}$$

From this, one can change the energy variables defined by the relation $|\vec{p}_1|d|\vec{p}_1| = E_1 dE_1$.

$$\begin{aligned}
 \text{Int}_{new} &= \frac{1}{8(2\pi)^5} \int_{m_1}^{\infty} dE_1 \frac{E_1}{E_1 E_2(E_1)} \delta(m_{12} - E_1 - E_2(E_1)) \frac{1}{|\vec{p}_3|}, \\
 &= \frac{1}{8(2\pi)^5} \int_{m_1}^{\infty} dE_1 \frac{1}{E_2(E_1)} \delta(m_{12} - E_1 - E_2(E_1)) \frac{1}{|\vec{p}_3|}.
 \end{aligned} \tag{H.10}$$

Supposing that the Dirac's delta property

$$\delta(f(x)) = \sum_i \frac{1}{|f'(x_i)|} \delta(x - x_i), \tag{H.11}$$

where x_i is the zeroth of the function ($f(x_i) = 0$). We find the delta function of Eq. (H.10) since this function is fixed by the energy variable in terms of the particle

masses.

$$m_{12} - E_1 - E_2(E_1) = 0,$$

$$m_{12}^2 + E_1^2 - 2E_1 m_{12} = E_1^2 - m_1^2 + m_2^2, (\because E_2(E_1) = \sqrt{E_1^2 - m_1^2 + m_2^2}) \quad (\text{H.12})$$

$$E_1 = \frac{m_{12}^2 - m_2^2 + m_1^2}{2m_{12}}, \text{ and } E_2(E_1) = \frac{m_{12}^2 + m_2^2 - m_1^2}{2m_{12}}.$$

The derivative of the delta dunction term become

$$\frac{d}{dE_1}(m_{12} - E_1 - E_2(E_1)) = -\frac{E_2(E_1) + E_1}{E_2(E_1)} = -\frac{m_{12}}{E_2(E_1)}. \quad (\text{H.13})$$

Turning to the explicity calculation of outgoing momentum $|\vec{p}_3|$ from the zero component of energy q in the CM frame, we start the law of conservation of momentum

$$\vec{P} = \vec{p}_1 + \vec{p}_2 + \vec{p}_3 = \vec{q} + \vec{p}_3, \quad (\because p_1 + p_2 = q = (q, \vec{0})),$$

$$0 = \vec{P} + \vec{p}_3, \quad |\vec{p}_3| = |\vec{P}|, \quad (\text{H.14})$$

$$E_3 = \sqrt{|\vec{P}|^2 + m_3^2} = \sqrt{E_p^2 - m_\Delta^2 + m_3^2} = E_3(E_p).$$

Recall that the relation at the zeroth component

$$E_p - q - E_3(E_p) = 0,$$

$$E_p^2 + q^2 - 2E_p q = E_p^2 - m_\Delta^2 + m_3^2, \quad (\text{H.15})$$

$$E_p = \frac{q_0^2 - m_3^2 + m_\Delta^2}{2q_0}, \quad E_3 = \frac{m_\Delta^2 - m_3^2 - q_0^2}{2q_0}.$$

At the same time, the center of mass momentum $|\vec{p}_3|$ in terms of the masses is given by

$$|\vec{p}_3| = \sqrt{E_3^2 - m_3^2} = \left(\left(\frac{m_\Delta^2 - m_3^2 - q^2}{2q} \right)^2 - m_3^2 \right)^{\frac{1}{2}}, \quad (\text{H.16})$$

$$\begin{aligned}
|\vec{p}_3| &= \frac{1}{2q} (m_\Delta^4 + m_3^4 + q^4 - 2m_\Delta^2 m_3^2 - 2m_\Delta^2 q^2 - 2q^2 m_3^2)^{\frac{1}{2}}, \\
&= \frac{1}{2q} \lambda^{1/2}(q^2, m_\Delta^2, m_3^2),
\end{aligned} \tag{H.17}$$

with the Källén function $\lambda(x, y, z) = x^2 + y^2 + z^2 - 2(xy + yz + zx)$. Since we have the value of energy, the energy integration is now supposed to rewrite

$$\begin{aligned}
\text{Int}_{new} &= \frac{1}{8(2\pi)^5} \int_{m_1}^{\infty} dE_1 \frac{1}{E_2(E_1)} \frac{E_2(E_1)}{m_{12}} \delta\left(E_1 - \frac{m_{12}^2 - m_1^2 + m_2^2}{2m_{12}}\right), \\
&= \frac{1}{8(2\pi)^5} \int_{m_1}^{\infty} dE_1 \frac{1}{m_{12}|\vec{p}_3|} \delta\left(E_1 - \frac{m_{12}^2 - m_1^2 + m_2^2}{2m_{12}}\right), \\
&= \frac{1}{8(2\pi)^5} \frac{1}{m_{12} \times \frac{\lambda^{1/2}[q^2, m_\Delta^2, m_3^2]}{2m_{12}}} \Theta(m_{12} - (m_1 + m_2)), \\
&= \frac{1}{4(2\pi)^5} \frac{\Theta(q^2 - (m_1 + m_2)^2) \Theta(q)}{\lambda^{1/2}[q^2, m_\Delta^2, m_3^2]},
\end{aligned} \tag{H.18}$$

with the representation of step function refers to

$$\Theta(m_{12} - (m_1 + m_2)) = \Theta(q^2 - (m_1 + m_2)^2) \Theta(q). \tag{H.19}$$

When we insert all expressions of Eq. (H.18) into Eq. (H.4), the integral of phase-space write as below

$$\begin{aligned}
\text{Int}_{\text{phasespace}} &= \int d^4q \int \frac{d^3p_3}{(2\pi)^3 2E_3} (2\pi)^4 \delta^{(4)}(P - q - p_3) \delta(m_{12}^2 - q^2) \\
&\times \frac{1}{4(2\pi)^5} \frac{\Theta(q^2 - (m_1 + m_2)^2) \Theta(q)}{\lambda^{1/2}(q^2, m_\Delta^2, m_3^2)}.
\end{aligned} \tag{H.20}$$

Focusing on the part of integration over q in the integral above,

$$\begin{aligned}
& \int d^4 q \delta(m_{12}^2 - q^2) \Theta(q^2 - (m_1 + m_2)^2) \Theta(q) (2\pi)^4 \delta^{(4)}(P - q - p_3) \\
&= \int d^3 \vec{q} \int dq \delta(q^2 - \vec{q}^2 - m_{12}^2) \Theta(q^2 - (m_1 + m_2)^2) \Theta(q) (2\pi)^4 \\
&\quad \times \delta^{(4)}(P - q - p_3), \\
&= \int d^3 \vec{q} \frac{1}{2E_q} \Theta(q^2 - (m_1 + m_2)^2) (2\pi)^4 \delta^{(4)}(P - q - p_3).
\end{aligned} \tag{H.21}$$

Here, we use $\int dp \delta(q^2 - \vec{q}^2 - m_{12}^2) \Theta(q) = \frac{1}{2E_q}$ since the delta function $\delta(q_0^2 - \vec{q}^2 - m_{12}^2)$ satisfies with the energy-momentum definition $q = \pm \sqrt{\vec{q}^2 + m_{12}^2} = E_q$. After the integration over q in the Eq. (H.21),

$$\begin{aligned}
\text{Int}_{\text{Phasespace}} &= \int \frac{d^3 p_3}{(2\pi)^3 2E_3} \int d^3 \vec{q} \frac{1}{2E_q} (2\pi)^4 \delta^{(4)}(P - q - p_3) \\
&\quad \times \frac{\Theta(q^2 - (m_1 + m_2)^2)}{4(2\pi)^5 \lambda^{1/2}(q^2, m_\Delta^2, m_3^2)}, \\
&= \frac{1}{16(2\pi)^4} \int \frac{d^3 p_3}{E_3} \int \frac{d^3 \vec{q}}{E_q} \frac{\Theta(q^2 - (m_1 + m_2)^2)}{\lambda^{1/2}(q^2, m_\Delta^2, m_3^2)} \\
&\quad \times \delta^{(4)}(P - q - p_3), \\
&= \frac{1}{16(2\pi)^4} \int \frac{d^3 p_3}{E_3} \int \frac{d^3 \vec{q}}{E_q} \delta(m_\Delta - E_q - E_3) \delta^{(3)}(-\vec{q} - \vec{p}_3) \\
&\quad \times \frac{\Theta(q^2 - (m_1 + m_2)^2)}{\lambda^{1/2}(q^2, m_\Delta^2, m_3^2)}.
\end{aligned} \tag{H.22}$$

Now this expression is exactly the same as the two-body phase space integration, so it is easy to prove the momentum integration in a typical way of considering where the particle exists at rest frame, $\vec{P} = 0$. In this frame, we have $\vec{P} = \underbrace{\vec{p}_1 + \vec{p}_2}_{\vec{q}} + \vec{p}_3$,

that is $|\vec{q}| = |\vec{p}_3|$ and the energy variable

$$E_3 = \sqrt{|\vec{p}_3|^2 + m_3^2} = \sqrt{|\vec{q}|^2 + m_3^2} = \sqrt{E_q^2 - m_{12}^2 + m_3^2} = E_3(E_q). \quad (\text{H.23})$$

Getting rid of the \vec{p}_3 from the delta function, one finds

$$\begin{aligned} \text{Int}_{\text{phasespace}} &= \frac{1}{16(2\pi)^4} \int d^3\vec{q} \frac{1}{E_q E_3(E_q)} \delta(m_\Delta - E_q - E_3) \\ &\quad \times \frac{\Theta(q^2 - (m_1 + m_2)^2)}{\lambda^{1/2}(q^2, m_\Delta^2, m_3^2)}, \\ &= \frac{1}{16(2\pi)^4} \int_{m_{12}}^\infty d|\vec{q}| \frac{|\vec{q}|^2}{E_q E_3(E_q)} \frac{\delta(m_\Delta - E_q - E_3)}{\lambda^{1/2}(q^2, m_\Delta^2, m_3^2)} \\ &\quad \times \Theta(q^2 - (m_1 + m_2)^2) \int_{-1}^1 d(\cos \theta) \int_0^{2\pi} d\phi, \\ &= \frac{4\pi}{16(2\pi)^4} \int_{m_{12}}^\infty d|\vec{q}| \frac{|\vec{q}|^2}{E_q E_3(E_q)} \delta(m_\Delta - E_q - E_3(E_q)) \\ &\quad \times \frac{\Theta(q^2 - (m_1 + m_2)^2)}{\lambda^{1/2}(q^2, m_\Delta^2, m_3^2)}. \end{aligned} \quad (\text{H.24})$$

Changing the momentum $|\vec{q}|$ integration to the energy integration, we get

$$\begin{aligned} \text{Int}_{\text{phasespace}} &= \frac{1}{8(2\pi)^3} \int_{m_{12}}^\infty dE_q \frac{E_q |\vec{q}|}{E_q E_3(E_q)} \delta(m_\Delta - E_q - E_3(E_q)) \\ &\quad \times \frac{\Theta(q^2 - (m_1 + m_2)^2)}{\lambda^{1/2}(q^2, m_\Delta^2, m_3^2)}, \\ &= \frac{1}{8(2\pi)^3} \int_{m_{12}}^\infty dE_q \frac{|\vec{q}|}{E_3(E_q)} \delta(m_\Delta - E_q - E_3(E_q)) \\ &\quad \times \frac{\Theta(q^2 - (m_1 + m_2)^2)}{\lambda^{1/2}(q^2, m_\Delta^2, m_3^2)}. \end{aligned} \quad (\text{H.25})$$

In the similar way, the energy values in terms of the masses can directly be calculated from the delta function with respect to the Dirac's property. That is

$$m_\Delta - E_q - E_3(E_q) = 0,$$

$$E_q = \frac{m_\Delta^2 + m_{12}^2 - m_3^2}{2m_\Delta}, \quad E_3(E_q) = \frac{m_\Delta^2 - m_{12}^2 + m_3^2}{2m_\Delta}, \quad (\text{H.26})$$

$$|\vec{q}| = \sqrt{E_q^2 - m_{12}^2} = \frac{1}{2m_\Delta} \lambda^{1/2}(q^2, m_\Delta^2, m_3^2),$$

and the derivative of input delta function becomes

$$\frac{d}{dE_q}(m_\Delta - E_q - E_3(E_q)) = -1 - \frac{1}{2} \frac{2E_q}{\sqrt{E_q^2 - m_{12}^2 + m_3^2}} = -\frac{m_\Delta}{E_3(E_q)}. \quad (\text{H.27})$$

The phase space part is then obtained as

$$\text{Int}_{\text{Phasespace}} = \frac{1}{8(2\pi)^3} \frac{1}{2m_\Delta^2} \frac{\lambda^{1/2}(q^2, m_\Delta^2, m_3^2)}{\lambda^{1/2}(q^2, m_\Delta^2, m_3^2)} \Theta(q^2 - (m_1 + m_2)^2) \\ \times \Theta(m_\Delta - m_3 - m_2), \quad (\text{H.28})$$

$$\text{Int}_{\text{Phasespace}} = \frac{1}{16(2\pi)^3 m_\Delta^2} \Theta(q^2 - (m_1 + m_2)^2) \Theta(m_\Delta - m_3 - m_2).$$

The expression of the double differential decay rate is

$$\frac{d\Gamma}{dm_{12}^2 dm_{23}^2} = \frac{1}{2m_\Delta} \langle |m_{\Delta \rightarrow Ne^+e^-}|^2 \rangle \times \text{Int}_{\text{Phasespace}},$$

$$\frac{d\Gamma}{dm_{12}^2 dm_{23}^2} = \frac{1}{32(2\pi)^3} \frac{1}{m_\Delta^3} \langle |m_{\Delta \rightarrow Ne^+e^-}|^2 \rangle, \quad (\text{H.29})$$

$$\frac{d\Gamma}{dq^2 d(\cos \theta)} = \frac{-2|\vec{p}_{\Delta^0}||\vec{p}_{e^-}|}{32(2\pi)^3} \frac{1}{m_\Delta^3} \langle |m_{\Delta \rightarrow Ne^+e^-}|^2 \rangle.$$

It is the full derivation of the phase space integration part for the relation Eq. (5.24). The kinematical boundaries of m_{12}^2 and m_{23}^2 which depend on the Lorentz invariant

combinations of the four-momenta are introduced as

$$\begin{aligned} (m_1 + m_2)^2 &\leq m_{12}^2 \leq (m_\Delta - m_3)^2, \\ (m_{23}^2)_{\min} &\leq m_{23}^2 \leq (m_{23}^2)_{\max}. \end{aligned} \quad (\text{H.30})$$

For the decay process in the system with m_Δ at rest, the kinematical boundary for m_{12}^2 is maximum when the energy of particle E_3 is minimum. Hence,

$$(m_{12}^2)_{\max} = (m_\Delta - m_3)^2 = m_\Delta^2 + m_3^2 - 2m_\Delta m_3 = m_\Delta^2 + m_3^2 - 2m_\Delta E_3. \quad (\text{H.31})$$

If $|\vec{p}_1| = |\vec{p}_2| \rightarrow 0$, minimum is possible since we have the energy-momentum relation $m_{12}^2 = (p_1 + p_2)^2 = (E_1 + E_2)^2 \geq (m_1 + m_2)^2$. Thus

$$(m_{12}^2)_{\min} \geq (m_1 + m_2)^2. \quad (\text{H.32})$$

For the kinematical limits $(m_{23}^2)_{\min} \leq m_{23}^2 \leq (m_{23}^2)_{\max}$, it is easiest to begin with the kinematic relation in the frame defined by $\vec{p}_1 + \vec{p}_2 = 0$;

$$m_{23}^2 = (p_2^2 + p_3^2) = (E_2 + E_3)^2 - \vec{p}_2^2 - \vec{p}_3^2 - 2|\vec{p}_2||\vec{p}_3|\cos\theta, \quad (\text{H.33})$$

and the respective energy variables are given by

$$E_2 = \frac{m_{12}^2 + m_2^2 - m_1^2}{2m_{12}}, \quad E_3 = \frac{m_\Delta^2 - m_3^2 - m_{12}^2}{2m_{12}}. \quad (\text{H.34})$$

If the direction of the outgoing particles p_2 and p_3 are parallel, the polar angle θ is equivalent to zero. Then

$$\begin{aligned} (m_{23}^2)_{\min} &= (E_2 + E_3)^2 - (\vec{p}_2 + \vec{p}_3)^2, \\ &= (E_2 + E_3)^2 - \left(\sqrt{E_2^2 - m_2^2} + \sqrt{E_3^2 - m_3^2} \right)^2. \end{aligned} \quad (\text{H.35})$$

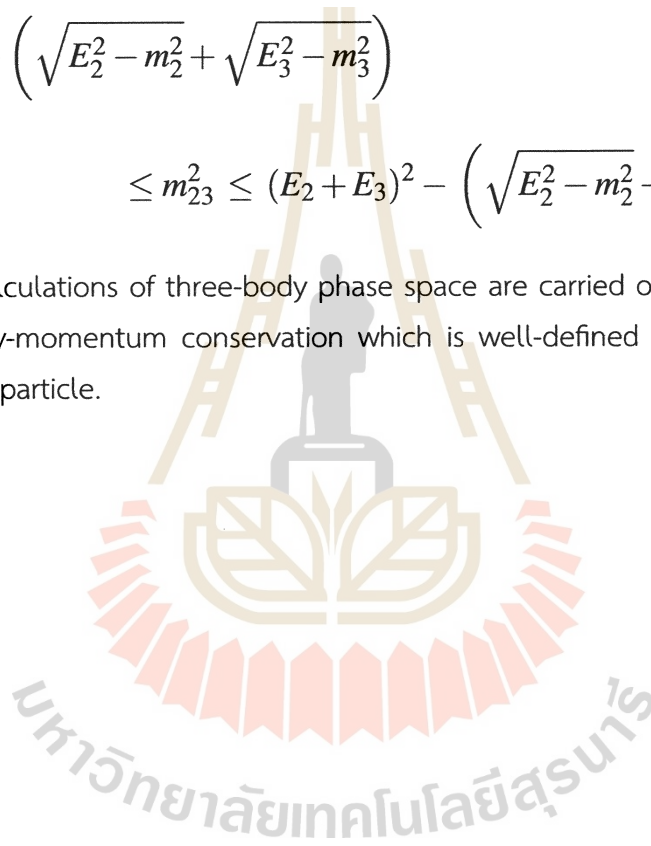
If the direction of the outgoing particles p_2 and p_3 are anti-parallel, the polar angle θ is equal to π . Then we get

$$\begin{aligned} (m_{23}^2)_{\max} &= (E_2 + E_3)^2 - (|\vec{p}_2| - |\vec{p}_3|)^2, \\ &= (E_2 + E_3)^2 - \left(\sqrt{E_2^2 - m_2^2} - \sqrt{E_3^2 - m_3^2} \right)^2. \end{aligned} \quad (\text{H.36})$$

That leads to write the kinematical boundary for m_{23} as a clearly form

$$\begin{aligned} (E_2 + E_3)^2 - \left(\sqrt{E_2^2 - m_2^2} + \sqrt{E_3^2 - m_3^2} \right)^2 \\ \leq m_{23}^2 \leq (E_2 + E_3)^2 - \left(\sqrt{E_2^2 - m_2^2} - \sqrt{E_3^2 - m_3^2} \right)^2. \end{aligned} \quad (\text{H.37})$$

The whole calculations of three-body phase space are carried out analytically based on the energy-momentum conservation which is well-defined in the rest frame of the decaying particle.



CURRICULUM VITAE

NAME: Moh Moh Aung **GENDER:** Female

NATIONALITY: Myanmar **DATE OF BIRTH:** Jan 30, 1991

EDUCATIONS:

- B.Sc (Hons), Department of Physics, University of Kyaukse, Myanmar, 2011.
- M.Sc, Department of Physics, University of Mandalay, Myanmar, 2014.
- M.Res, Department of Physics, University of Mandalay, Myanmar, 2015.
- Ph.D, School of Physics, Institute of Science, Suranaree University of Technology, Thailand, 2024.

AWARDS during PhD study:

- [1] Honorable mention award of Siam Physics Congress in Chiang Mai (SPC 2023)
- [2] Best oral presentation award of Science Postgrad Annual Research Conference in SUT (SPARC 2024)

PUBLICATION

Moh Moh Aung, Stefan Leupold, Elisabetta Perotti and Yupeng Yan, “Electromagnetic form factors of the transition from the Delta to the nucleon”, (2024). *arXiv:hep-ph/2401.17756 [hep-ph]*